The Role of Chromatin Associated Protein HMGB2 in Setting up Permissive Chromatin States for Direct Glia to Neuron Conversion

Dissertation der Graduate School of Systemic Neurosciences der Ludwig-Maximilians-Universität München

Tjaša Lepko

18.04.2018

This work was supervised by Prof. Dr. Jovica Ninkovic and carried out at the Institute of Stem Cell Research, Helmholtz Zentrum München and Biomedical Center Munich, Germany

Supervisor: Prof. Dr. Jovica Ninkovic
2nd reviewer: Prof. Dr. Magdalena Götz
3rd reviewer: Prof. Dr. Dieter Chichung Lie

Date of submission: 18.04.2018
Date of oral defense: 25.09.2018

Table of Contents

List of Figures

Abstract

The adult mammalian brain has a limited capacity to replace the loss of neurons following the traumatic brain injury or disease, therefore requiring innovative strategies to promote tissue regeneration and functional repair of the central nervous system (CNS). Direct lineage reprogramming of non-neuronal cell types (reactive astrocytes and oligodendrocytes), resident within the injured CNS to generate new neurons is a promising approach to repair damaged brain. Despite very good conversion rate of isolated postnatal astrocytes in vitro and recent advances to produce induced neuronal cells in vivo, the molecular understanding of the reprogramming process remains largely unknown. Toward this end, we developed an in vitro model with adjusted growth factor composition lacking epidermal growth factor (EGF) that reduces the reprogramming efficiency of astroglia into neurons to the rate similar to reactive astrocytes in vivo. By comparing the cultures prone and resistant to reprogramming we aimed to identify molecular features required for the efficient conversion. The proteome analysis of EGF+FGF and FGF cultures revealed the chromatin state changes as the main factor that could maintain the astrocytes in the glial lineage even after neurogenic factor overexpression. To test this hypothesis, we overexpressed the most regulated chromatin-related protein, HMGB2, together with NEUROG2 and analysed the reprogramming efficiency. Indeed, the simultaneous overexpression of both factors in the astrocytes resistant to the fate transition significantly increased direct reprogramming suggesting the role of chromatin-associated proteins in bypassing the lineage roadblocks. To understand the role of global chromatin rearrangement, we performed ATAC-sequencing comparing both culture conditions and searched for HMGB2 induced changes in the chromatin compaction. The chromatin accessibility analysis revealed an enrichment of opened promoters assigned to the neuronal genes in the astrocytes with good reprogramming capacity and the ability of HMGB2 to open these specific promoters in the culture resistant to reprogramming. In order to access the transcriptional changes induced by HMGB2 and NEUROG2 overexpression, we performed RNA-sequencing that indicated the involvement of HMGB2 in

repression of the myogenic alternative fate, possibly by the opening the repressor binding sites. Taken together, we identified the novel candidate HMGB2 in the prospect of direct neuronal reprogramming making the chromatin states in the glial cells permissive for lineage conversion and thereby enabling acquisition of the neuronal phenotype in the cultures with limited reprogramming capacity.

1 Introduction

In most mammalian species, the main part of neurogenesis occurs during embryonic development. During this time, the majority of the neurons are generated, which will, later on, contribute to the formation of a complex brain structure. In the adult mammalian brain, neurogenesis persists only in a few restricted areas, while the remainder of the brain exhibits highly gliogenic characteristics (Ninkovic and Götz, 2013). This means, only the astroglia-like cells in the neurogenic niches continuously progress towards neurogenic lineage, whereas astroglial progenitors in all the other regions normally do not generate neurons (Berninger et al., 2007), but almost exclusively the cells of the oligodendrocyte lineage (Ninkovic and Götz, 2013). This might be an issue especially after the traumatic brain injury and in neurodegenerative diseases, which lead to a critical loss of neurons that in mammals cannot be replaced by the organism itself. In order to reactivate and reinstruct neurogenesis after the neuronal loss in otherwise non-neurogenic areas, a detailed understanding of the underlying molecular mechanisms of neurogenesis is required. Therefore, a considerable research is focused on mechanisms allowing neural stem cells to successfully generate neurons during embryonic neurogenesis as well as in the restricted regions in the adult brain where neurogenesis continues to occur and implementation of these mechanisms to elicit neurogenesis. Indeed, in the past 15 years, a great progress has been made in uncovering key transcription factors and other modulators of neurogenesis, which led to a novel avenue for repair, namely eliciting neurogenesis from glial cells outside of the neurogenic niches. The field of direct neuronal reprogramming from non-neuronal cells in vitro and recently as well in vivo has shown promising results in replacing damaged or lost neurons. Recent advances in understanding of molecular basics of the reprogramming highlighted that the changes in chromatin structure may be an important player to achieve the neuronal cell fate acquisition. A group of chromatin architectural proteins, High Mobility Group B proteins are due to their high and specific expression in the adult neurogenic niches, very interesting candidates to examine the chromatin-associated changes and their importance in our ability to reprogram the cell fates.

The following sections will lead through the general concept of neurogenesis by describing the basic features of embryonic and adult neurogenic areas. Furthermore,

the recent advances of direct neuronal reprogramming in vitro and in vivo will be discussed. Finally, the members of the High Mobility Group (HMG) protein family will be presented, summarizing the knowledge about their functional motifs, mechanisms of action, their expression and potential roles in the mammalian brain.

1.1 Mammalian brain development

1.1.1 Regionalization of the neural tube and patterning of the forebrain

The mammalian central nervous system (CNS) develops from the neural plate, a structure of ectodermal origin. During primary neurulation, neural plate folds into a neural tube, filled with cerebrospinal fluid (CSF). In the mouse, neurulation begins at the embryonic day E8.5 and ends at day E10.5, when the neural tube closure is completed. Following anterior-posterior regionalization, the front part of the neural tube gives rise to the brain, whereas the middle and caudal portions form the spinal cord. However, even before the closure of the posterior neural tube is completely finished, the formation of three primary vesicles occurs anteriorly: forebrain (prosencephalon), midbrain (mesencephalon), and hindbrain (rhombencephalon) (Fig. 1). In the next step, five secondary brain vesicles are formed. The forebrain subdivides into the anterior telencephalon (future cortex and basal ganglia) and more posterior diencephalon (future thalamus, hypothalamus, and retina). The hindbrain further separates into an anterior metencephalon (future pons and cerebellum) and posterior myelencephalon (future medulla) (Fig. 1) (Gilbert, 2014; Sanes et al., 2012).

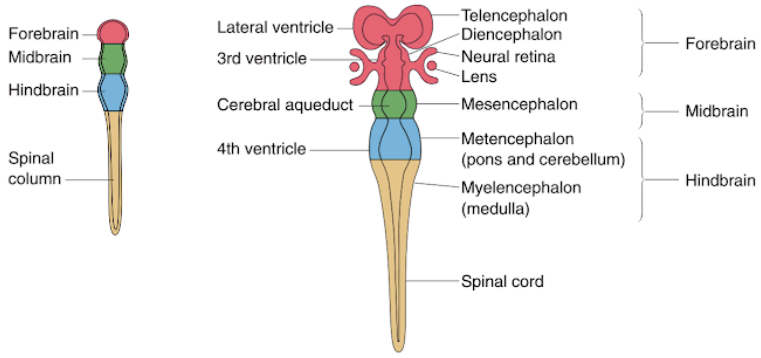

Figure 1: Formation of primary and secondary brain vesicles from the neural tube.

Anterior part of the neural tube divides primarily into three brain vesicles: the forebrain (prosencephalon), midbrain (mesencephalon) and hindbrain (rhombencephalon). The next step of subdivisions generates two secondary brain ventricles from the forebrain: telencephalon and diencephalon, as well as two from the hindbrain: metencephalon and the myelencephalon. At the end of anterior-posterior regionalisation, the caudal part of the neural tube gives rise to the spinal cord.
Adapted by permission from Elsevier: Elsevier Books, (Sanes et al., 2012), 4318200138020, (2012)
https://www.sciencedirect.com/science/book/9780080923208

Within the telencephalon, the patterning continues along the dorsal-ventral axis generating two main regions: dorsal telencephalon (pallium) and ventral telencephalon (subpallium). Dorsal telencephalon gives rise to the cerebral cortex, hippocampus, cortical hem, and choroid plexus. The ventral telencephalon is subdivided to the lateral ganglionic eminence (LGE), medial ganglionic eminence (MGE) and caudal ganglionic eminence (CGE) (Fig. 2). While the telencephalon is specified by the induction of the transcription factor FOXG1 at about E8.5, its subdivisions into specific domains are controlled by extrinsic signaling gradients, named morphogens such as sonic hedgehog (SHH), fibroblast growth factors (FGF), Wingless-Int proteins (WNT) and bone morphogenic proteins (BMP). They define the expression and activity of specific transcription factors in each domain (Hébert and Fishell, 2008; Nat et al., 2013; Tole and Hébert, 2013) (Fig. 2). The expression of BMP and WNT proteins is involved in the specification of dorsal fate by inducing transcription factors like EMX1/2 and PAX6. SHH promotes the formation of all

ventral telencephalic subdivisions by positively regulating the expression of Nkx2.1, Dlx-genes, and Ascl1 (Hébert and Fishell, 2008; Nat et al., 2013).

1.1.2 Neuronal specification during early development

Extrinsic signaling gradients are not only involved in patterning of distinct regions of developing brain, but they also initiate transcriptional cascades that instruct neural stem cells and their progenitors to generate specific neuronal and glial subtypes (Masserdotti et al., 2016). The dorsal telencephalon generates primarily glutamatergic neurons, while the ventral telencephalon produces mainly GABAergic neurons (Hébert and Fishell, 2008; Tole and Hébert, 2013). Glutamatergic neuronal fate in the dorsal telencephalon is driven by the expression of downstream targets of NEUROG1 and NEUROG2 such as NeuroD and the T-box brain genes Tbr2 (also know as Eomes) and Tbr1 (Fode et al., 2000; Guillemot, 2007; Mattar et al., 2004). Glutamatergic neurons originate from the regions of high Wnt expression, where neural stem cells positive for PAX6 and EMX1/2 up-regulate the proneural basic helix-loop-helix (bHLH) transcription factors NEUROG1 and NEUROG2 (Ohtaka-Maruyama and Okado, 2015). GABAergic neurons are specified by Ascl1 and Dlx genes in the ventral telencephalon (Casarosa et al., 1999; Petryniak et al., 2007) from where they subsequently migrate dorsally into the developing cortex (Hébert and Fishell, 2008; Nat et al., 2013) (Fig. 2).

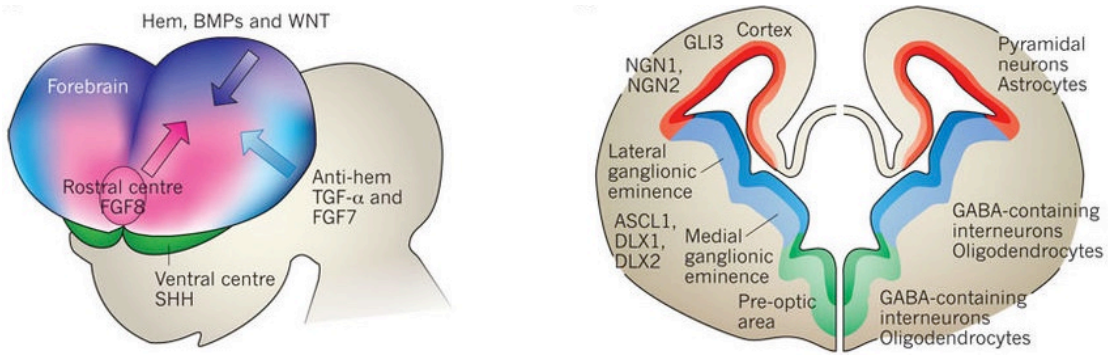

Figure 2: Morphogens are involved in the generation of unique domains that give rise to specific neuronal and glial subtypes.

The forebrain patterning (left picture) is organized by signaling gradients: sonic hedgehog (SHH) presented in green, fibroblast growth factors (FGF) in pink and light

blue, Wingless-Int proteins (WNT) and bone morphogenic proteins (BMP), both shown in purple. They divide telencephalon to the dorsal region labeled with red and ventral region labeled in blue and green on the right picture. The dorsal region includes the cortex, a source of pyramidal glutamatergic neurons and astrocytes. The ventral region is subdivided into the lateral, medial and caudal ganglionic eminences and the pre-optic area, which give rise to GABAergic interneurons and oligodendrocytes. Transcription factors that are associated with the corresponding area are indicated.
Adapted by permission from Macmillan Publishers Ltd: Nature, (Rowitch and Kriegstein, 2010), 4310920713940, (2010)
https://www.nature.com/articles/nature09611

1.1.3 Neurogenesis in the cortex

Most of our understanding of neurogenesis in the telencephalon is derived from studies in the cerebral cortex, however, the basic principles of cortical neurogenesis are mostly transferable also to the other brain regions (Kriegstein and Alvarez-Buylla, 2009). In the mouse telencephalon, neurogenesis occurs about E9-10 and continues until about E18, having its peak at E14. Neurogenesis starts at the stage of the neuroepithelium, composed of a single layer of rapidly dividing neuroepithelial cells (NC) lining the cerebral ventricles. These neuroepithelial cells begin to acquire neural stem cell features and transform into so-called apical radial glial cells (aRG) (Taverna et al., 2014) (Fig. 3), expressing markers such as astrocyte-specific glutamate transporter (GLAST), brain lipid-binding protein (BLBP) and intermediate filament proteins including nestin and vimentin. Radial glia are located at the apical surface of the ventricular zone (VZ) having a contact to the ventricle via apical process and to the outer pial surface via basal process (Fig. 3). During the thickening of the cortex throughout neurogenesis, the basal process is extended in order to maintain contact with both the ventricle and the pial surface (Fig. 3) (Kriegstein and Alvarez-Buylla, 2009; Paridaen and Huttner, 2014). At early neurogenic stages at about E11, the apical radial glia mainly undergo symmetric cell divisions in order to expand their pool (Götz and Huttner, 2005). After that, they start dividing asymmetrically to self-renew and generate a population of transit-amplifying progenitors (basal or intermediate progenitors) or neurons (Kriegstein and Alvarez-Buylla, 2009; Noctor et al., 2007). The basal process contacting the pial surface serves as a scaffold to guide neuronal migration to their final destination layer (Fig. 3). Newly generated basal progenitors

do not contact the ventricle or pial surface but have multipolar nature (Kriegstein and Alvarez-Buylla, 2009). In addition to apically located radial glia, another type of radial glial cells has been identified, termed as subapical progenitors due to their dividing properties at subapical positions (Pilz et al., 2013). Moreover, some more cells having radial glia features were observed, positioned more basally outside the ventricular zone and having apically and/or basally directed processes. They are named basal radial glial cells or outer radial glial cells and are mostly present in species with gyrencephalic brains, while lissencephalic species animals like mice show only low numbers of basal radial glia in the developing dorsal telencephalon (Borrell and Götz, 2014; Paridaen and Huttner, 2014). A high number of newly generated basal progenitors leads to the formation of the subventricular zone (SVZ) in the cortex (Fig. 3). In contrary to apical radial glial cells, which mostly undergo asymmetric divisions at the peak of neurogenesis, basal progenitors divide symmetrically to produce two neurons or self-renew to generate two additional intermediate progenitors (Kriegstein and Alvarez-Buylla, 2009; Noctor et al., 2007) (Fig. 3). These progenitors are important for cortical expansion in some mammals during evolution (Paridaen and Huttner, 2014).

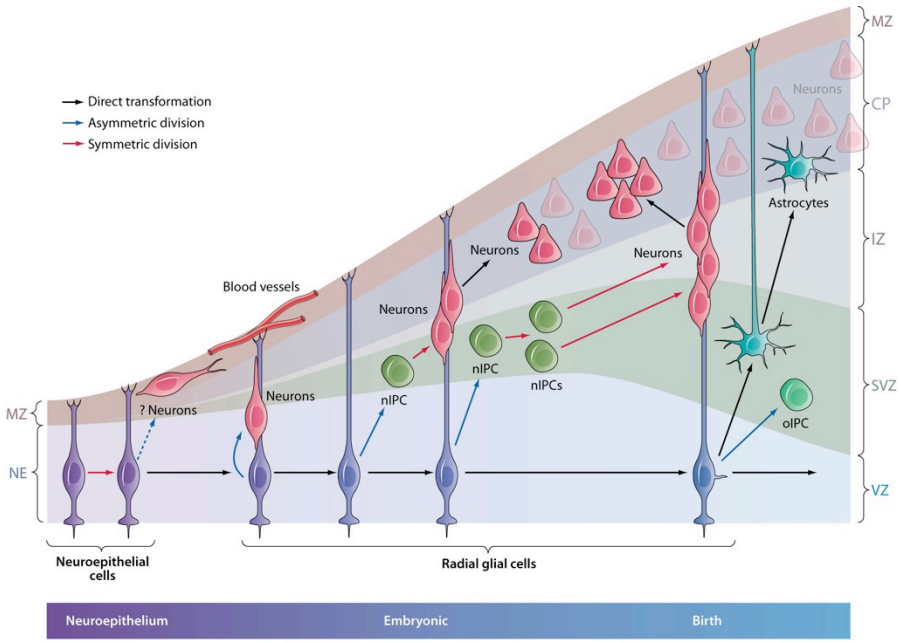

Figure 3: Neurogenesis during cortical development.

At early stages, neuroepithelial cells divide to generate radial glia. As the brain development proceeds, they convert into radial glial cells that divide both

symmetrically to self-renew and asymmetrically to generate basal progenitors (nIPCs) and neurons. Neurons move along basal processes of radial glia out to the developing cortical plate. At later stages of embryogenesis, neurogenic radial glia become gliogenic to produce astrocytes and oligodendrocytes (oIPC). Colored arrows present symmetric, asymmetric or direct transformation. Abbreviations: NE, neuroepithelium; CP, cortical plate; IZ, intermediate zone; MZ, marginal zone; nIPC, neurogenic intermediate progenitor cell; oIPC, oligodendrocytic intermediate progenitor cell; RG, radial glia; SVZ, subventricular zone; VZ, ventricular zone.
Adapted by permission from Annual Reviews: Annual Review of Neuroscience, (Kriegstein and Alvarez-Buylla, 2009), 4318211074016, (2009)
https://doi.org/10.1146/annurev.neuro.051508.135600

1.1.4 Cortical layer formation

Progenitors residing the dorsolateral ventricular and subventricular zone generate the projection neurons from embryonic day E11.5 to E17.5 in a precisely controlled temporal order. Projection neurons are glutamatergic neurons, having pyramidal morphology and spreading their projections between different regions of the cortex and regions of the brain (Molyneaux et al., 2007). Newly generated neurons in the cortex radially migrate through the intermediate zone (IZ) and form six-layered cortical plate (CP) in an inside-out manner, meaning that early-born neurons colonize deeper cortical layers VI and V, and late-born neurons migrate past them to form more superficial layers IV and II/III (Greig et al., 2013) (Fig. 4). Correspondingly, early-born neurons are situated close to the ventricle, while the late-born neurons are close to the pial surface. The earliest-born neurons appear around E11.5 and form the preplate close to the intermediate zone. Later-born neurons migrate into the preplate, dividing it into the marginal zone and subplate, and establishing the multilayered cortical plate in-between (Greig et al., 2013; Molyneaux et al., 2007). At E12.5, layer VI corticothalamic neurons are generated (Fig. 4), expressing transcription factors FOXP2 and TBR1. Next, at E13.5, layer V CTIP2 positive sub-cortical neurons are produced, followed by layer IV excitatory spiny neurons at E15.5 (Fig. 4) expressing SATB2 (Arlotta et al., 2005; Greig et al., 2013; Lodato and Arlotta, 2015; Molyneaux et al., 2007). Some layer II/III callosal projection neurons that are CUX1+ are being produced already at E12.5, with a peak of their production around E15.5 (Molyneaux et al., 2007). Layer I is composed of neurons termed Cajal-Retzius cells (Fig. 4), which are generated in early stages of development, but have a

different origin from three different regions outside the cortex (Greig et al., 2013). In addition to cortical projection neurons, cortex is also colonized by GABAergic projection neurons and interneurons derived from GE. They are produced between E11 and E18 and migrate tangentially to their final locations within the cortex. Majority of them originate from MGE and CGE in the ventral telencephalon, while the LGE contributes interneurons to the striatum and olfactory bulb (Molyneaux et al., 2007; Taverna et al., 2014). Once the projection neurons in the embryonic cortex migrate to the correct layer, they undergo terminal neuronal differentiation, dendrite and axon formation, synaptogenesis, and the establishment of neuronal connectivity (Taverna et al., 2014) that is mostly completed by postnatal day P21. Neurogenesis is followed by gliogenesis, myelination, angiogenesis, and formation of the blood-brain barrier (Taverna et al., 2014).

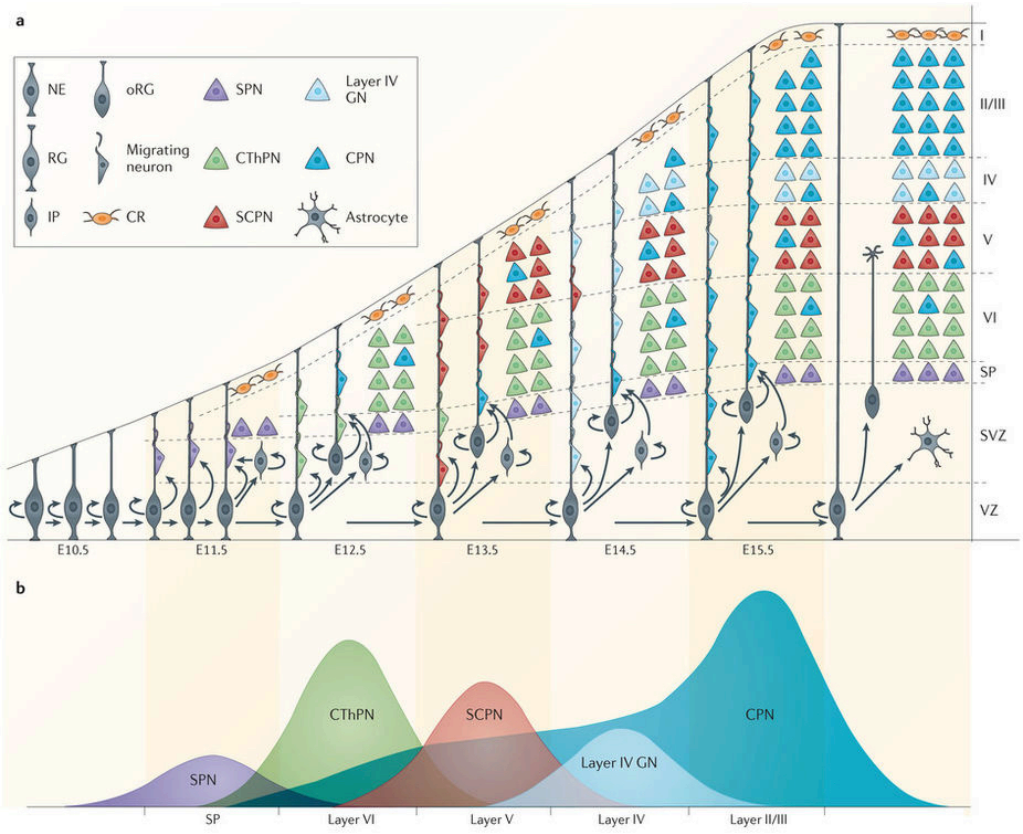

Figure 4: Layer specific neuronal formation in the dorsal telencephalon.

(a) Sequential generation of different neuronal subtypes and formation of a 6-layered cortical plate over the time course of neurogenesis. (b) Specific subtypes of projection neurons are born in sequential waves of neurogenesis. The peak of subplate neurons (SPN) generation occurs at E11.5, corticothalamic layer VI neurons

(CThPN) at E12.5, subcortical layer V neurons (SCPN) at E13.5 and granular layer IV neurons (GN) at E14.5. Most of callosal layer II/III neurons are born between E14.5 and E16.5. Peak sizes represent approximate amount of neurons generated on each embryonic day. Abbreviations: NE, neuroepithelial cell; oRG, outer radial glia; SPN, subplate neuron; GN, granular neuron; RG, radial glial cells; CThPN, corticothalamic projection neuron; CPN, callosal projection neuron; IP, intermediate progenitor, CR, Cajal-Retzius cell; SCPN, subcortical projection neuron; VZ, ventricular zone; SVZ, subventricular zone; SP, subplate.
Adapted by permission from Macmillan Publishers Ltd: Nature Reviews Neuroscience, (Greig et al., 2013), 4311050235529, (2013)
http://www.nature.com/articles/nrn3586

1.1.5 Generation of astrocytes and oligodendrocytes

Following neurogenesis, from E18 until early postnatal stages, astrocytes, oligodendrocytes, and ependymal cells are generated (Kriegstein and Alvarez-Buylla, 2009; Paridaen and Huttner, 2014; Rowitch and Kriegstein, 2010). Astrocytes are mainly generated from radial glia that lose their ventricular contact and migrate toward the cortical plate (Kriegstein and Alvarez-Buylla, 2009) (Fig. 3). Oligodendrocytes originate from different telencephalic regions and are during development born at early embryonic stages as well as later stages. There are three known waves of oligodendrocyte production (Fig. 5). First cortical oligodendrocytes are generated in the MGE, migrate towards the cortex and arrive there at the beginning of day E16 (Fig. 5). In the second wave, oligodendrocytes are produced more dorsally in the LGE and CGE and migrate to dorsal cortex (Fig. 5). Finally, in the third wave starting after E18, cortical oligodendrocytes are locally born from cortical progenitors in the dorsal cortex (Fig. 5). Interestingly, in the adult cortex, only late-born oligodendrocytes remain, while most of the early born oligodendrocytes disappear. Oligodendrocytes are also generated postnatally, however, the exact origin of progenitors generating these oligodendrocytes is still unknown. Some evidence indicate that at least a subpopulation of these cells, including new NG2+ progenitors, is derived from the adult neurogenic niche subventricular zone (Kriegstein and Alvarez-Buylla, 2009).

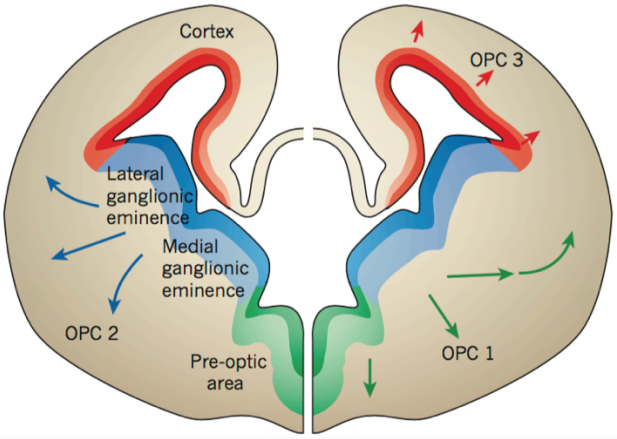

Figure 5: Three sequential waves of oligodendrocyte generation in the mammalian telencephalon.

The first wave of OPC (green arrows) arises from MGE, the second wave of OPC (blue arrows) emerges from precursors in the MGE and CGE, and the third wave of OPC (red arrows) is generated in the cortex.
Adapted by permission from Macmillan Publishers Ltd: Nature, (Rowitch and Kriegstein, 2010), 4310120093154, (2010)
https://www.nature.com/articles/nature09611

Embryonic radial glial cells do not only give rise to neurons and glia during brain development but are also the source of neural stem cells in the adult brain (Merkle et al., 2004). Adult neural stem cells maintain some cellular and molecular hallmarks of their embryonic counterparts, like epithelial apico-basal organization, contact with the blood vessels, apical processes with specialized apical junctions and a primary cilium at the ventricle (Kriegstein and Alvarez-Buylla, 2009) and the expression of many radial glial and astroglial genes including GFAP and GLAST (Falk et al., 2017). However, they differ in their proliferation rate and their genome-wide gene expression patterns (Götz et al., 2016). Labelling with BrdU and retroviral lineage tracing revealed that the majority of the adult neural stem cells were generated from embryonic cells that divided between E13.5 and E15.5. They remain relatively quiescent until postnatal life when they are reactivated to produce olfactory bulb neurons in the process known as adult neurogenesis (Fuentealba et al., 2015).

1.2 Adult neurogenesis

1.2.1 Neurogenic niches in the adult mouse brain

Adult neurogenesis, defined as a process of generating functional neurons from adult neural stem cells (NSC) (Ming and Song, 2011), includes many processes recapitulated from embryonic development such as neuronal differentiation, migration, maturation, and cell death (Alvarez-Buylla et al., 2008). Adult neurogenesis occurs throughout life in two restricted regions of adult the mammalian brain (Ming and Song, 2011). These two neurogenic niches where endogenous neural stem cells reside are the subventricular zone (SVZ) of the lateral ventricle and the subgranular zone (SGZ) in the dentate gyrus (DG) of the hippocampus (Bond et al., 2015; Ming and Song, 2011) (Fig. 6,7a). Adult neural stem cells in the subventricular zone (also named type B cells) are located beyond the ependymal cell layer, but contact the cerebrospinal fluid (CSF) in the ventricle with a primary cilium that projects from the apical surface (Fig. 6). In addition, they extend long basal process ending on blood vessels (Mirzadeh et al., 2008; Tong et al., 2014) (Fig. 6). Type B NSCs give rise to transient amplifying progenitor cells (TAPs or type C cells), which divide a few times before generating migratory neuroblasts (type A cells). Neuroblasts then form a complex network of chains, called rostral migratory stream (RMS) and migrate towards olfactory bulb. After arriving to the olfactory bulb, neuroblasts detach from chains, migrate radially, differentiate into multiple types of interneurons and finally integrate into the preexisting circuits (Alvarez-Buylla et al., 2008; Bond et al., 2015; Doetsch et al., 1999; Lim et al., 2006; Ming and Song, 2011; Taupin and Gage, 2002). The second neurogenic niche, subgranular zone in the dentate gyrus of the hippocampus, is a thin area between the granule cells layer and the hilus (Gonçalves et al., 2016). Radial glia-like NSCs (RGLs or type 1 cells) reside the SGZ and span their radial process through the granule cell layer to the upper molecular cell layer (Fig. 6). They give rise to intermediate progenitor cells (IPCs), which exhibit limited rounds of proliferation before generating neuroblasts. Neuroblasts migrate tangentially along the SGZ and develop into immature neurons. Finally, these neurons migrate radially into the granule cell layer to differentiate into dentate granule neurons (Bond et al., 2015). In other parts of adult brain

neurogenesis is generally believed to be very limited under normal physiological conditions but could be induced after injuries (Ming and Song, 2011). Some studies reported the signs of neurogenesis also in the hypothalamus (Kokoeva et al., 2005; Rojczyk-Gołębiewska et al., 2014), however, it is mostly restricted to early postnatal stages (Goodman and Hajihosseini, 2015; Robins et al., 2013).

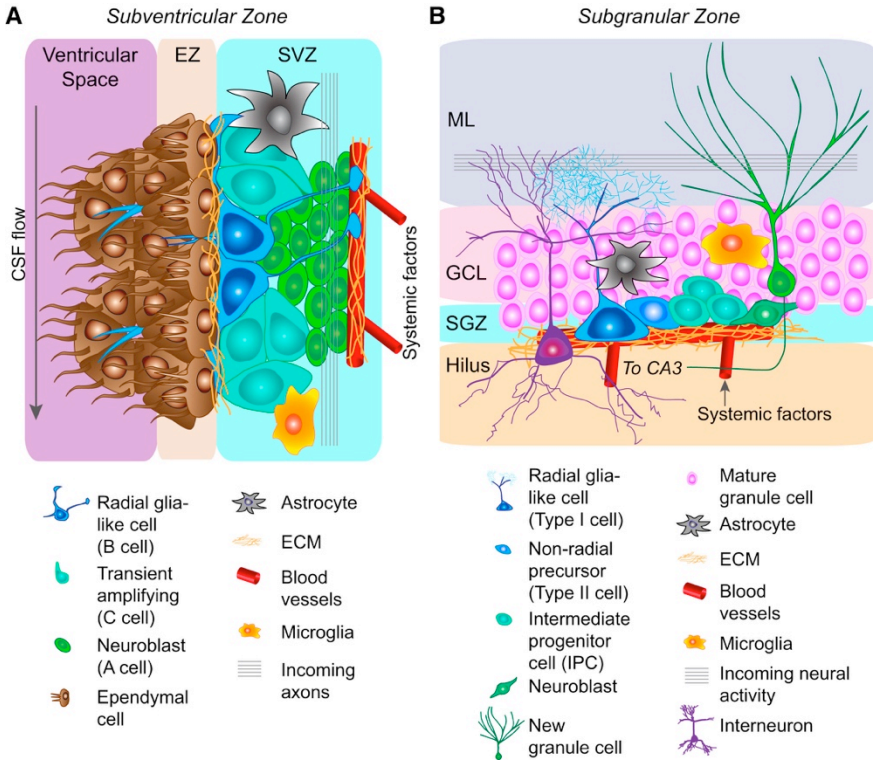

Figure 6: Neurogenic niches in the adult mammalian brain.

(a) A schematic representation of the neural stem cell niche in the subventricular zone (SVZ). Ependymal cells line the lateral ventricle and separate radial glia-like neural stem cells (type B cells) from the ventricular lumen. They are in the contact with blood vessels and extend a single cilium through the ependymal layer to contact the CSF. Once adult neural stem cells get activated, they give rise transient amplifying type C cells and migratory neuroblasts (type A cells). (b) Graphical illustration depicting the composition of the SGZ niche. Radial glia-like NSCs (type 1 cells) have cell bodies that reside in the SGZ and the process that extend into the molecular layer of the DG. Type 1 cells give rise to type 2 cells that differentiate into neuroblasts that become immature neurons and then mature into dentate granule cells, which finally migrate into the granule cell layer of the dentate gyrus. In addition to the described cell types, astrocytes, microglia, endothelial cells, mature neurons and components of the extracellular matrix contribute to the cellular architecture of both neurogenic niches. Abbreviations: CSF, cerebrospinal fluid; ECM, extracellular

matrix; EZ, ependymal zone; GCL, granule cell layer; ML, molecular layer; SGZ, subgranular zone; SVZ, subventricular zone.
Adapted by permission from Elsevier: Cell Stem Cell, (Bond et al., 2015), 4311840816388, (2015)
http://www.cell.com/cell-stem-cell/fulltext/S1934-5909(15)00410-5

1.2.2 Adult neurogenesis in the adult mouse and human brain

Two neurogenic niches SVZ and SGZ appear to be well conserved amongst the mammals, including humans (Bergmann et al., 2015). While the neural stem cells in the SVZ generate neurons for the olfactory bulb, the human SVZ supplies the neighboring striatum with new interneurons (Ernst et al., 2014) (Fig. 7). Olfactory bulb neurogenesis in mammals plays an important role in odor discrimination (Lazarini and Lledo, 2011), whereas the functional significance of striatal neurogenesis and the integration of the new neurons into existing neuronal circuits in humans remains to be explored (Ernst et al., 2014). New neurons continue to be generated also in the mammalian SGZ (Fig. 7a), linked to learning and memory, pattern separation (Gonçalves et al., 2016) and possibly to some neuropsychiatric disorders (Hsieh, 2012). In humans, some studies reported a substantial turnover of dentate granule cells (Spalding et al., 2013), while the other studies found much less putative new neurons (Dennis et al., 2016; Eriksson et al., 1998; Knoth et al., 2010) (Fig. 7b). Very recently, two contradictory studies were published, despite using very similar immunohistochemical approaches to detect newly generated neurons (Boldrini et al., 2018; Sorrells et al., 2018). The study from Alvarez-Buylla lab showed the rapid decrease of the young neurons production in the primate hippocampus within the first years of life. They propose that neurogenesis in the dentate gyrus does not continue in adult humans or is extremely rare, raising the questions about the differences in human and rodent hippocampal plasticity (Sorrells et al., 2018). On the other hand, Boldrini and colleagues found the persistent adult hippocampal neurogenesis into the eighth decade of life (Boldrini et al., 2018). This long-standing debate, whether and to what extent adult human neurogenesis occurs, will continue. Therefore, further studies are clearly needed, including new and more reliable methods to track neurogenesis in human adults.

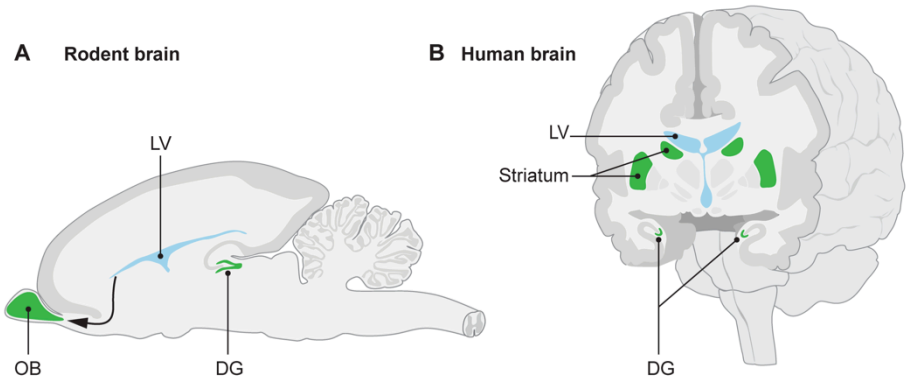

Figure 7: Comparison of the adult neurogenesis in the adult rodent and human brain.

(a) In rodents, new neurons (labeled in green) are generated in the subventricular zone lining the lateral ventricle, from where they migrate to the olfactory bulb. The second source of new neurons in the rodent brain is the subgranular zone in the dentate gyrus. (b) In humans, neurons are generated in the subventricular zone but integrate into the adjacent striatum. Some of the studies also reported the continuous generation of new neurons in the dentate gyrus of the human brain. Abbreviations: OB, olfactory bulb; LV, lateral ventricle; DG, dentate gyrus.
Adapted by permission from PLOS: PLOS Biology, (Ernst and Frisén, 2015), Open Access article distributed under the terms of the Creative Commons Attribution License, (2015)
http://journals.plos.org/plosbiology/article?id=10.1371/journal.pbio.1002045

1.3 Direct neuronal reprogramming

The adult mammalian brain lacks the capacity to replace the loss of neurons upon the traumatic brain injury or neurodegeneration. Therefore, functional replacement of depleted neurons appears to be one of the major challenges for regenerative therapies. Stem-cell-based therapeutic approaches primary focus on differentiation of either embryonic stem cells or induced pluripotent stem cells to induced neural stem cells or neural progenitors that could be used as a source for cell transplantation (Dametti et al., 2016) (Fig. 8). An alternative way to create the cells to be used for the transplantation is direct reprogramming of the patient's skin fibroblasts into induced neurons in vitro (Fig. 8). Direct neuronal reprogramming allows the conversion of a differentiated cell into neuronal cell type without passing through a pluripotent stage. Direct neuronal reprogramming is not only the valuable source of patient-derived neurons for the transplantations but also crucial application in the field of human disease modeling and drug discovery. Importantly, induced neurons maintain the age and epigenetic signatures of the donor, which is critical due to the fact that many neurodegenerative diseases are age-related (Arenas et al., 2015; Drouin-Ouellet et al., 2017; Huh et al., 2016; Mertens et al., 2015).

Recently, in vivo direct neuronal reprogramming, which makes the use of endogenous CNS cells in the adult brain to generate induced neurons in situ, emerged as a new approach to circumvent cell transplantation (Arenas et al., 2015; Chen et al., 2015) (Fig. 8). Astrocytes, one of the most abundant and widely distributed cell type in the adult brain (Doetsch et al., 1999), become in response to traumatic brain injury or neurodegeneration reactive, a subpopulation of them starts dividing (Bardehle et al., 2013; Buffo et al., 2008; Sirko et al., 2013, 2015) and they contribute to the scar formation (Ghasemi-Kasman et al., 2015; Mattugini et al., 2018). Reactive gliosis and glial scars are initially protective in order to limit further damages but later on present both physical and biochemical barriers for the axonal regeneration (Burda and Sofroniew, 2014; Silver et al., 2014; Sofroniew, 2009). A novel approach to convert resident astrocytes to the induced neurons has a potential to reduce the scar formation and provides a new source of neurons at the injury site. Thus, direct lineage reprogramming of non-neuronal cell types resident within the

central nervous system to generate new neurons is a promising strategy to repair damaged brain.

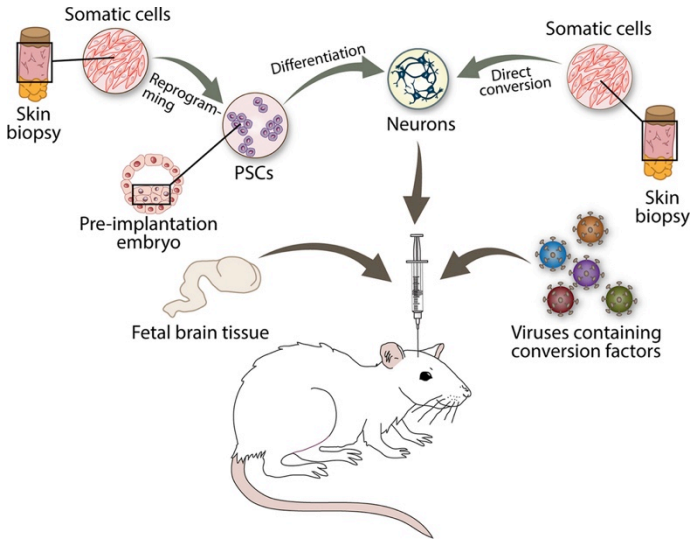

Figure 8: Therapeutic approaches to replace the loss of neurons after the traumatic brain injury or neurodegeneration.

Schematic representation depicting the possible strategies for the brain repair, which include the transplantation of fetal brain tissue, neurons generated from induced pluripotent stem cells originating from blastocyst or reprogrammed from fibroblasts. An alternative approach the transplantation of induced neurons directly reprogrammed from patient's skin fibroblasts. Direct reprogramming could also be performed directly in vivo in the adult brain by applying the viruses encoding for neurogenic transcription factors to generate desired neuronal subtypes from non-neuronal cell types. Abbreviation: PSCs, pluripotent stem cells.
Adapted by permission from John Wiley and Sons: Journal of Internal Medicine, (Grealish et al., 2016), 4312050467516, (2016)
https://onlinelibrary.wiley.com/doi/full/10.1111/joim.12475

1.3.1 Direct reprogramming of different non-neuronal cell types into induced neurons in vitro

The first successful experiment to reprogram non-neuronal cells types isolated from the brain into induced neurons was reported 15 years ago (Heins et al., 2002), opening new avenues towards a potential use of endogenous astroglia for brain repair (Heinrich et al., 2010). Our group has pioneered the conversion of astroglia into functional neurons in vitro by overexpression of neurogenic transcription factor

Pax6 (Heins et al., 2002). This encouraged many other researchers and resulted in a huge progress in direct neuronal reprogramming field in vitro. Many follow up studies showed that astroglia from the postnatal mouse cortex can be redirected towards neurogenesis following overexpression of transcription factors that have been discovered to play critical roles in the regulation of neurogenesis and neural stem cells, for example PAX6, ASCL1, NEUROG2, DLX2, BRN2, NEUROD1, NEUROD2, SOX2, SOX11, NEUROD4 and others (Amamoto and Arlotta, 2014; Berninger et al., 2007; Blum et al., 2011; Buffo et al., 2005; Gascón et al., 2016; Heinrich et al., 2010; Heins et al., 2002; Masserdotti et al., 2015; Ninkovic et al., 2013) (Fig. 9b). By forced expression of neurogenic transcription factors, also other non-neuronal cell types have been shown to adopt a neuronal fate, for example prenatal or postnatal mouse fibroblasts (Caiazzo et al., 2011; Colasante et al., 2015; Gascón et al., 2016; Tsunemoto et al., 2015; Vierbuchen et al., 2010) (Fig. 9d-f), human fibroblasts (Colasante et al., 2015; Drouin Ouellet et al., 2017; Pang et al., 2011; Pfisterer et al., 2011; Tsunemoto et al., 2015) (Fig. 9d-f), human pericytes (Karow et al., 2012) (Fig. 9a), and mouse hepatocytes (Marro et al., 2011) (Fig. 9c). In addition, many other transcription factors, microRNAs, and small molecules have been discovered and implemented into the reprogramming protocols, largely enhancing the efficiency and maturation state of induced neurons (Gascón et al., 2017). Two of the most used and studied neurogenic transcription factors in the direct reprogramming paradigm are ASCL1 and NEUROG2 (Masserdotti et al., 2016). During mammalian brain development, ASCL1 is required and sufficient to instruct stem and progenitor cells to acquire GABAergic interneuron identity within the ventral telencephalon, while NEUROG2 instructs dorsal progenitors towards glutamatergic neuronal fate (Casarosa et al., 1999; Fode et al., 2000). Resembling their role in the developing brain, the overexpression of ASCL1 in the cortical astroglial cells in vitro triggers the generation of GABAergic neurons and forced expression of NEUROG2 results in the acquisition of glutamatergic phenotype (Heinrich et al., 2010; Masserdotti et al., 2015). Interestingly, the efficiency of neuronal conversion differs between two factors, NEUROG2 can induce neurons with 70-80% efficiency, while ASCL1 generates only about 40% of induced neurons from transduced cells (Heinrich et al., 2010). Furthermore, the outcome of reprogramming largely depends on the starting populations, which may represent a permissive or repressive environment to fulfill their neurogenic potential (Masserdotti et al., 2016). ASCL1 overexpression in the

other cell types, such as midbrain astrocytes or MEFs, induces a mix of glutamatergic and GABAergic neurons or mainly glutamatergic neurons (Chanda et al., 2014; Liu et al., 2015; Masserdotti et al., 2016). NEUROG2 alone is on the other site, not able to induce any neurogenesis in the fibroblasts and only in combination with small molecules or other factors can generate somatic motor neurons (Liu et al., 2013, 2016; Smith et al., 2016; Son et al., 2011; Vierbuchen et al., 2010), contrary to glutamatergic program induced in astrocytes. This suggests that the efficiency of reprogramming largely depends on the cellular context and that the very same neurogenic transcription factor induces different downstream targets dependent on starter cells and the presence or absence of the other co-factors.

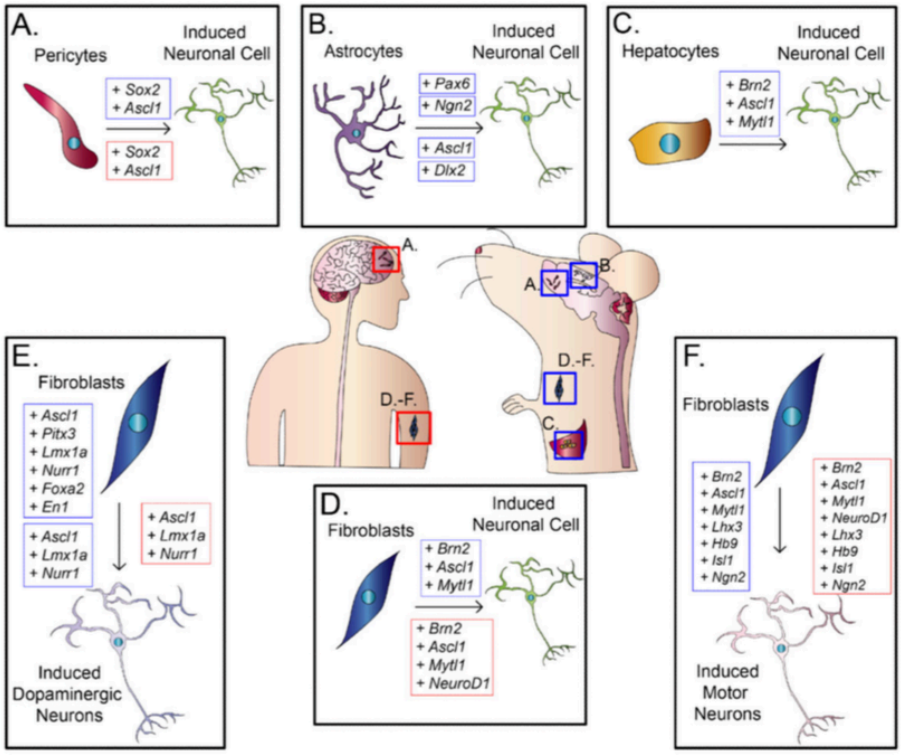

Figure 9: Direct reprogramming of different cell types into induced neurons in vitro using defined transcription factors.

In vitro cultured pericytes (a), astrocytes (b), hepatocytes (c), and fibroblasts (d-f) can be reprogrammed into induced neuronal cells by defined factors depicted in the boxes. Blue boxes represent reprogramming factors that efficiently convert different cell types isolated from mouse, while red boxes depict factors used for human pericytes or fibroblasts reprogramming.

Adapted by permission from PubMed Central: Science, (Amamoto and Arlotta, 2014), Free from known copyright as described by the Creative Commons Public Domain Mark 1.0., (2014)
https://www.ncbi.nlm.nih.gov/pmc/articles/PMC4122114/

1.3.2 The role of proliferation in direct neuronal reprogramming

In regard to starting cell populations, the cells selected for the reprogramming in vitro like astroglial cells or fibroblasts, are mostly proliferative. However, the proliferative state of the cell is not essential for the efficient conversion (Fishman et al., 2015), but has rather detrimental effects. Induction of the proliferation in fibroblasts by Myc overexpression, reduced the reprogramming efficiency (Fishman et al., 2015), while genetically or chemically induced cell-cycle exit improved neuronal reprogramming (Patel et al., 2012). Continuous live cell imaging of postnatal astrocytes or pericytes during the reprogramming process revealed that most of the cells directly convert into neurons without any cell division (Gascón et al., 2016; Heinrich et al., 2010; Karow et al., 2012). Furthermore, direct neuronal reprogramming can be efficiently induced also from postmitotic cells like hepatocytes, neurons, and astrocytes (Marro et al., 2011; Masserdotti et al., 2015; Rouaux and Arlotta, 2013).

1.3.3 Metabolic switch during reprogramming of astroglial cells to the induced neurons

Active proliferation of the starting populations might not be prerequisite for the efficient reprogramming, however the metabolic state of the starter cells that largely depends also on cell-cycle phase (Ito and Suda 2014), has been recently discovered as a major hurdle for the efficient conversion from one cell type to the other (Gascón et al., 2016) (Fig. 10). Astrocytes that in their in vivo environment play important functions in energy production, utilization, delivery and storage (Bélanger et al., 2011), rely mostly on the glycolysis to meet the high-energy needs. Glycolysis leads due to the fast degradation of glucose to low ATP production but efficiently generates precursors of amino acids, lipids, nucleotides, and co-factors like NADPH (Lunt and Vander Heiden, 2011). On the other side, neurons use an oxidative phosphorylation (OxPhos) as the main source of energy, where the glucose is more efficiently catabolized through the complete oxidation inside the mitochondria and results in a

high outcome of ATP. Direct conversion from astrocytes to induced neurons, therefore, requires a metabolic switch from glycolysis to oxidative phosphorylation (Magistretti and Allaman, 2015), that leads to an increased intracellular level of oxidative stress and reactive oxidative species (ROS) production (Quadrato et al., 2016). ROS include the superoxide anion (O2−), hydrogen peroxide (H2O2), and hydroxyl radicals (OH') that can act as signaling molecules but can also damage lipids, proteins, and DNA (Schieber and Chandel, 2014) and induce cell death (Ito and Suda 2014). The increase of oxidative stress and elevated levels of ROS turned out to be one of the major hurdles for the efficient cellular conversion (Gascón et al., 2016) (Fig. 10). The activation of OxPhos during metabolic switch exceeds the levels of antioxidant molecules produced by protective machinery, making the cells incapable to properly cope with the new metabolic profile (Gascón et al., 2017) (Fig. 10). However, the overexpression of BCL-2, other antioxidant treatments, and ferroptosis inhibitors help to overcome this critical barrier by restoring redox homeostasis and result in more than 90% reprogramming efficiency when converting reactive astrocytes into neurons in vitro (Gascón et al., 2016) (Fig. 10). To sum up, the metabolic state of the starter cell population plays an important role for the conversion into another cell type (Gascón et al., 2017). The reduction of the oxidative stress during the metabolic shift is not only necessary to allow survival of the neurons during reprogramming but also a prerequisite for the efficient cell fate transition (Gascón et al., 2017). However, the downstream molecular targets of redox metabolism remain to be identified (Quadrato et al., 2016) as well as understanding how these targets are regulated by the neurogenic transcription factors itself. This would help us understand the relationship between the induction of neurogenesis and metabolic changes, as well as the target level of expression needed for such an efficient conversion rate.

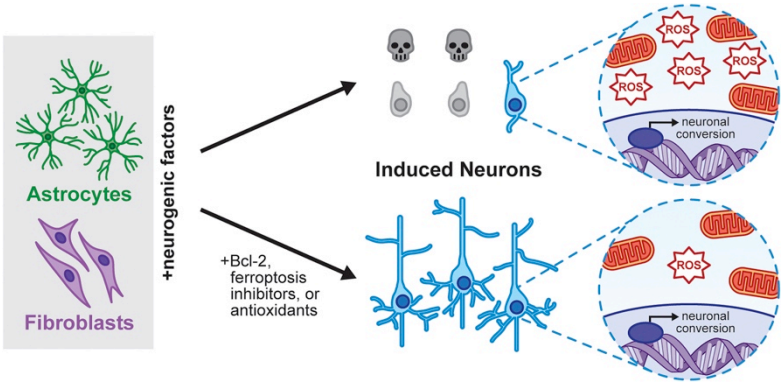

Figure 10: The reduction of the oxidative stress is crucial for the efficient neuronal reprogramming.

Graphical illustration showing that high levels of oxidative stress limit successful direct neuronal reprogramming with neurogenic transcription factors NEUROG2 and ASCL1 from astrocytes or fibroblasts. Inhibitors of ferroptosis, antioxidants or BCL-2 restore redox homeostasis remarkably improve the efficiency of reprogramming. Abbreviation: ROS, reactive oxygen species.
Adapted by permission from Elsevier: Cell Stem Cell, (Quadrato et al., 2016), 4312361301913, (2016)
http://www.cell.com/cell-stem-cell/fulltext/S1934-5909(16)00070-9

1.3.4 Chromatin dynamics, transcriptional initiation, and repression during direct neuronal reprogramming

While the transcription factors that can efficiently reprogram non-neuronal cells to induced neurons have been largely identified, the molecular understanding of the reprogramming process remains largely unknown. On a mechanistic level, it is unclear how the expression of a single transcription factor can accomplish such a biologically complex task of converting one differentiated cell type into another. To elicit the reprogramming event, transcription factors must be able to engage genes that are originally not expressed in the donor cells and are typically embedded in the closed chromatin. In addition, the original program has to be silenced in order to suppress the non-neuronal identity of the donor cells. A subset of transcription factors that have a special ability to access their targets in a non-permissive chromatin state are described as “pioneer factors” (Iwafuchi-Doi and Zaret, 2014; Wapinski et al., 2017) (Fig. 11). Their access at the closed chromatin sites typically enables the subsequent binding of other transcription factors (non-pioneers),

cofactors and chromatin modifying and remodelling enzymes, initiating the expression of genes required to adopt a new cell fate. However, how such transcription factors interact with their chromatin targets and the mechanisms underlying chromatin remodeling in response to pioneer factor binding is only starting to be explored (Pataskar et al., 2016).

One of the important factors in the neuronal reprogramming, ASCL1, has an ability to access its targets in closed chromatin regions, therefore being described as ‘‘on-target’’ pioneer factor (Chanda et al., 2014; Iwafuchi-Doi and Zaret, 2014; Wapinski et al., 2013) (Fig. 11). While its on-target pioneering nature was previously well examined, the recent studies focused on changes in chromatin dynamics during ASCL1 mediated reprogramming of mouse embryonic fibroblasts (MEFs) into induced neurons using ATAC-seq assay (Wapinski et al., 2017) (Fig. 11). ATAC-seq, Assay for Transposase Accessible Chromatin with high-throughput sequencing, is a rapid and sensitive technique based on transposase-mediated insertion of sequencing primers into open chromatin regions to study chromatin accessibility (Buenrostro et al., 2013, 2015). The data from this study revealed that reprogramming is a highly dynamic process, whereby pioneer factor ASCL1 opens closed chromatin at its target sites already within 12 hours after the induction. However, more than 80% of the accessibility changes occurred between days 2 and 5 of the reprogramming process (Fig. 11). Interestingly, later on, during morphological and functional maturation of induced neurons, only minor chromatin changes were observed (Wapinski et al., 2017). The chromatin reconfiguration reflects the previously described transcriptional response to ASCL1 (Treutlein et al., 2016), with the enrichment of sites related to neuronal and muscle GO terms, suggesting also the determination of the alternative myogenic cell fate. This could be explained by a common ASCL1 and MYOD1 (a myogenic bHLH transcription factor) E-box binding motif (Wapinski et al., 2017) that makes ASCL1 inefficient to restrict conversion only to the neuronal fate (Treutlein et al., 2016). Similar to ASCL1, NEUROG2 also acts as a pioneer transcription factor accessing closed chromatin (Smith et al., 2016). The majority of its binding events identified by ChiP-seq occurred at the sites that could not be detected with ATAC-seq (Smith et al., 2016). While NEUROG2 is sufficient to reprogram glial cells into neurons, somatic fibroblasts reprogramming requires the help of the forskolin (FK) and dorsomorphin

(DM) (Liu et al., 2013). Upon NEUROG2 overexpression only a modest increase in open chromatin was detected, however, FK+DM significantly enhanced the accessibility of the chromatin at NEUROG2 binding sites and other pro-neural genetic regulatory elements. Small molecules simultaneously activate signaling cascade that induces Sox4 expression and promotes SOX4 dependent chromatin remodeling. That enhances NEUROG2 chromatin occupancy and induces the expression of diverse pro-neural transcription factors, leading to a new neuronal cell fate (Smith et al., 2016). The influence of chromatin status on direct neuronal reprogramming was until now poorly understood (Gascón et al., 2017), but recent studies proposed rapid chromatin switch during reprogramming driven by pioneer transcription factors. Thus, these factors are capable of binding their closed target sites, rapidly reorganize the chromatin structure, and activate its target program that can subsequently facilitate a conversion of the cell fate to the target identity (Wapinski et al., 2017) (Fig. 11).

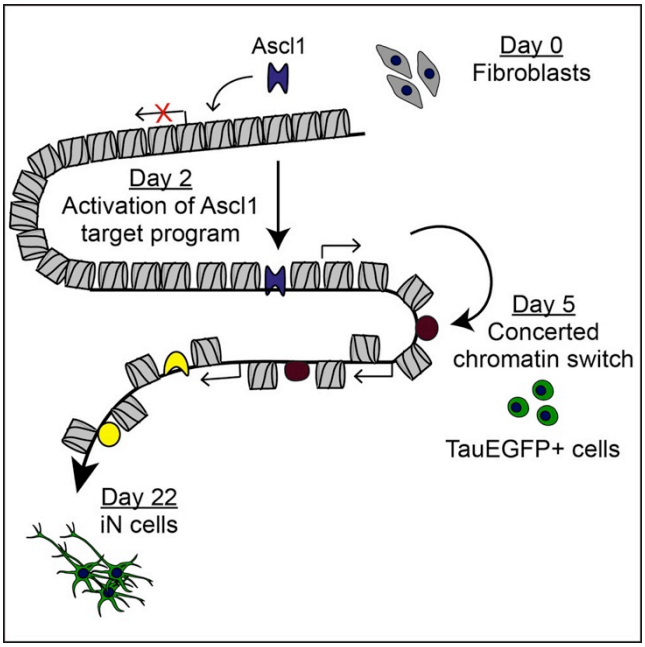

Figure 11: Pioneer activity of ASCL1 during neuronal reprogramming of fibroblasts.

Schematic illustration of ASCL1 binding to nucleosome rich, closed chromatin, inducing chromatin reorganization during day 2 and 5 that leads to the activation of neuronal program and generation of mature induced neurons by day 22.

Induced reprogramming requires not only the activation of target cell program but also silencing of original cellular identity and removal of the repressors that might not allow the acquisition of new non-donor cell program (Heinrich et al., 2015; Mall et al., 2017). In addition, with the induction of a new cellular fate, also some alternative fate programs might emerge as reported in the fibroblast reprogramming (Mall et al., 2017; Treutlein et al., 2016; Wapinski et al., 2017). One of the cell type-specific guardians relevant for reprogramming is the RE-1 transcription repressor complex (REST) that is expressed in non-neuronal cells where it represses neuronal genes (Jørgensen et al., 2009). By inhibiting the genes that should be activated to induce neuronal fate it acts as an obvious barrier for the efficient reprogramming. Indeed, down-regulation of REST in astrocytes results in dramatically increased NEUROG2 induced neuronal reprogramming reaching almost 90% efficiency (Masserdotti et al., 2015). Similarly, the repression of the RNA binding polypyrimidine tract binding (PTB) protein, is sufficient to induce reprogramming of mouse embryonic fibroblasts into functional neurons by microRNA associated reduction of REST activity and derepression of neuronal genes (Xue et al., 2013). However, efficient neuronal reprogramming from the human fibroblasts requires also the inactivation of the PTB paralog nPTB and its crosstalk with BRN2 and miR-9 (Xue et al., 2016). Recent studies identified also the importance of the repressors of the non-neuronal fates during reprogramming, like MYT1L. MYT1L binds preferentially to gene promoters and represses many fibroblasts genes, suggesting its role in establishment and maintenance of the neuronal identity during fibroblasts to neuron conversion (Mall et al., 2017). Taken together, cell fate re-specification critically depends on the removal of repressors of the targeted cell fate program as well as on the presence of repressors of the donor cell program (Gascón et al., 2017).

1.3.5 In vivo direct neuronal reprogramming

Encouraged by in vitro reprogramming studies, several groups attempted to reprogram the cells directly in the brain parenchyma (Brulet et al., 2017; Buffo et al.,

2005; Gascón et al., 2016; Grande et al., 2013; Guo et al., 2014; Heinrich et al., 2014; Kronenberg et al., 2010; Niu et al., 2013, 2015; Rivetti di Val Cervo et al., 2017; Torper et al., 2013, 2015). Despite very low efficiency, the initial in vivo direct neuronal reprogramming experiments delivered exciting proof of principle that reactive glial cells at the injury site can be converted into young neurons in vivo (Buffo et al., 2005). Follow up experiments mostly focused on the targeting of two cellular populations: the astrocytes and the oligodendrocyte progenitors/NG2 glia in two regions of the brain: in the cortex or striatum (Gascón et al., 2017) (Fig. 12). The cortex is a favorable model for the in vivo reprogramming trials due to well-established and studied model of stab wound injury. Striatum and generation of midbrain dopaminergic neurons or medium-sized spiny neurons are of great interest because of their loss in Parkinson's disease or Huntington's disease (Amamoto and Arlotta, 2014; Masserdotti et al., 2016). After the traumatic brain injury, astrocytes became reactive and enter the cell cycle, while NG2 glia increase their number and become a major population surrounding the lesion site (Wang and Zhang, 2018). Astrocytes become also more plastic as they can form self-renewing multipotent neurospheres when cultured in vitro (Buffo et al., 2008; Sirko et al., 2013, 2015). Therefore they are good targets for the retroviral delivery of neurogenic genes such as Neurog2, NeuroD1, and Sox2. Moreover, they can be involved in the scar formation and inflammatory processes (Robel et al., 2011; Sofroniew, 2009; Sofroniew and Vinters, 2010), therefore the direct conversion of these cells might be beneficial to reduce the glial scar and at the same time provide new source of neurons at the injury site (Grade and Götz, 2017). For direct in vivo neuronal reprogramming in the intact striatum, the viral vectors like AAVs or lentiviruses encoding for neurogenic transcription factors were used, allowing the targeting of non-proliferative astrocytes or slow-proliferating NG2 (Buffo et al., 2008; Torper et al., 2013, 2015) (Fig. 12). This suggests that in vivo direct neuronal reprogramming does not require proliferation, similarly to the in vitro direct conversion. However, regional differences and starting population strongly influence the efficiency of reprogramming (Gascón et al., 2017; Grade and Götz, 2017). Astrocytes in the striatum seem to be more susceptible for the reprogramming, as shown using SOX2 reprogramming factor that was not able to induce any neurogenesis in cortical astrocytes or NG2 glia (Heinrich et al., 2014) but was sufficient to convert striatal astrocytes to induced neurons with the addition of brain-derived neurotrophic factor (BDNF) induced by

valproic acid (VPA) (Niu et al., 2013, 2015) (Fig. 12). Furthermore, Guo and colleagues showed that reactive glial cells in the cortex after the injury or in Alzheimer's disease (AD) model mice can be converted into glutamatergic neurons, following expression of single neurogenic transcription factor NEUROD1, while NG2 cells were reprogrammed into glutamatergic and GABAergic neurons (Guo et al., 2014) (Fig. 12). Simultaneous overexpression of ASCL1, LMX1A, and NURR1 in the intact striatal NG2 glial cells converted them into mainly GABAergic and some glutamatergic neurons, but not dopaminergic neurons (Torper et al., 2015). However, dopaminergic neurons were obtained from striatal astrocytes when using the combination of ASCL1, LMX1A, and NEUROD1 together with miR218 (Rivetti di Val Cervo et al., 2017). Although the efficiency was relatively low, the induced dopaminergic neurons were functional and could even partially rescue some aspects of motor behavior in Parkinson's disease animal model (Rivetti di Val Cervo et al., 2017).

A real breakthrough in the field of direct in vivo neuronal reprogramming, was, however, achieved since we learned from in vitro cultures that the increase of oxidative stress at the intracellular level during the metabolic switch from glycolysis in the astrocytes to oxidative phosphorylation in the neurons, functions as a barrier for an efficient cellular conversion. This metabolic obstacle interferes also with efficient glia to neuron conversion in vivo but can be overcome by co-expression of single neurogenic factor, NEUROG2 with BCL-2 and addition of antioxidants, such as vitamins D and E. Excessive levels of reactive oxygen species lead to cell death by ferroptosis characterized by accumulation of lipid peroxidation products (Klempin et al., 2017). However, ROS inhibition increases the efficiency of reprogramming up to 90% when converting reactive glial cells into neurons upon the stab injury in the cerebral cortex. Importantly, these induced neurons survive until late time points and acquire a deep layer identity in the cortex (Gascón et al., 2016).

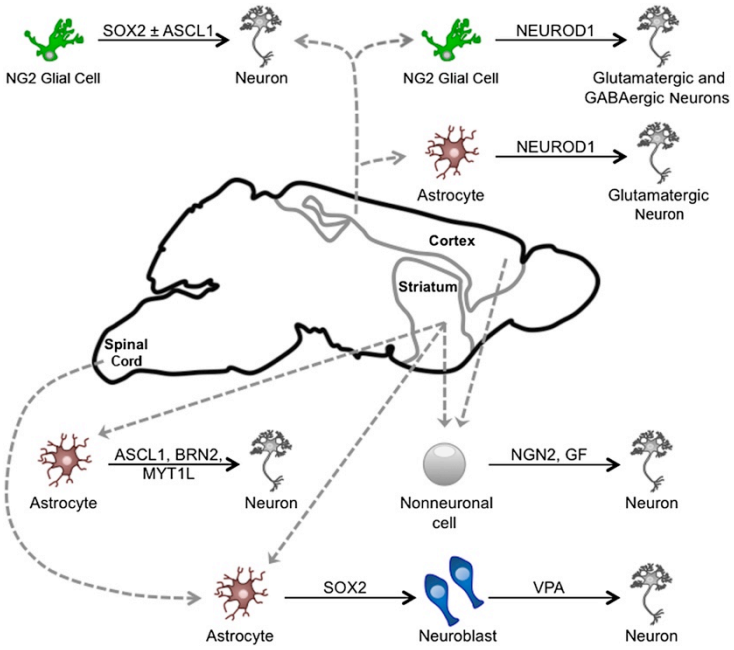

Figure 12: Direct in vivo reprogramming of cortical and striatal NG2 glia and astrocytes by the forced expression of neurogenic transcription factors.

Graphical scheme depicting some in vivo reprogramming studies that demonstrated the generation of induced neurons from non-neuronal cells directly in the adult brain in vivo. The induction of neurons from astrocytes was achieved by lentiviral expression of SOX2 and VPA treatment in the adult mouse striatum and spinal cord (Niu et al., 2013; Su et al., 2014). Cortical astrocytes and NG2 glia were reprogrammed after the brain injury into different neural subtypes by NEUROD1 overexpression (Guo et al., 2014). NG2 glia in the cortex can be also converted by a combination of SOX2 and ASCL1 (Heinrich et al., 2014). Astrocytes in the intact striatum were reprogrammed by ASCL1, BRN2, and MYT1L (Torper et al., 2013). The induction of neuronal fate from both, striatal NG2 glia and astrocytes can be achieved by NEUROG2 overexpression and exposure to growth factors (Grande et al., 2013). Abbreviations: GF, growth factor; VPA, valproic acid.
Adapted by permission from Elsevier: The American Journal of Pathology, (Smith and Zhang, 2015), 4312580340664, (2015)
http://ajp.amjpathol.org/article/S0002-9440(15)00258-8/fulltext

1.4 High Mobility Group (HMG) proteins are chromatin architectural proteins

The ability of neurogenic transcription factors or other regulatory factors to access their target sites to alter the gene expression is largely depended on the chromatin structure. Nuclear proteins involved in maintaining or altering the chromatin structure are named “chromatin architectural proteins”. These structural proteins lack enzymatic activity but are able to bind to nucleosomes without DNA sequence specificity and change the local and global architecture of chromatin. There are two major groups of architectural proteins: linker histone H1 protein family, which is the most abundant family of chromatin binding proteins, and High Mobility Group (HMG) protein family (Postnikov and Bustin, 2016). The linker histone H1 binds to the DNA entering and exiting the nucleosomal core particle and has an important role in establishing and maintaining higher-order chromatin structures (Izzo et al., 2008). In general, H1 proteins promote and stabilize the compacted chromatin structures, while HMG proteins promote chromatin decompaction and higher accessibility. Thus, HMG family of chromatin binding proteins, which are involved in changing chromatin configuration, can affect many DNA dependent processes such as transcription, replication, and the repair of damaged DNA (Postnikov and Bustin, 2016). Thereby they can control the expression of several genes by interacting with nucleosomes, transcription factors, nucleosome-remodeling machines and with histone H1 (Bianchi and Agresti, 2005).

1.4.1 HMG protein families and their functional motifs

The HMG superfamily is subdivided into three families, based on their DNA binding domains: HMGA (containing AT-hooks), HMGB (containing HMG-boxes) and HMGN (containing nucleosomal binding domains) (Bianchi and Agresti, 2005; Bustin, 2001; Catez and Hock, 2010) (Fig. 13a). Following their specific functional motif, there is a common C-terminal chromatin regulatory domain, important for protein-protein interactions (Furusawa and Cherukuri, 2010; Hock et al., 2007) (Fig. 13a). HMGA proteins contain AT-hooks, nine amino acid segments which bind AT-rich DNA stretches in the minor groove (Bianchi and Agresti, 2005; Postnikov and Bustin,

2016) (Fig. 13a). HMGB proteins contain two highly conserved HMG Boxes and a negatively charged C-terminal tail containing about ~40 highly acidic residues (Kalinowska-Herok and Widłak, 2008; Postnikov and Bustin, 2016; Štros, 2010; Štros et al., 2007) (Fig. 13a). HMG boxes are 80 amino acid long domains that bind to the minor groove of DNA with limited or no sequence specificity (Agresti and Bianchi, 2005). The HMGN protein family is characterized by nuclear localization signal (NLS), positively charged nucleosomal binding domain (NBD) and C-terminal regulatory domain (Postnikov and Bustin, 2016) (Fig. 13a). HMGN proteins bind inside nucleosomes, between the DNA spires and the histone octamer (Bianchi and Agresti, 2005).

1.4.2 HMG proteins: the mechanisms of action

High mobility group (HMG) proteins are architectural chromatin-associated proteins, that have been implicated in many DNA-dependent processes at the chromatin level (Štros, 2010). All members bind to chromatin in a dynamic and reversible way, either directly inside nucleosomes (in the case of HMGN), or to multiprotein complexes of transcription factors and cofactors (HMGA) or to both nucleosomes and transcription factors (HMGB) (Bianchi and Agresti, 2005). Although HMG proteins do not possess intrinsic transcriptional activity, they have the ability to modulate transcription of their target genes by altering the chromatin structure by a variety of different mechanisms (Ozturk et al., 2014) (Fig. 13b). First, they can bend the DNA and facilitate the binding of the other factors, which preferentially bind to the distorted DNA (Fig.13 b_i) (Hock et al., 2007). They use so-called ‘hit and run’ mechanism whereby the HMG box prebends DNA to favour the binding of transcription factors with DNA (Malarkey and Churchill, 2012). The induction of the changes in DNA conformation by HMG is one of the major mechanisms to enhance the access of transcription factors to their target sequences (Ueda and Yoshida, 2010). Second, by altering the chromatin structure they either prevent or enable an access of modulating factors on their targets on chromatin or nucleosomal DNA (Fig.13 b_ii) (Hock et al., 2007). Third, they can promote assembly of regulatory nucleoprotein complexes, such as enhanceosomes and transcription initiation complexes (Fig.13 b_iii) (Hock et al., 2007; Ozturk et al., 2014). Enhanceosomes are dynamic multiprotein 3D-structures of transcription factors (Agresti and Bianchi, 2003). Fourth, HMG proteins introduce

structural changes like DNA bending at sites to which they bind together with the specific regulatory factors (Fig.13 b_iv) (Hock et al., 2007). They can also participate in enhancing and stabilising the binding of interacting transcription factors to their target sequences. Their protein-protein interactions are usually transient or unstable and appear only when the complex is bound to chromatin (Ueda and Yoshida, 2010). Fifth, they facilitate nucleosome positioning and thereby accessibility of DNA to transcription factors (Fig.13 b_v) (Ozturk et al., 2014). Mostly they assist in loosening the histone–DNA contacts within the nucleosome through interactions with chromatin modifying enzymes, histone chaperones and ATP-dependent chromatin remodelling complexes (Malarkey and Churchill, 2012; Reeves, 2015). Sixth and the last mechanism is their competition with other nuclear proteins for chromatin binding sites, altering the local or global structure of the chromatin fibre (Hock et al., 2007) (Fig.13 b_vi). One example is displacement of histone H1 leading to chromatin decompaction (Ozturk et al., 2014), that has been demonstrated by different techniques including fluorescence recovery after photobleaching (FRAP), nuclear fractionation analysis and micrococcal nuclease digestion (MNase) assays (Catez and Hock, 2010; Kishi et al., 2012).

The interaction of HMG proteins with chromatin is not associated with specific sites but is rather highly dynamic. Each HMG molecule can scan the nucleosomes for potential binding sites and continuously move from one binding site to another in a “stop and go” fashion (Gerlitz et al., 2009; Hock et al., 2007). In the nucleus, they are one of the most mobile and dynamic nuclear proteins (Štros, 2010). HMG proteins can recognize the DNA structure rather than a specific nucleotide sequence and are able to bind to in a sequence-independent fashion via their respective functional domain (Reeves, 2001).

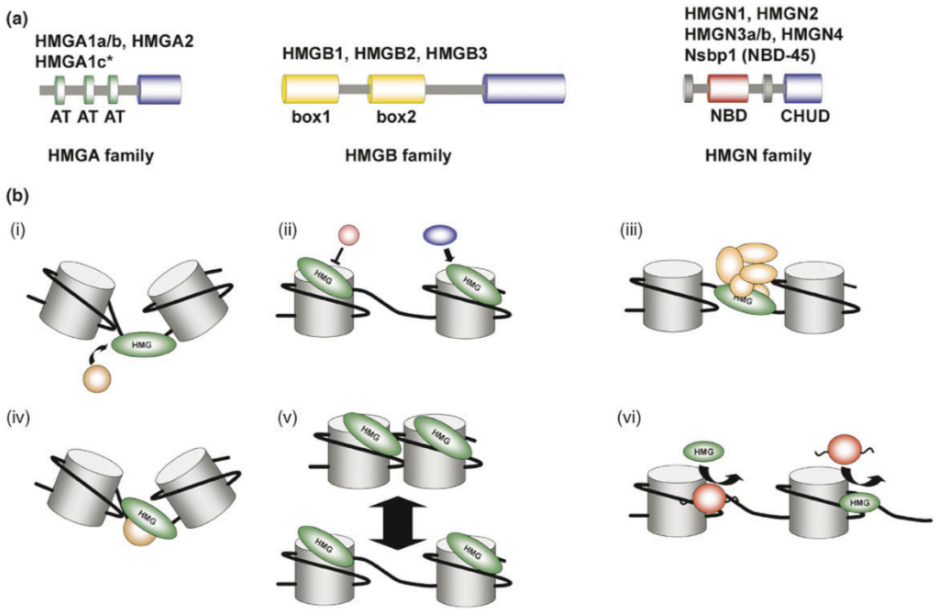

Figure 13: Architectural functions of HMG proteins.

(a) The main structural domains of three HMG families. Family members are listed above each schematic drawing. HMGAs contain three AT-hooks in green and an acidic C-terminal part in blue, except HMGA1c that contains only two AT-hooks. HMGB family members have two HMG boxes depicted in yellow and an extended acidic C-terminus labelled in blue. The HMGN proteins contain two nuclear localization signal domains (NLS, grey), a positively charged nucleosomal binding domain (NBD, red), and a negatively charged C-terminal region named chromatin unfolding domain (CHUD, blue). (b) HMG proteins (green) alter chromatin structure by a variety of mechanisms and facilitate the binding of additional factors (round shapes of various colours), described in detail in the text above. Abbreviations: NBD, nucleosomal binding domain; CHUD, chromatin unfolding domain.
Adapted by permission from Elsevier: Trends in Cell Biology, (Hock et al., 2007), 4312661474794, (2007)
http://www.cell.com/trends/cell-biology/fulltext/S0962-8924(06)00338-2

HMG proteins also play an important role in modulating DNA damage recognition and repair in the context of chromatin in eukaryotic cells. They modulate the efficiency of DNA repair by all of the major cellular pathways: nucleotide excision repair, base excision repair, double-strand break repair and mismatch repair (Reeves, 2015).

1.4.3 HMG protein family members, their expression and potential roles in the brain

1.4.3.1 HMGA proteins

HMGA family is comprised of four proteins HMGA1a, HMGA1b, HMGA1c and HMGA2 (Fig. 13a), encoded by two genes Hmga1 and Hmga2. The Hmga1 transcript is alternatively spliced and gives rise to three proteins (Ozturk et al., 2014). HMGA proteins are very small proteins with the molecular weight about 10 kDa (Agresti and Bianchi, 2003), highly expressed during embryonic development in various undifferentiated tissues. At later stages, their levels are strongly reduced (Bianchi and Agresti, 2005). HMGA1 can be still detected in some adult tissues, like testis, skeletal muscles, and thymus. Similarly, HMGA2 expression is rarely detectable in healthy adult tissues, except testis, skeletal muscle cells, and adipose tissues (Ozturk et al., 2014). HMGA2 protein is also highly expressed in fetal neural stem cells, where it increases their self-renewal, partly by repressing the expression of p16Ink4a and p19Arf. HMGA2 expression declines with age due to negative regulation via let-7b microRNA, resulting in reduced self-renewal and loss of the stem cell function. This study indicated an important role of HMGA2 in regulating age-related changes in neural stem cell numbers (Nishino et al., 2008). The contribution of HMGA proteins to the neurogenic and self-renewal potential of neural precursor cells (NPCs) in the early stages of neocortical development, was also shown by Kishi and colleagues (Kishi et al., 2012). They found that the chromatin of neocortical NPCs becomes globally more condensed and less dynamic during the time frame of cortical neurogenesis. This leads to the restriction of the differentiation potential of NPCs, which start to preferentially produce glial cells at postnatal stages. High expression of HMGA proteins in NPCs during the early developmental stage is therefore essential to keep chromatin open at the global scale and consequently for the neurogenic potential of NPCs. They proposed that HMGA proteins are able to antagonize the function of linker histone H1 and therefore loosen the chromatin fibre, which eventually leads to an open chromatin state (Kishi et al. 2012). The changes in the chromatin opening might be also important in the process of direct reprogramming (Yu et al., 2015b). Recently it was reported that HMGA2 overexpression in combination with SOX2 facilitates direct reprogramming of different human somatic cells (human adult fibroblasts, senescent somatic cells, and blood cells) into human induced neural stem cells (hiNSCs) and promotes their self-renewal (Yu et al., 2015b).

1.4.3.2 HMGN proteins

HMGN are small proteins with the molecular weight around 10 kDa (Reeves, 2015). Their nucleosome binding domain flanked by nuclear localization signals (NLS) allows them to recognize the structure of the 146-bp nucleosome core (Bustin, 1999) and specifically bind inside the nucleosomes (Bianchi and Agresti, 2005). The HMGN protein family is composed of 5 closely related proteins: HMGN1, HMGN2, HMGN3, HMGN4 and HMGN5 (Reeves, 2015) (Fig. 13a). The HMGN3 protein has two splice variants: HMGN3a and HMGN3b (Furusawa and Cherukuri, 2010) (Fig. 13a). HMGN genes are ubiquitously expressed in all embryonic tissues and are required for the proper development and differentiation (Furusawa and Cherukuri, 2010). During mouse embryogenesis, they are progressively down-regulated throughout the entire embryo, except in the stem cells and stem cell derived transiently amplifying progenitors (Furusawa and Cherukuri, 2010; Hock et al., 2007). HMGN1, HMGN2, HMGN3 are reported to be expressed in the brain during development but also in adult animals (Ito and Bustin, 2002; Nagao et al., 2014). Their expression was detected in neural progenitor cells (NPCs), glial progenitors, and astrocytes in the perinatal and adult brains and proposed their role in promoting astrocyte and oligodendrocyte differentiation during brain development (Deng et al., 2017; Ito and Bustin, 2002; Nagao et al., 2014). In the adult subventricular zone, HMGN1 is expressed in the NESTIN+ neural progenitor cells. The number of NESTIN-positive cells in the SVZ was decreased by 40% in the Hmgn1-/- animals, suggesting that loss of HMGN1 interferes with the differentiation or with the survival of NPCs (Deng et al., 2013).

1.4.3.3 HMGB proteins

The High Mobility Group Box (HMGB) proteins are most abundant HMG proteins with both nuclear and extracellular roles in key biological processes (Hock et al., 2007; Moleri et al., 2011). HMGB family consists of four members: HMGB1, HMGB2, HMGB3 and HMGB4 (Fig. 13a). They are highly homologous with more than 80% similarity and are also very conserved amongst all mammals (Müller et al., 2004). HMGB1-3 proteins have a molecular weight in the range of about 25 kDa (Agresti

and Bianchi, 2003). HMGB4 protein has a molecular mass of 21 kDa and like other 3 members contains two HMG-boxes but lacks the acidic tail (Štros, 2010).

HMGB proteins preferentially bind to the minor groove of DNA using the HMG box domains that fold up into the typical shape of three α-helices (Kalinowska-Herok and Widłak, 2008). Applying electrostatic and hydrophobic interactions these domains can unfold the minor groove and induce a bend towards the major groove (Malarkey and Churchill, 2012). Therefore, the main function of HMGB box domains is bending and unwinding of DNA. HMGB proteins with high affinity recognize non-linear DNA structures (Štros, 2010) and prefer binding on distorted and damaged DNA (Postnikov and Bustin, 2016; Ueda and Yoshida, 2010). HMGB also binds to nucleosomes with linker DNA, but not to the nucleosome core particle. This indicates that the primary binding target of HMGB proteins is the linker DNA adjacent to the entry or exit sites of the nucleosome, which is close to the histone H1 binding site. Therefore, they continuously compete with each other for these adjacent binding sites (Ueda and Yoshida, 2010). Despite their HMGB transient contact with the chromatin (Ueda and Yoshida, 2010), HMGB proteins are known to be involved in many important biological processes such as transcription, replication, recombination, DNA repair (Reeves, 2015; Štros, 2010), transposition, in the maintenance of genome integrity and V(D)J recombination (Bianchi and Agresti, 2005).

All four members of HMGB protein family are highly expressed during embryogenesis, but only HMGB1, which is the most abundant member of this family (Kalinowska-Herok and Widłak, 2008), continues to be broadly expressed in adult organs (Bianchi and Agresti, 2005). Hmgb1-/- animals die within 24 hours after birth due to an inability to use glycogen stored the liver (Moleri et al., 2011). HMGB2 protein has a limited presence in adult organs, being prominently expressed in thymus, testes and lymphoid organs (Bianchi and Agresti, 2005; Ronfani et al., 2001). The HMGB3 protein expression in the adult mouse appears to be restricted to hematopoietic stem cells within the bone marrow (Bianchi and Agresti, 2005; Moleri et al., 2011). Mouse mutants lacking the Hmgb2 or Hmgb3 genes have less severe defects, which correlate with their expression patterns. Male Hmgb2-/- mice show reduced fertility and defects in spermatogenesis (Ronfani et al., 2001), while Hmgb3

deficiency alters the generation and differentiation of primitive hematopoietic progenitor cells (Moleri et al., 2011). The HMGB4 protein expression is limited to testis, suggesting its important role in the spermatogenesis (Catena et al., 2009). The knockout experiments indicate that HMGB proteins are functionally not completely redundant and therefore suggest their distinct roles in different biological processes (Ueda and Yoshida, 2010).

1.4.3.3.1 HMGB1

During development, the expression of the HMGB1 protein is restricted to newly generated neurons in the cortical plate. In the adult mouse brain, its expression remains only in the areas of continuous neurogenesis. This suggests its high expression in less differentiated cells - neural stem cells, whereas differentiated cells such as mature neurons show only low or undetectable expression levels (Guazzi et al., 2003; Müller et al., 2004). Oppositely, more recent studies reported its expression in various adult brain regions such as cortex, hippocampus, and striatum, where they found its predominant localization in the nuclei of neurons and astrocytes. During aging, HMGB1 expression levels reduce specifically in neurons (Enokido et al., 2008).

Following traumatic brain injury, HMGB1 acts as an important pro-inflammatory cytokine mediating inflammation, neuronal apoptosis and tissue damage (Li et al., 2014) (Fig. 14). Despite its role in the nucleus, under inflammatory conditions, it translocates to the cytoplasm and is actively released into the extracellular space by innate immune cells, such as macrophages and dendritic cells (Fig. 14). HMGB1 is also passively released from damaged and necrotic neurons, which serves as an endogenous “danger signal” that alerts the immune system to the presence of injured cells (Fig. 14). This results in an increased infiltration of neutrophils, monocytes, cytokines, natural killer cells, and activates the microglia (Fig. 14). Outside the cell, HMGB1 binds to the transmembrane Toll-Like receptors (TLR) 2 and 4, and the Receptor for Advanced Glycation End products (RAGE). Activation of these receptors leads to the phosphorylation of several MAP kinases that activate the downstream transcription factor NF-κB and induce an immediate inflammatory

response. Moreover, this signalling cascade leads to further release of HMGB1 other pro-inflammatory cytokines, thereby propagating inflammation (Parker et al., 2017) (Fig. 14). Although HMGB1 contributes to the pathogenesis after the brain injury, some studies reported its beneficial effects during the recovery stage of brain injury. HMGB1 promotes neurovascular remodelling by recruiting endothelial progenitor cells and increasing their proliferation (Li et al., 2014).

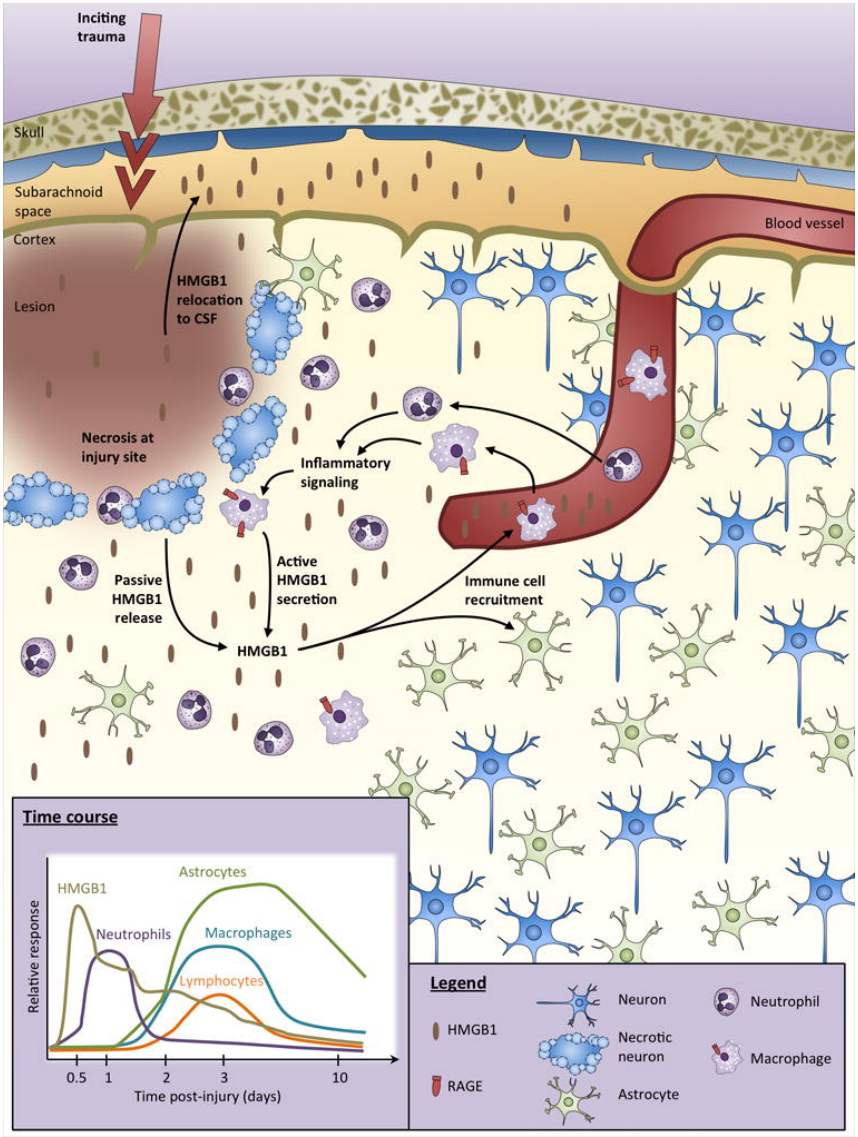

Figure 14: HMGB1 signaling after the traumatic brain injury.

Upon the brain injury, HMGB1 is secreted from the cells to the extracellular space, CSF and serum. Extracellular HMGB1 exhibits cytokine activity and acts as a damage-associated molecular pattern (DAMP) molecule that stimulates the release of proinflammatory factors and immune cell recruitment. This leads to an excessive immune response and inflammation following the injury.

https://doi.org/10.1080/02699052.2016.1217045

An increased expression of HMGB1 has been also found in the Alzheimer's diseased brain (Guazzi et al., 2003; Müller et al., 2004), where it plays a proneurogenic role by promoting neuronal differentiation of adult hippocampal neural progenitors via RAGE/NF-κB axis activation (Meneghini et al., 2013).

1.4.3.3.2 HMGB2

The HMGB2 protein is widely expressed during embryonic development and its expression pattern in the brain becomes evident already at E12.5. The strongest signal is detected in the ventricular zone, containing proliferating neuroepithelial cells. At E17, HMGB2 protein localizes in the ventricular and subventricular zone as well as in the differentiated cortex. At the postnatal stages, the expression remains only in the granular layer of the cerebellum and hippocampus (Ronfani et al., 2001). In the adult brain, the expression patterns still remain elusive. Single cell RNA-sequencing based transcriptome analysis revealed the enrichment of Hmgb2 (and Hmgb1) mRNA in the adult NSCs isolated from the hippocampus (Shin et al., 2015). Recently Kimura and colleagues investigated the expression and function of the HMGB2 protein in the dentate gyrus of the adult mouse brain and showed that HMGB2 is expressed in the subset of neural stem cells and progenitors cells but not in the granule neurons. On the contrary, HMGB1 expression was detected in the entire granule cell layer of the dentate gyrus. They observed the strong association of HMGB2 expression with the transition from the quiescent to the proliferative state of NSCs, supporting the hypothesis that HMGB2 participates in the activation of quiescent NSCs. These findings propose HMGB2 as a novel marker to identify NSCs primed for activation in the adult hippocampus and its involvement in the regulation of adult neurogenesis (Kimura et al., 2018).

In the second adult neurogenic niche, the SVZ, HMGB2 has been reported to potentially regulate NSCs proliferation (Abraham et al., 2013), however, the

expression in the specific populations residing neurogenic niche and precise function remained to be explored. Therefore we decided to perform the immunostaining against HMGB2 protein in the adult mouse brain and explore its colocalization within different cell types in the SVZ. To distinguish between the major cell populations in the SVZ, we used cellular and proliferation markers that showed distinct colocalization with HMGB2 in two cell populations of the SVZ: transit-amplifying progenitors (TAPs) and neuroblasts (Lepko, 2012). Furthermore, we have also prospectively isolated the neural stem cells and its progeny using fluorescence-activated cell sorting (FACS) (Beckervordersandforth et al., 2010; Fischer et al., 2011) and examined gene expression of the Hmgb members. We confirmed the high expression of Hmgb2 in the progeny of neural stem cells compared to the other populations. Interestingly, Hmgb1 showed very similar expression pattern with the highest expression in TAPs and neuroblasts (Lepko, 2012). Due to the similar expression of Hmgb2 and Hmgb1 in the subventricular zone and their possible redundancy, we also performed the immunostaining for the HMGB1 protein that showed its high abundance in the whole brain in contrast to the published data (Guazzi et al., 2003; Müller et al., 2004). The restricted expression of the HMGB2 protein in neurogenic niches prompted us to explore its potential functional role in the neurogenesis. Preliminary data from HMGB2 gain and loss of function experiments (Lepko, 2012) support the hypothesis that HMGB2 has a role in the proliferation of the neuronal progenitors and their progression toward neurogenic fate. Recent findings highlight the importance of HMGB2 in the regulation of neurogenesis in both neurogenic niches, therefore it is an interesting candidate to be explored in the context of forced neurogenesis during the direct reprogramming of the glial cells into induced neurons.

2 Aims of the thesis

Direct neuronal reprogramming opened a new venue in our understanding of the cellular plasticity, but more importantly, it is also a promising approach for potential treatments of brain injuries and neurological diseases. Despite very high efficiency of reprogramming in the cultured cells in vitro and recent advances to produce induced neuronal cells from somatic cells residing within the injured brain, the molecular understanding of the reprogramming process remains largely unknown. A number of important issues need to be explored, such as the influence of the starting population to be reprogrammed into induced neurons, essential pathways that must be induced or repressed and the role of the environment surrounding the conversion place in vivo. In my PhD thesis, I aimed at getting a better understanding of the molecular mechanisms underlying reprogramming process, which is the key for the potential future neuronal replacement therapies.

A general limitation to study molecular mechanisms of the direct neuronal conversion in vivo is the complexity of the injury microenvironment. Several signaling factors are released simultaneously in response to the injury, therefore it is very difficult to identify which of them have the beneficial effects on the permissiveness of astroglial cells to the forced neurogenesis and which would rather inhibit this process. To that end, a well-controlled cell culture models are essential to gain a better mechanistic understanding of direct reprogramming process and to identify potential barriers for in vivo lineage reprogramming. Most of the astroglia-to-neuron reprogramming studies rely on in vitro model resulting in very high conversion rate that can be achieved already by applying a single neurogenic transcription factor. Despite being an attractive model system to study the role of neurogenic transcription factors, such system alleviates reprogramming hurdles. Therefore, to challenge the established reprogramming paradigms I aimed to establish a new in vitro model that better recapitulates in vivo environment following the brain injury with a rather limited number of neurons induced by an individual neurogenic transcription factor.

Using this new in vitro model, my first aim of the thesis was to explore the intrinsic differences of two different starting populations used for neuronal reprogramming, one being very susceptible for the direct conversion and the other with limited

reprogramming capacity. I aimed to identify the molecular features and possible candidates that would be involved in maintaining the astrocytes in the glial lineage even after neurogenic factor overexpression.

With this approach, I identified the differential expression of chromatin architectural protein HMGB2 between two cultures with different reprogramming capacities. The next objective of the present study was, therefore, to exploit whether the manipulation of the HMGB2 levels in both astrocyte cultures has any effect on the reprogramming efficiency in vitro. Based on these findings, I next aimed at testing its potential to reprogram reactive glial cells directly at the injury site in vivo.

Having achieved improved astro-to-neuronal conversion efficiency upon induced expression of HMGB2 in the culture with limited reprogramming capacity, my next goal was to examine the chromatin-associated changes and their importance in cellular plasticity and fate decisions using the direct reprogramming as a model system. Supported with the establishment of novel genome-wide methods, I aimed at unravelling the molecular role of this protein in the chromatin compaction with an ultimate goal to identify the crucial chromatin regions that have to undergo chromatin rearrangement to enable efficient direct conversion from gliogenic to neurogenic fate.

With the combined effort of integrating several high-throughput approaches and reprogramming experiments using the novel in vitro system, I asked the question what are the transcriptional changes induced by neurogenic transcription factors and our novel candidate HMGB2 during the reprogramming process. To this aim, I explored the transcriptomes of two cultures transduced with NEUROG2 and HMGB2 and tried to discover, how are these changes dependent on the cellular context and investigated which of them are crucial to elicit the proper neuronal program from glial the cells.

This work is aiming to dissect the molecular network underlying the forced conversion of astroglial cells into neurons by studying their proteomes, chromatin organisation and transcriptomes. A better understanding of the molecular features of the reprogramming will not only provide new insights into the mechanisms

maintaining cell identity but also contribute to the breakdown of such cellular barriers in direct reprogramming in vivo.

3 Results

3.1 Different responsiveness of glial cultures to the neurogenic fate determinants

Direct reprogramming of primary postnatal cortical astroglial cells into functional neurons in vitro can be achieved by forced expression of neurogenic transcription factors that instruct neurogenesis during development (Berninger et al., 2007; Blum et al., 2011; Buffo et al., 2005; Heinrich et al., 2010; Heins et al., 2002; Masserdotti et al., 2015). So far, in vitro studies of direct lineage reprogramming described initial culturing conditions for astroglial cells using two common growth factors, epidermal growth factor (EGF) and basic fibroblasts growth factor (bFGF, also known as FGF2) in order to retain their proliferating capacity and expand the amount of the cells that can be used for the reprogramming. To convert these astroglial cells into induced neurons, neurogenic transcription factors were applied by the retroviral delivery and this resulted in general in a very high reprogramming capacity. Despite very good conversion rate of isolated postnatal astrocytes in vitro, the molecular understanding and the possible barriers appearing during the reprogramming process, remain largely unknown.

In order to investigate the molecular mechanisms involved in direct reprogramming of astroglial cells into neurons, we established a new in vitro model with adjusted growth factor composition. We decided to withdraw the EGF from the culturing medium, similarly to the in vivo conditions generated at the injury site. Upon the brain injury, the levels of EGF increase with the peak within the first 24 h and return to baseline levels by 3 days. On the contrary, the increase in FGF occurs already 4 h after the injury and persist for 14 days (Addington et al., 2015). Therefore, we cultured astroglial cells obtained from postnatal mouse cerebral cortex for 10 days in two different culturing conditions with two growth factors EGF+FGF or only one growth factor FGF. Next, the cells were re-plated and transduced with retroviral vectors expressing fluorescent protein only (GFP or dsRED) as a control, or single neurogenic transcription factors Neurog2, Brn2 or Sox11 together with dsRED or GFP reporter protein (Fig. 15a). After 24 h, the medium was replaced with the one

that did not contain any growth factors and the cells were kept in the reprogramming process for the following 7 days. After one week we assessed the reprogramming efficiency by morphology and doublecortin immunostaining (Fig. 15b). Doublecortin (DCX) is a microtubule-associated protein expressed by neuronal precursor cells and immature neurons and is used as a marker for neurogenesis. Only DCX+ cells that fulfilled the previously published criteria (Gascón et al., 2016), having ellipsoid soma with at least one thin process 3x longer than the soma, were quantified as reprogrammed neuronal cells.

In both culturing conditions EGF+FGF and FGF, we first quantified the proportion of induced neurons out of all GFP or dsRED+ transduced cells (Fig. 15c,d). Cells transduced with control retroviral vector (GFP+ or dsRED+) did not generate any DCX+ neurons. The small amount of DCX+ cells in the control condition (2.59±1.63% in EGF+FGF and 1.20±0.12% in FGF) represents transduced neuronal progenitors that were co-isolated together with the cortical astroglia. In general, only astroglial cells can be maintained as a monolayer in the primary culture, however, some escapers of neurogenic origin can still be found. Next, we assessed the proportion of neurons generated by different neurogenic transcription factor overexpression in both cultures. As expected, the astroglia cultured with two factors EGF+FGF could be converted into induced neurons with a very high efficiency rate. The percentage of reprogrammed neuronal cells out of all transduced cells was with Neurog2 85.71±3.41%, with Brn2 62.99±5.59%, and with Sox11 52.43±8.18% (Fig. 15c,d). However, we observed a considerable decrease in the reprogramming capacity of the cells cultured with FGF only. Cultures were analyzed at 3.41±2.05%, 10.42±3.96%, and 33.70±14.94% of induced neurons following transduction with Neurog2, Brn2, and Sox11, respectively (Fig. 15c,d). While the astroglia can be converted into functional neurons with high efficiency when cultured with both growth factors EGF and FGF, removing the EGF from the culture resulted in decreased number of generated induced neurons using the same neurogenic transcription factors.

We identified a new in vitro model to culture the cells that can be successfully reprogrammed (EGF+FGF culture) or the cells that became resistant to reprogramming (FGF culture). Comparing both cultures could help us to identify

unique molecular features required for the efficient direct reprogramming and the possible barriers maintaining the cells in the glial lineage even after the neurogenic transcription factor overexpression.

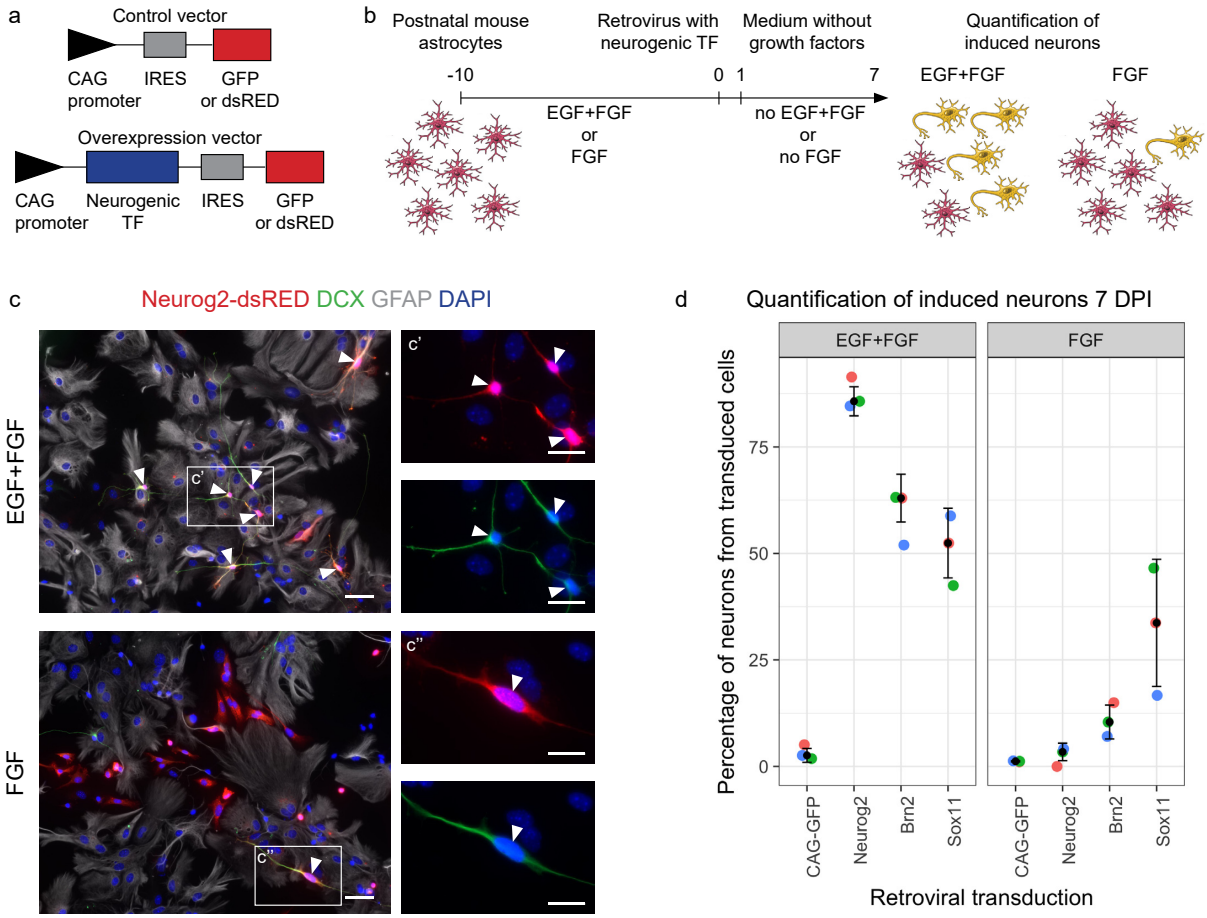

Figure 15: Growth factor composition defines the reprogramming capacity of glial cultures in vitro.

(a) Schematic structure of the control retroviral vector and retroviral vector to overexpress neurogenic transcription factors. (b) Graphic representation of the reprogramming protocol with two different growth factor conditions. (c) Micrographs showing astroglial culture transduced with Neurog2-dsRED, 7 days post-transduction. White arrowheads point to cells reprogrammed into induced neurons. Boxed areas correspond to the higher magnification images of induced neurons (c', c''). (d) Dot plot showing quantification of reprogramming efficiency in two cultures 7 DPI with different neurogenic transcription factors. Abbreviations: IRES, internal ribosomal entry site; TF, transcription factor; DPI, days post induction. Data are shown as median±IQR; each of the single dots represents independent biological replicate. Scale bars (c) 50 µm, (c', c'') 25 µm.

3.2 Comparison of the cellular and molecular features of astroglial cells grown in two culture conditions

In order to address the question what are the intrinsic differences of the cells cultured in two different growth factor conditions that are possibly responsible for their different reprogramming capacity, we performed the set of experiments to explore their identity as described in following chapters. The primary astroglial cultures are quite heterogeneous, containing different cells types that could respond differently to the forced neurogenic factors overexpression. Removal of EGF from the culturing medium could induce an expansion of the populations resistant to the reprogramming which would result in a decreased amount of induced neurons. To test this hypothesis, we immunostained the cultures for different proteins that label astrocytes and other populations that could be co-isolated from the postnatal mouse cortex. In addition, we decided to explore the differences in the global protein expression in both culturing conditions and to this aim performed proteome analysis using liquid chromatography (LC) with mass spectrometry (MS) in collaboration with Dr. Stephanie Hauck (Research Unit Proteome Science, Helmholtz Zentrum München).

3.2.1 Cellular markers expression of EGF+FGF and FGF cultures based on immunocytochemistry

To investigate how similar are the cultures based on their identity markers, we performed immunostaining for several proteins (GFAP, S100β, DCX, OLIG2, αSMA, Ki67, PH3) 24 hours upon transduction with the control retrovirus encoding for the GFP. Retroviruses can exclusively transduce dividing cells, meaning that only proliferating cells within the culture represent the targeting population for the reprogramming. Therefore, we investigated the cellular marker expression specifically in the population labeled by the control retrovirus. We observed that the majority of cells express astrocyte marker S100β in both EGF+FGF and FGF cultures, 92.84±3.81% and 91.19±4.14%, respectively (Fig. 16a,b). The proportion of GFAP+ cells was a bit lower, 57.03±2.17% in EGF+FGF and 63.07±2.13% in FGF culture (Fig. 16a,b). Importantly, we confirmed the minimal contamination with the neuronal progenitors labeled with DCX (Fig. 16a,b). We also tested for the OLIG2

expression and observed 79.70±3.28% positive cells in EGF+FGF treated cells and 80.35±2.25 in FGF culture (Fig. 16c,d). On the other hand, we observed only a tiny proportion of αSMA+ pericytes in both cultures (0.30±0.43% in EGF+FGF and 2.15±0.26% in FGF) (Fig. 16c,d). Based on the immunostaining experiments, we concluded that two cultures do not differ in their cellular composition and their marker expression. However, we observed an interesting feature during their expansion phase in the first 10 days of culturing. When starting with the same amount of the postnatal cortical tissue in both conditions, we constantly observed 2-3 times lower number of single cells in the FGF condition at day 10, when cells were counted and re-plated prior to viral transduction. This suggested the lower proliferation capacity in the FGF culture. Therefore, we assessed the proliferation in two different culture conditions using immunocytochemistry against Ki67 that labels all cycling cells and PH3 labeling mitotic cells. Indeed, we observed a significant decrease in the amount of proliferating cells in the culture grown with FGF alone compared to cultures grown with both EGF and FGF. In the EGF+FGF culture, there were around 18.79±1.64% Ki67+ cells, while in the FGF culture this number is reduced to 12.59±1.11% (Fig. 16d,e), both calculated from the GFP transduced cells. Similar reduction could be also observed using a PH3 marker (Fig. 16d,e). While we counted 9.07±0.86% of PH3+ cells in the EGF+FGF condition, in the FGF there was 6.03±0.60% PH3+ cells (Fig. 16d,e). In addition to different cell cycle properties, the increased cell death in the FGF culture could also account for the lower number of the cells after the expansion phase. To address the proportion of the cells that undergo apoptosis, we performed the TUNEL assay (Gavrieli et al., 1992) in both cultures. Apoptotic cells undergo an extensive DNA degradation during the last stage of apoptosis and the blunt ends of double-stranded DNA breaks can be enzymatically labeled and visualized by ApopTag technology (Millipore). We observed very few TUNEL+ cells in both conditions (Fig. 16j), 1.68% out of all DAPI+ nuclei in EGF+FGF culture and 2.49% in FGF cultured cells. Taken together, removal of the EGF from culturing medium does not change the proportion of different cell types within the culture, but it results in the decreased proliferation rate of the cultured cells. Therefore, we cannot confirm our hypothesis of an expansion of the populations resistant to the reprogramming in the FGF culture that would explain its lower conversion rate.

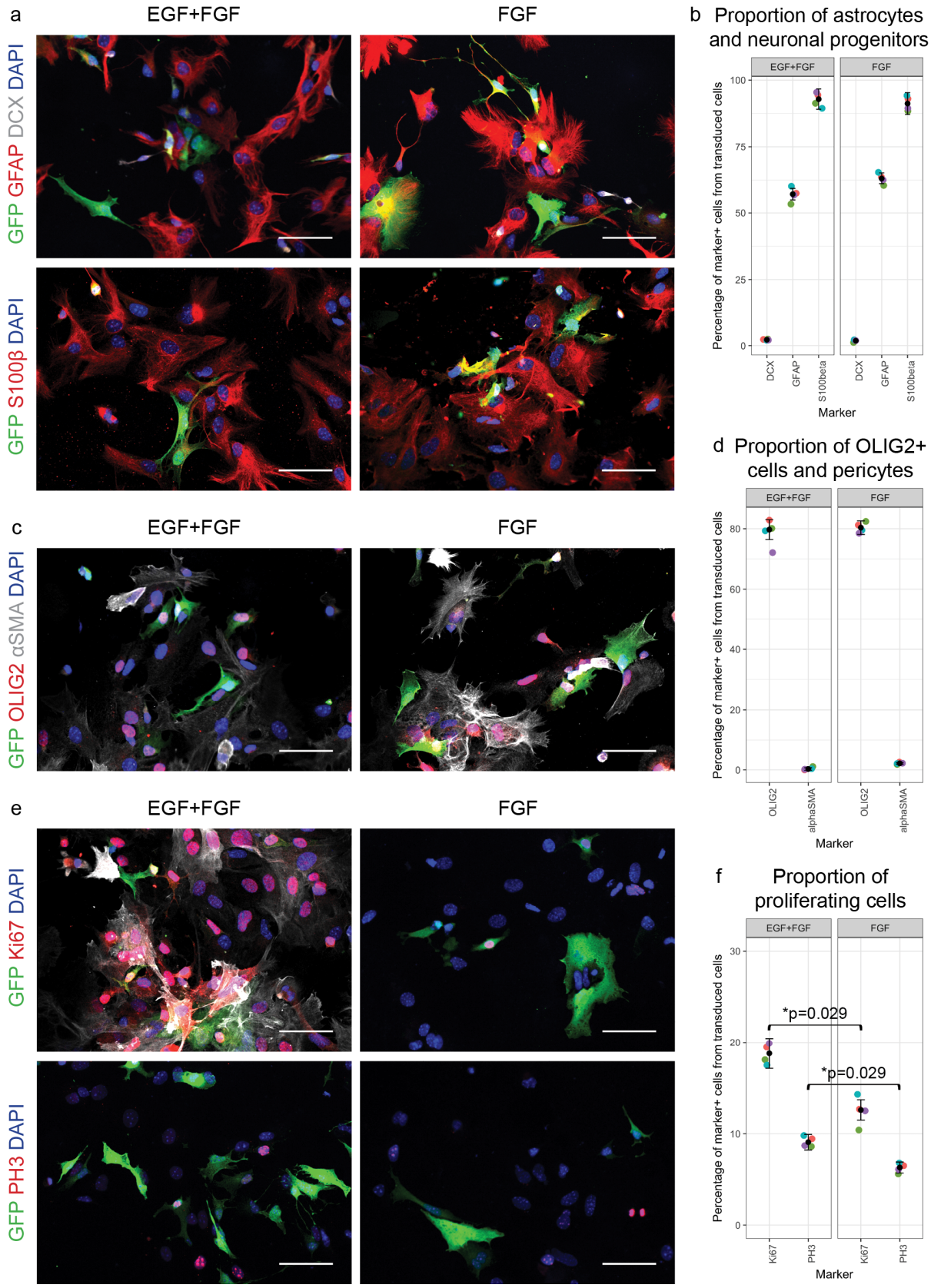

* continues on the next page

*

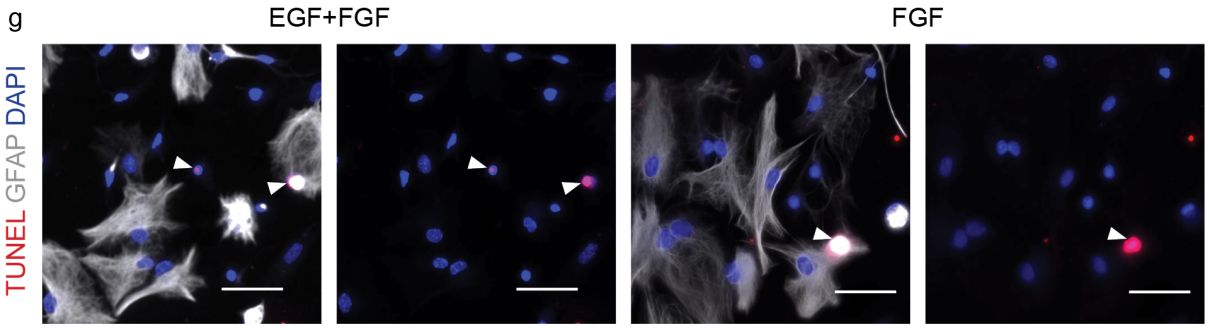

Figure 16: Immunocytochemistry reveals the similarity of the EGF+FGF and FGF cultures based on their marker expression and differences in their proliferation rate.

(a) Micrographs depicting immunostaining for S100β, GFAP and DCX in EGF+FGF and FGF cultures 24 h after transduction with the control virus. (b) Quantification of the S100β+ and GFAP+ astrocytes and DCX+ neuronal progenitor cells out of transduced cells. (c,d) Astroglial cultures in two conditions stained for OLIG2 and αSMA (c) and proportion of the positive cells out of control transduced cells fixed 1 DPI (d). (e) Micrographs showing the examples of KI67+ cells or PH3+ cells in both cultures. (f) Dot plot showing quantifications of both proliferation markers expressed as a percentage of GFP+ cells at the time point 24 h. (g) Micrographs depicting the TUNEL+ cells (white arrowheads) in EGF+FGF or FGF culture. Abbreviation: OPC, oligodendrocyte progenitor cell. Data are shown as median±IQR; each of the single dots represents independent biological replicate; significance was tested by non-parametric Mann-Whitney U test. Scale bars (a, c, e, g) 50 μm.

3.2.2 Proteome analysis of EGF+FGF and FGF cultures

With the previous analysis based on identity markers, we did not observe any heterogeneity between the cultures that could explain the different reprogramming capacity of the cells. However, we were able to test only for few proteins by immunostaining and might miss the differences that could explain their different responsiveness to the neurogenic transcription factor overexpression. Therefore, we decided to perform the proteome analysis of astrocytes prone and resistant to reprogramming to address the possible differences in global protein expression in both cultures. To test the differences in initial populations, we collected the cells for the proteome analysis after 10 days of culturing with EGF+FGF or FGF growth factors and prior to viral transduction. We submitted them to our collaborators at the

Research Unit Proteome Science (Helmholtz Zentrum München) for the label-free LC-MSMS based protein quantification (Fig. 17a). They detected about 1700 proteins from which 174 showed significantly changed levels (1.5-fold change, $p<0.05$). 81 proteins were significantly enriched in the EGF+FGF culture, 93 had higher levels in the FGF culture (1.5-fold change, $p<0.05$) while the vast majority was common for both cultures (Fig. 17a,b). Using the DAVID 6.8 Gene Ontologies tool (Huang et al., 2009a, 2009b), we performed the GO enrichment analysis of the proteins enriched in astroglia more and less prone to reprogramming (Fig. 17c,d). Focusing on the category cellular components, we found that the proteins enriched specifically in the FGF cultured cells were related to GO terms cytoskeleton or muscle tissue (Fig. 17c), suggesting some morphological differences in the FGF culture. The GO term analysis of 81 proteins, highly enriched in EGF+FGF astroglia revealed the mitochondrial respiration and chromatin remodeling as most regulated categories between two cellular populations (Fig. 17d-f), suggesting that both have an important role for the efficient reprogramming process.

We decided to focus more on the changes in the chromatin states that could maintain the astrocytes in the glial lineage even after neurogenic factor overexpression. Looking through the candidates related to category chromatin reassembly, we found the chromatin architectural protein High Mobility Group B2 (HMGB2) having 1.88-fold higher protein levels in the EGF+FGF culture (Fig. 17f). We confirmed its 2-fold enrichment in the EGF+FGF culture with the Western blot (Fig. 17g). Interestingly, we also observed the enrichment of the HMGB1 protein, which belongs to the same family (Fig. 17f). In the adult mouse brain, HMGB2 is specifically expressed in cells committed to neurogenic lineage (transit amplifying progenitors, neuroblasts) in both neurogenic niches, suggesting that it might contribute to the specification of neuronal cell identity (Lepko, 2012). On the other side, the immunostaining for the HMGB1 in the sections from the adult mouse brain revealed its high abundance in the most of the brain regions (data not shown). We, therefore, hypothesized that HMGB2 might be a good candidate to enable the better transition of the EGF+FGF astrocytes during reprogramming process and we speculated its possible involvement in setting up the permissive chromatin states for direct glia to neuron conversion.

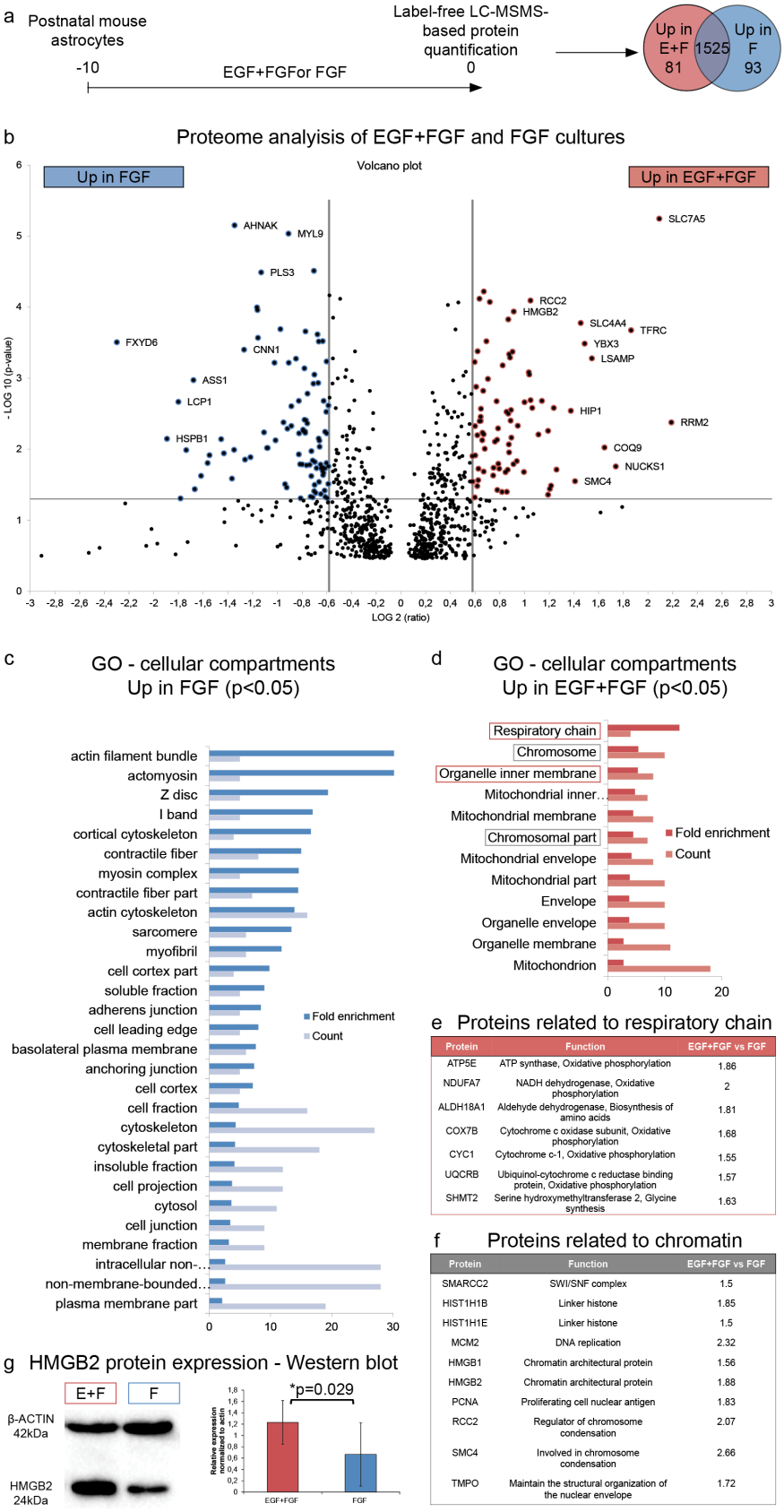

Protein	Function	EGF+FGF vs FGF
ATP5E	ATP synthase, Oxidative phosphorylation	1.86
NDUFA7	NADH dehydrogenase, Oxidative phosphorylation	2
ALDH18A1	Aldehyde dehydrogenase, Biosynthesis of amino acids	1.81
COX7B	Cytochrome c oxidase subunit, Oxidative phosphorylation	1.68
CYC1	Cytochrome c-1, Oxidative phosphorylation	1.55
UQCRB	Ubiquinol-cytochrome c reductase binding protein, Oxidative phosphorylation	1.57
SHMT2	Serine hydroxymethyltransferase 2, Glycine synthesis	1.63

Protein	Function	EGF+FGF vs FGF
SMARCC2	SWI/SNF complex	1.5
HIST1H1B	Linker histone	1.85
HIST1H1E	Linker histone	1.5
MCM2	DNA replication	2.32
HMGB1	Chromatin architectural protein	1.56
HMGB2	Chromatin architectural protein	1.88
PCNA	Proliferating cell nuclear antigen	1.83
RCC2	Regulator of chromosome condensation	2.07
SMC4	Involved in chromosome condensation	2.66
TMPO	Maintain the structural organization of the nuclear envelope	1.72

Figure 17: Different reprogramming capacity of two cultures in vitro is possibly influenced by metabolic states and chromatin accessibility landscapes.

(a) Schematic illustration of the protocol to collect astroglial cells for the proteome analysis 10 days after culturing with EGF+FGF or FGF growth factors. (b) Volcano plot showing 93 proteins enriched specifically in FGF culture and 81 proteins enriched in EGF+FGF culture (fold change>1.5; p value<0.05). (c,d) GO terms – cellular components of the proteins present at higher levels in the FGF culture (c) or proteins having higher levels in the EGF+FGF culture (d) (p value<0.05). (e,f) List of proteins related to respiratory chain (e) and chromatin organisation (f), two overrepresented GO terms in EGF+FGF culture. (g) WB for HMGB2 protein in both cultures and bar chart showing its 2-fold enrichment in the EGF+FGF culture. Abbreviations: LC-MSMS, liquid chromatography tandem-mass spectrometry; GO, gene ontology; E, EGF; F, FGF. Data are shown as median±IQR; n=4; significance was tested by non-parametric Mann-Whitney U test.

3.3 Testing the Hmgb2 overexpression vector

To test whether HMGB2 protein could be involved in the reprogramming process, we decided to perform retroviral-driven overexpression of HMGB2 in the astroglial cultures. To do so, we first produced the retrovirus encoding for Hmgb2 (see Materials and methods) and tested its efficiency by immunostaining in the primary cortical astrocytes isolated from Hmgb2 full knock out animals (Fig. 18a). This culture is the best tool to test the overexpression since the most of the mouse cell lines already contain a high level of HMGB2 (Ronfani et al., 2001). Astrocytes were prepared following standard protocol, transduced either with the control virus encoding for GFP only or Hmgb2 overexpression virus with the GFP reporter separated by IRES. 1 week after transduction we performed the immunostaining against HMGB2 and observed cells endogenously expressing HMGB2 protein in +/+ and +/- glial cultures, interestingly at different levels in different cell types. GFAP+ cells showed much lower levels than cells negative for this marker that are most possibly oligodendrocyte progenitor cells. Nevertheless, we could not detect any signal in the cells isolated from Hmgb2-/- animals that also confirmed the specificity of the HMGB2 antibody. Most importantly, the Hmgb2-GFP transduced Hmgb2-/- astrocytes showed a high amount of the HMGB2 (Fig. 18a), pointing out the efficient overexpression of this protein using our retroviral vector.

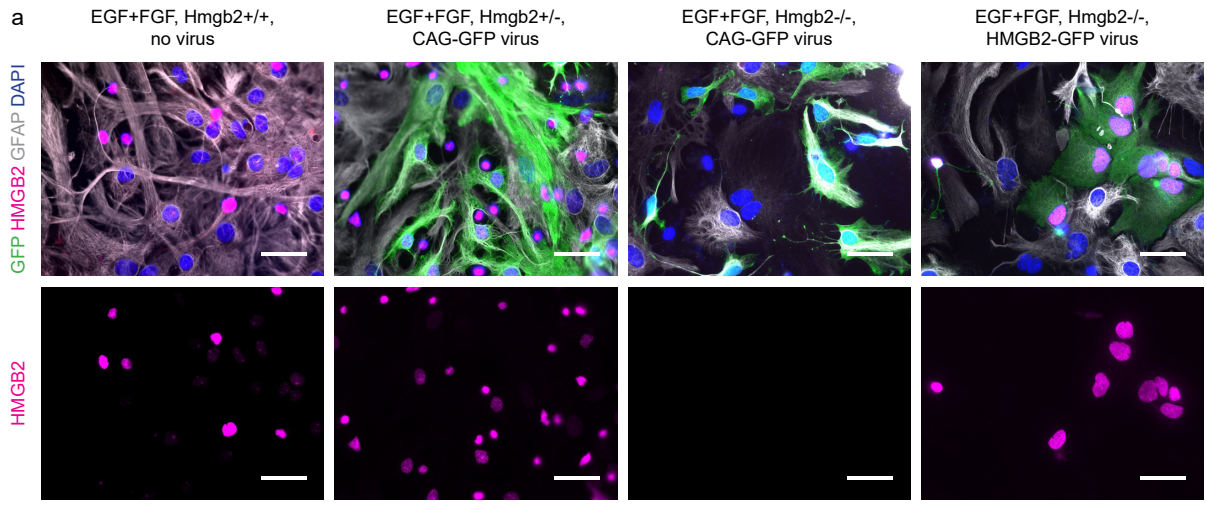

Figure 18: Testing the efficiency of HMGB2 overexpression in astrocytes isolated from Hmgb2 deficient animals.

(a) Micrographs showing the HMGB2 immunostaining in WT Hmgb2+/+ untransduced astroglial cells (left panel) and in CAG-GFP transduced Hmgb2+/- astroglial cultures (second left panel). The micrographs on the right present cells isolated from Hmgb2-/- animals, transduced with control virus to test the specificity of the Hmgb2 antibody (second from the right) and transduced with retrovirus encoding for Hmgb2 and GFP reporter to test the efficiency of overexpression. Pictures were taken 7 days after plating the cells. Scale bars (a) 50 μm.

3.4 HMGB2 protein increases the reprogramming efficiency in vitro in the FGF culture

3.4.1 Reprogramming of astroglial cultures by HMGB2 overexpression

Proteome analysis revealed 2-fold lower expression of HMGB2 protein in the astroglial cells that are less prone to be reprogrammed in comparison to the culture with high reprogramming efficiency. We, therefore, asked whether we could improve the acquisition of neuronal program from FGF astrocytes with the elevated levels of HMGB2 protein and thereby rescue the phenotype. To this aim, we overexpressed it in EGF+FGF and FGF cultures together with NEUROG2, a neurogenic transcription factor that showed the most dramatic differences in the conversion rate between two conditions. We performed our standard reprogramming protocol, first culturing the cells for 10 days in two different conditions, followed by retroviral transduction and 7 days of the reprogramming process. As shown previously, the reprogramming with single transcription factor NEUROG2, showed about 3-fold higher efficiency of reprogramming in the culture grown with EGF+FGF (56.28±13.50%) when compared to the FGF culture (17.47±10.17%) (Fig. 19a,b). We then transduced the astrocytes with two retroviruses encoding for Neurog2-dsRED and Hmgb2-GFP (Fig. 19a,b). Simultaneous overexpression of NEUROG2 and HMGB2 did not increase the amount of the induced neurons in the culture having already very good reprogramming capacity (57.19±15.41% induced neurons in EGF+FGF). However, we observed about 20% higher reprogramming rate in FGF culture when overexpressing both factors together (Fig. 19a,b). Addition of HMGB2 to neurogenic transcription factor NEUROG2 in FGF culture resulted in a significantly higher amount of induced neurons – from 17.47±10.17% with NEUROG2 alone to 40.71±25.12% together with HMGB2, respectively (Fig. 19b). This suggests that elevated levels of HMGB2 can rescue the low responsiveness to the forced neurogenesis in the culture lacking EGF and can help this culture to achieve better reprogramming capacity similar to double growth factors conditions.

Given its promising function to enhance the reprogramming process in the FGF culture, we next asked, whether the overexpression of HMGB2 alone is sufficient to

promote the conversion of astroglia into neurons. 7 days after transduction with the retrovirus encoding for Hmgb2 we did not observe any acquisition of neuronal phenotype in both cultures, indicating that HMGB2 alone is not sufficient to induce neurogenesis (Fig. 19b,c,d). The majority of the transduced cells remained GFAP+, similarly to the control transduction with the CAG-GFP retrovirus, suggesting that HMGB2 on its own does not change the cell identity (Fig. 19c,d). Interestingly, we observed a slightly higher proportion of GFAP negative cells within the control transduced cells in the FGF culture, meaning that we might initially target different starting population in the FGF culture when compared to the EGF+FGF culture. Taken together, HMGB2 protein on its own does not alter the cell fate, but together with the NEUROG2 overexpression induces the reprogramming in the FGF culture that otherwise exhibits a limited efficiency in neuronal conversion.

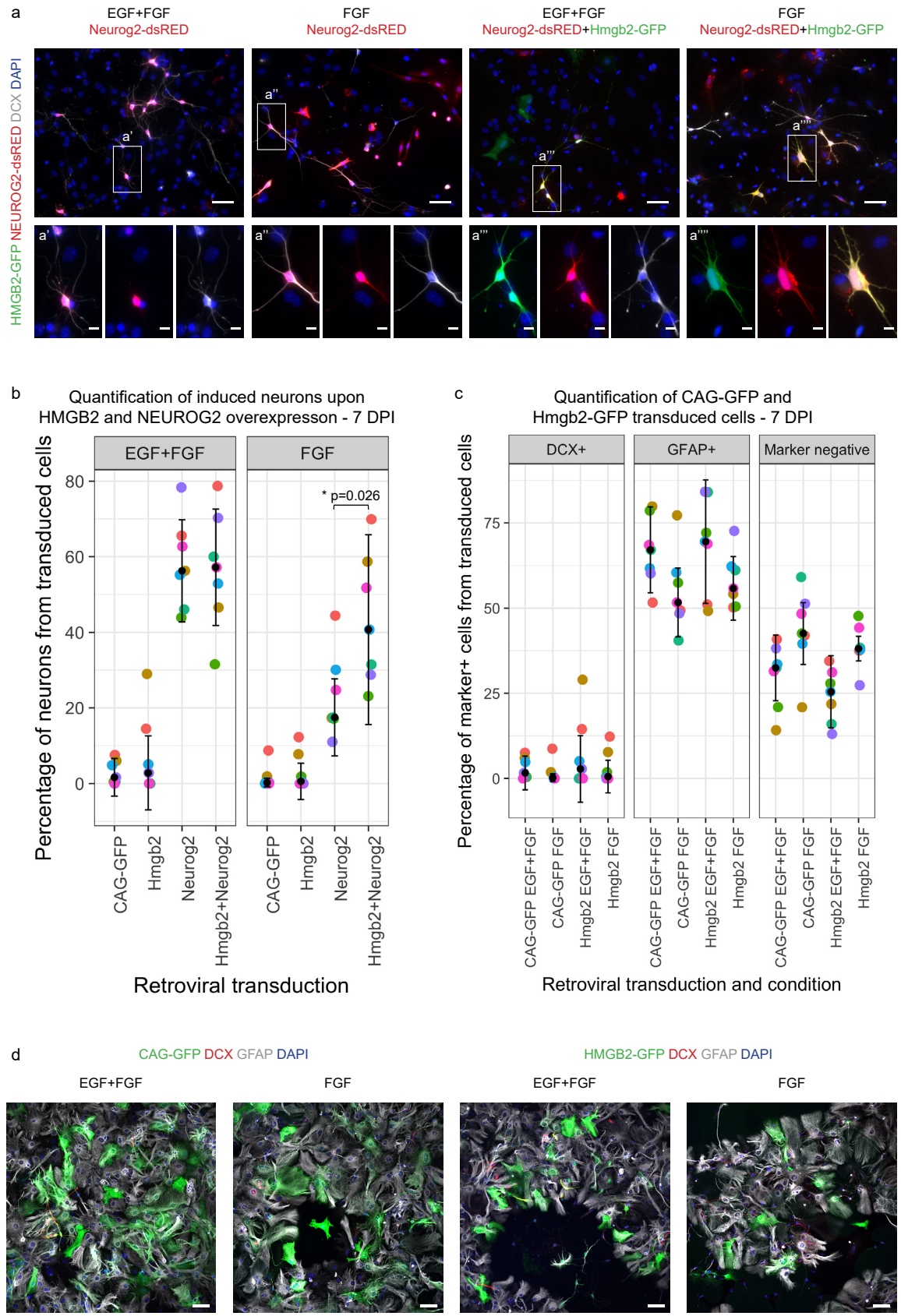

Figure 19: Simultaneous overexpression of HMGB2 and NEUROG2 improves the reprogramming efficiency in the FGF culture.

(a) Micrographs of the astroglial cultures after 7 days of the reprogramming process. Boxed areas correspond to the higher magnification images in adjacent panels (a', a'', a''' and a'''') and depict examples of induced neurons – in the first two panels transduced with Neurog2-dsRED and in the third and fourth panel double positive for HMGB2-GFP and NEUROG2-dsRED. (b) Quantification of the induced neurons in EGF+FGF or FGF cultures 7 days after transduction with Hmgb2 or Neurog2 alone or both together. The percentage of induced neurons is calculated as a proportion out of transduced cells. (c) Dot plot showing the quantification of the cells transduced with the CAG-GFP or Hmgb2-GFP retrovirus that express DCX or GFAP marker 7 DPI. (d) Z-stack confocal micrographs of astrocytes 7 DPI in two culturing conditions and transduced with control CAG-GFP or Hmgb2-GFP retrovirus. Abbreviation: DPI, days post induction. Data are shown as median±IQR; each of the single dots represents independent biological replicate. Significance in (b) was tested by non-parametric Mann-Whitney U test. Scale bars (a, d) 50 μm, (a', a'', a''', a'''') 10 μm.

3.4.2 Reprogramming of astroglial cultures by HMGB1 overexpression

HMGB1 is the second member of the HMGB protein family that was enriched in the EGF+FGF culture based on the proteome analysis (Fig. 17f). Despite their different expression pattern in the adult mouse brain, we were still speculating about their similar roles in the astroglial cultures and decided to test the HMGB1 potential in facilitating NEUROG2 reprogramming capacity. To this aim, we overexpressed it together with the NEUROG2 in the FGF culture and asked whether it would give similar results that we observed with NEUROG2 and HMGB2 overexpression (Fig. 20a,b). In two out of three experiments we did not observe higher amount of induced neurons after simultaneous overexpression of HMGB1 and NEUROG2 when compared to NEUROG2 alone (Fig. 20b). While HMGB2 boosts the acquisition of the neuronal phenotype and increases the final neuronal yield if the FGF culture, this was not obtainable with the HMGB1. However, the variability between the replicates was quite high and more experiments need to be done to verify it statistically.

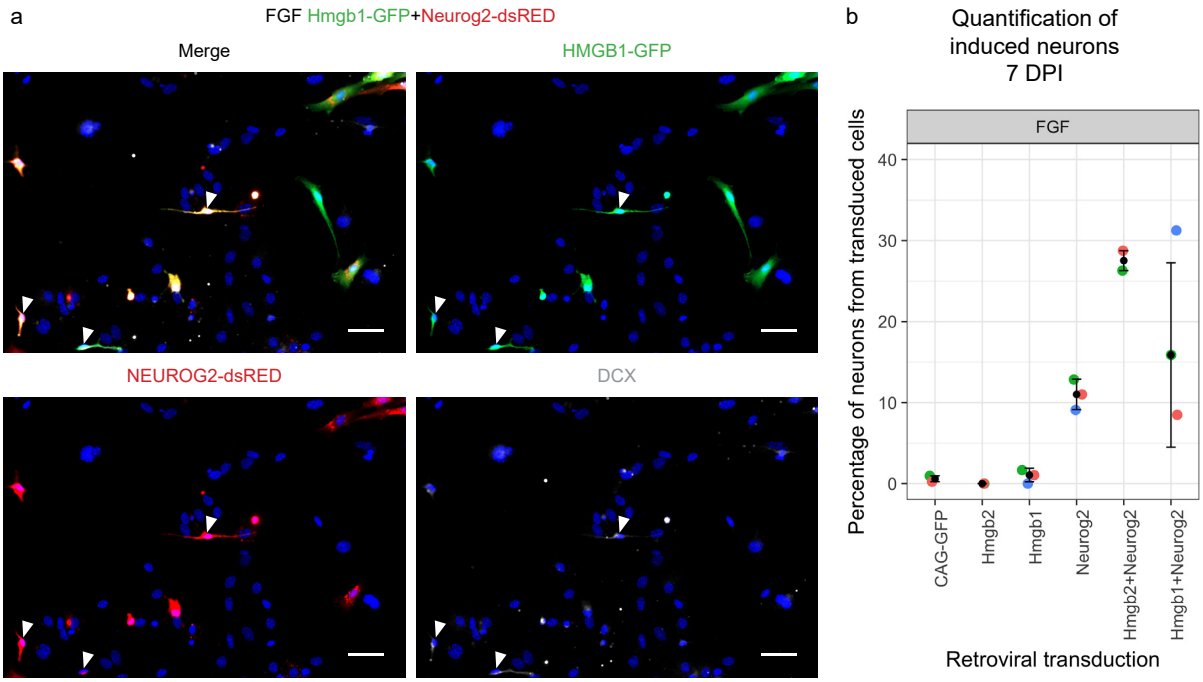

Figure 20: HMGB1 does not resemble the function of HMGB2 in the astroglial cells.

(a) Micrographs of the FGF culture 7 days after simultaneous overexpression of HMGB1 and NEUROG2 proteins. Arrowheads are pointing out the examples of GFP+ and dsRED+ double positive induced neurons. (b) Dot plot displaying the quantification of induced neurons in the FGF culture after HMGB2 and HMGB1 overexpression alone or together with NEUROG2. Abbreviation: DPI, days post induction. Data are shown as median±IQR; each of the single dots represents independent biological replicate. Scale bars (a) 50 μm.

3.4.3 Reprogramming of astroglial cultures by simultaneous overexpression of HMGB2 and BRN2

Since HMGB2 protein together with NEUROG2 showed a prominent effect in the reprogramming of the FGF culture, we next asked whether this is specific for one particular neurogenic transcription factor or it has more general effect in the astrocyte culture and could improve the reprogramming efficiency also in a combination with different neurogenic determinants. In order to address this question, we decided to test it together with the BRN2, the factor that was also not sufficient to promote the conversion of reactive glia into neurons in the FGF culture (Fig. 15d, Fig. 21a,b). Similarly to the NEUROG2, simultaneous overexpression of HMGB2 and BRN2 in

the EGF+FGF culture did not result in the higher amount of the induced neurons (37.82±14.42% with Brn2 and 32.36±22.16% with Hmgb2+Brn2) (Fig. 21a,b). On the contrary, in both performed experiments with HMGB2 and BRN2 co-expression in the FGF culture, we observed the increase in the reprogramming efficiency (from 15.71±5.37% with Brn2 to 42.88±5.75% with Hmgb2+Brn2), similar to the levels obtained in the EGF+FGF culture (Fig. 21a,b). This suggests that HMGB2 helps the reprogramming in the transcription factor-independent manner, however, we would need to prove this statistically by performing at least two more experiments with BRN2 and with other known reprogramming factors like ASCL1. Taken together, HMGB2 overexpression induces the intrinsic changes in the FGF cultured astroglia, which help the neurogenic transcription factors to trigger the generation of induced neurons.

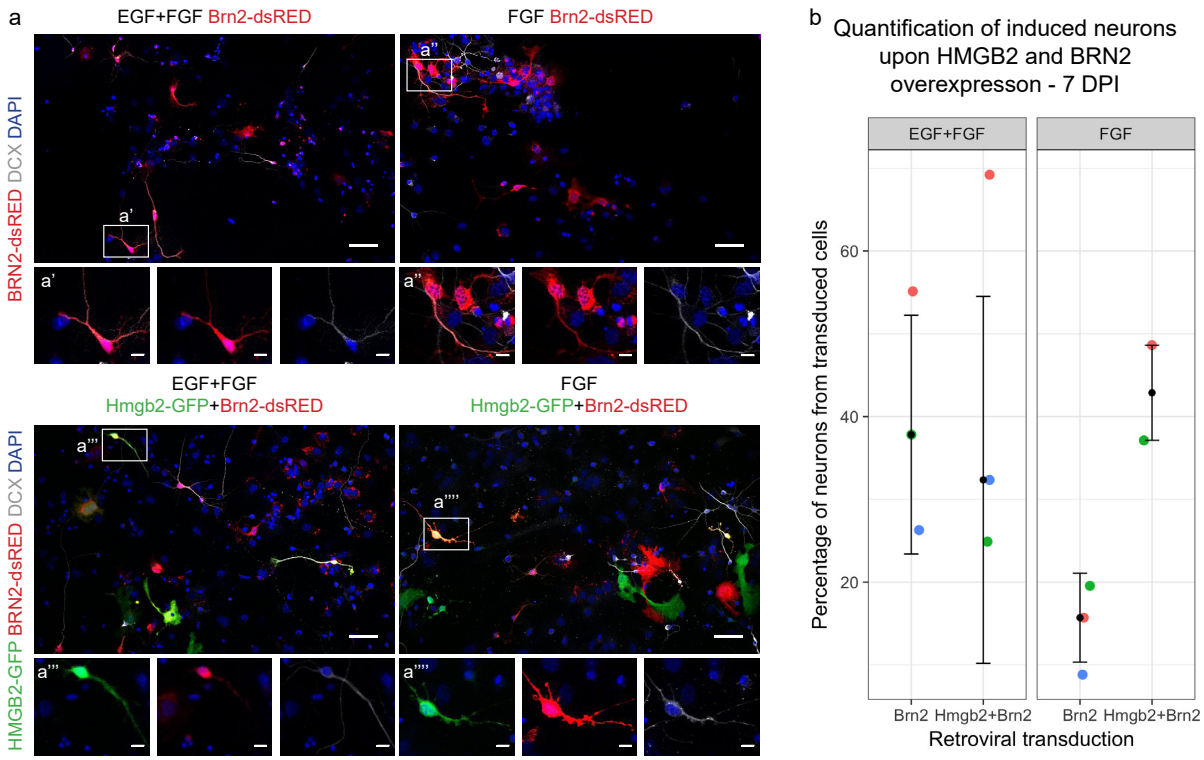

Figure 21: Simultaneous overexpression of HMGB2 and BRN2 improves the reprogramming efficiency in the FGF culture.

(a) Example pictures of astrocytes transduced with Brn2-dsRED alone (upper panels) or in combination with Hmgb2-GFP retrovirus (lower panels) 7 days post transduction in two culturing conditions. Boxed areas correspond to the magnified images in adjacent panels (a', a'', a''' and a'''') and show examples of induced neurons. (b)

Quantification of reprogramming efficiency after simultaneous overexpression of HMGB2 and BRN2 in EGF+FGF and FGF culture in comparison to BRN2 overexpression alone. Abbreviation: DPI, days post induction. Data are shown as median±IQR; each of single dots represents independent biological replicate. Scale bars (a) 50 µm, (a', a'', a''', a''') 10 µm.

3.4.4 Reprogramming of HMGB2 deficient astrocytes

In vitro reprogramming experiments in two different culturing conditions revealed the limited reprogramming capacity of the FGF culture that could be affected by lower levels of HMGB2 protein. To test whether this protein is necessary for the conversion of astroglial cells to induced neurons, we isolated the astroglia from the Hmgb2-/- animals, cultured them with EGF+FGF growth factors and induced neurogenesis by NEUROG2 overexpression. We first looked at the composition of the cultures isolated from the Hmgb2+/+, Hmgb2+/- and Hmgb2-/- siblings to prove that the loss of HMGB2 protein does not affect the cellular identity of the starting populations (Fig. 21a). More than half of the CAG-GFP transduced cells were positive for GFAP protein 7 days after the transduction; in Hmgb2+/+ astrocytes 57.77±22.83%, in Hmgb2+/- astrocytes 70.73±3.96% and in Hmgb2-/- astrocytes 66.04±14.99%, indicating the enrichment of cortical astrocytes in the culture regardless of their genotype. Based on the GFAP expression, cultures from Hmgb2 knock out animals do not seem to be different to the wild-type ones (Fig. 15a; Fig. 22a). The only observed difference compared to our previous reprogramming experiments was higher contamination of endogenous neuronal progenitors in the culture. However, it was not Hmgb2-/- specific but present in all astroglial cultures isolated from the siblings having different genotypes. Small proportion of these progenitors could be transduced by the retrovirus, as quantified by the proportion of DCX positive CAG-GFP transduced cells that was slightly higher compared to our initial experiments in wild-type astroglia: in Hmgb2+/+ astrocytes 5.77±12.92%, in Hmgb2+/- astrocytes 4.01±6.61% and in Hmgb2-/- astrocytes 3.17±14.02%, respectively. Nevertheless, we were able to recognize and exclude them based on their morphology, as they mostly formed clusters of cells and did not show mature neuronal phenotype having a long thin process like reprogrammed neurons. Finally, to address the question whether cultures lacking HMGB2 show the altered fate transition, we overexpressed NEUROG2 in all three conditions and followed our standard reprogramming protocol

(Fig. 22b,c). The reprogramming of Hmgb2+/+ astroglia was consistent with our previous experiments, demonstrating a relatively high reprogramming rate with 58.41±16.26% induced neurons out of Neurog2-dsRED transduced cells (Fig. 22b). We were also able to efficiently reprogram Hmgb2+/- astroglial cells with the efficiency of 51.44±23.91% (Fig. 22b). The conversion rate of Hmgb2 deficient astroglia was decreased, with 34.55±16.15% reprogrammed neurons from transduced cells (Fig. 22b). These results indicate a small gradual decrease in the number of induced neurons depended on the amount of the HMGB2 protein. The reduced reprogramming efficiency in Hmgb2-/- astrocytes, however, varied between different experiments and was therefore not significant. All in all, we observed that the neuronal phenotype can still be acquired in the cells lacking the HMGB2 protein, but the final neuronal yield is reduced, suggesting that HMGB2 is involved in facilitating the reprogramming process induced by NEUROG2.

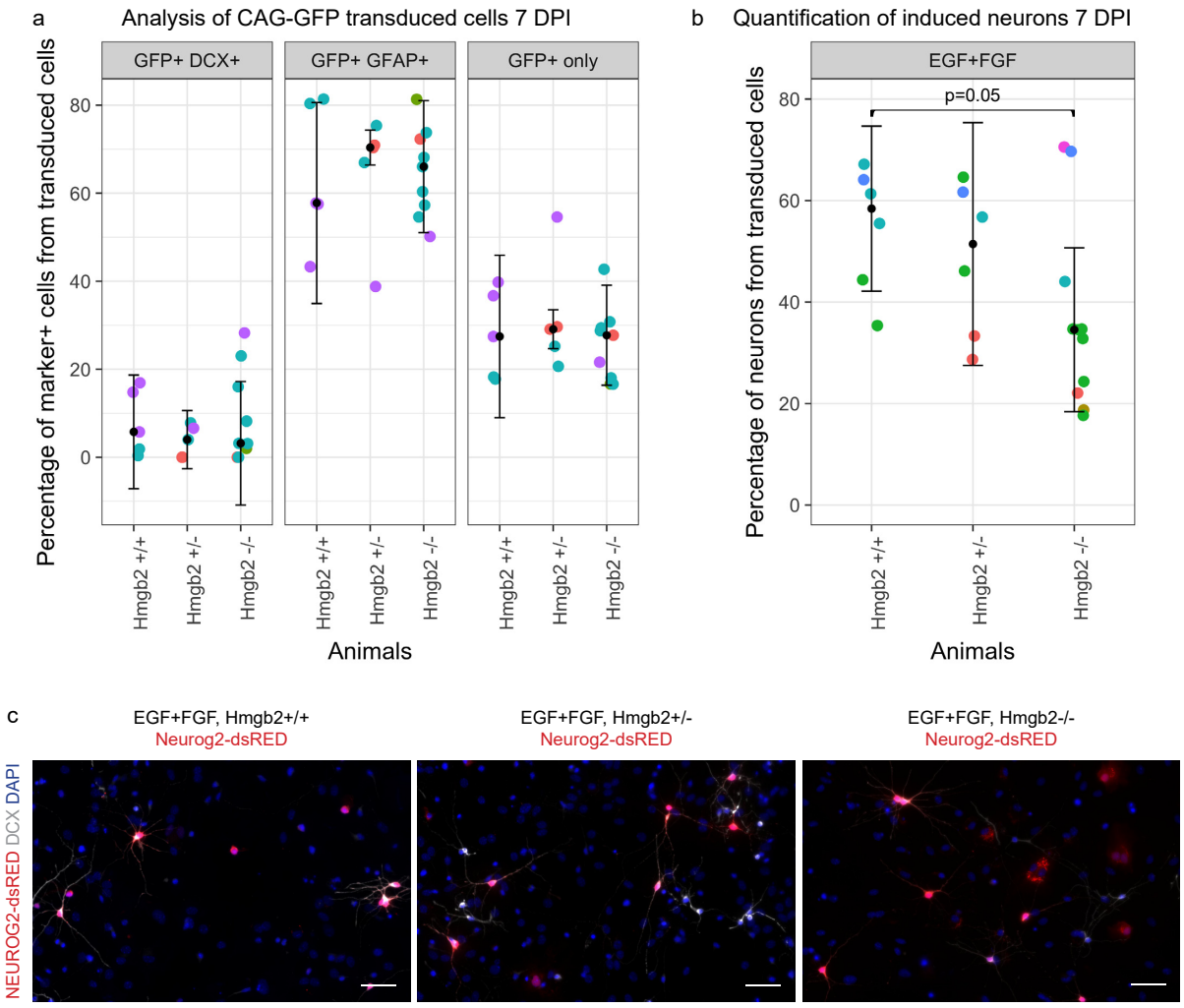

Figure 22: Astrocytes lacking HMGB2 protein are less efficiently reprogrammed into induced neurons.

(a) Dot plots showing the proportion of DCX and GFAP positive cells out of CAG-GFP transduced cells in the astroglial cultures isolated from Hmgb2+/+, Hmgb2+/- and Hmgb2-/- siblings. (b) Quantification of the converted cells out of Neurog2-dsRED transduced astroglia with different genotypes 7 DPI. (c) Micrographs depicting the reprogramming with the overexpression of NEUROG2 in the astrocytes lacking HMGB2 protein and homo or heterozygous controls. Abbreviation: DPI, days post induction. Data are shown as median±IQR; each of the single dots represents one animal, siblings from the same litter have same colors, separate experiments are labeled by separate colors. Significance in (b) was tested by non-parametric Mann-Whitney U test. Scale bars (c) 50 µm.

3.5 HMGB2 helps to reprogram reactive glial cells in vitro

Following the ability of HMGB2 to complement the neurogenic transcription factors in the FGF culture where the acquisition of the neuronal program is impaired, we decided to test it also in another in vitro model that appears to be rather challenging in the reprogramming context. We examined the reprogramming potential of reactive astroglia isolated from the adult injured cerebral cortex gray matter. Although these cells expanded as neurospheres can generate functional neurons upon forced expression of NEUROG2 (Heinrich et al., 2010), the direct conversion of reactive glial cells in adherent culture is rather limited. We, therefore, asked whether the role of HMGB2 could be also exerted in this culture and it could help NEUROG2 to achieve better reprogramming efficiency. We performed local stab wound lesion in the cortical gray matter of adult wild-type mice and dissociated injured cortical hemispheres 3 days later for subsequent adherent cultures. After 3 days of culturing, cells were transduced with different combinations of retroviruses and 7 days after the transduction we fixed and immunostained the cultures for neuronal marker β-III TUBULIN in order to quantify the amount of neuronal-like cells (Fig. 23a). In the control condition, we used two retroviruses encoding for GFP and dsRED and quantified the amount of GFP+ cells only, dsRED+ cells only or double positive cells (Fig. 23d). All the cells in the control conditions were negative for β-III TUBULIN – red dot in the graph (Fig. 23d). We obtained similar results when overexpressing HMGB2-GFP in combination with control CAG-dsRED virus (green dot, Fig. 23d), indicating that HMGB2 does not induce any neurogenesis in reactive glial cells in vitro. Next, we overexpressed neurogenic transcription factor NEUROG2-dsRED in combination with HMGB2-GFP (Fig. 23b). We compared the amount of the induced neurons in dsRED+ cells only to the double positive cells that have simultaneous overexpression of both factors (Fig. 23d, blue dot). We observed the appearance of some cells positive for β-III TUBULIN, which haven't yet developed a proper neuronal morphology, and we decided to quantify them in a special category called β-III TUBULIN+ "non-neuronal" cells (labeled with arrows in Fig. 23c). Forced expression NEUROG2 alone resulted in 5.3% β-III TUBULIN+ "non-neuronal" cells and no cells with mature neuronal morphology. Looking at the double transduced cells, there were 6.0% β-III TUBULIN+ "non-neuronal" cells, but we could also find 4.2% β-III

TUBULIN+ “neuronal” cells (Fig. 23b,d) that adopted elongated neuronal-like morphology (labeled with arrowheads in Fig. 23b). This result suggests that HMGB2 overexpression does not only help NEUROG2 to reprogram the reactive astroglia more efficiently but also boosts the acquisition of the neuronal phenotype. Gaining very promising results, we decided to test another neurogenic transcription factor ASCL1 that is broadly used in the reprogramming field. We transduced the adherent reactive glial culture with Ascl1-dsRED in combination with Hmgb2-GFP retrovirus and analyzed all single and double transduced cells for β-III TUBULIN expression. ASCL1 alone converted 3.8% of all transduced cells, however morphologically they were still not identified as induced neurons (Fig. 23c,d). Simultaneous overexpression of both factors together resulted in a noticeable increase in the β-III TUBULIN+ “non-neuronal” cells up to 22.4% and only 1.7% induced neurons (Fig. 23c,d). HMGB2 seems to help ASCL1 in at least starting the reprogramming process, but we would need to keep the cells longer in the reprogramming process to prove whether this 20% of the cells would manage to acquire the proper neuronal phenotype. To sum up, HMGB2 showed a good potential to increase the conversion efficiency of the culture that is otherwise very resistant to the reprogramming. Similarly to the postnatal astroglial cultures, its effect seems to be neurogenic transcription factor independent. We performed only one pilot experiment using adherent reactive gliosis culture, in order to test whether HMGB2 might have some potential to improve the reprogramming capacity also in the reactive astrocytes in vivo. Since it gave quite promising results, we definitely need to confirm the outcome in at least three more experiments but also try its potency after the brain injury in direct reprogramming in vivo.

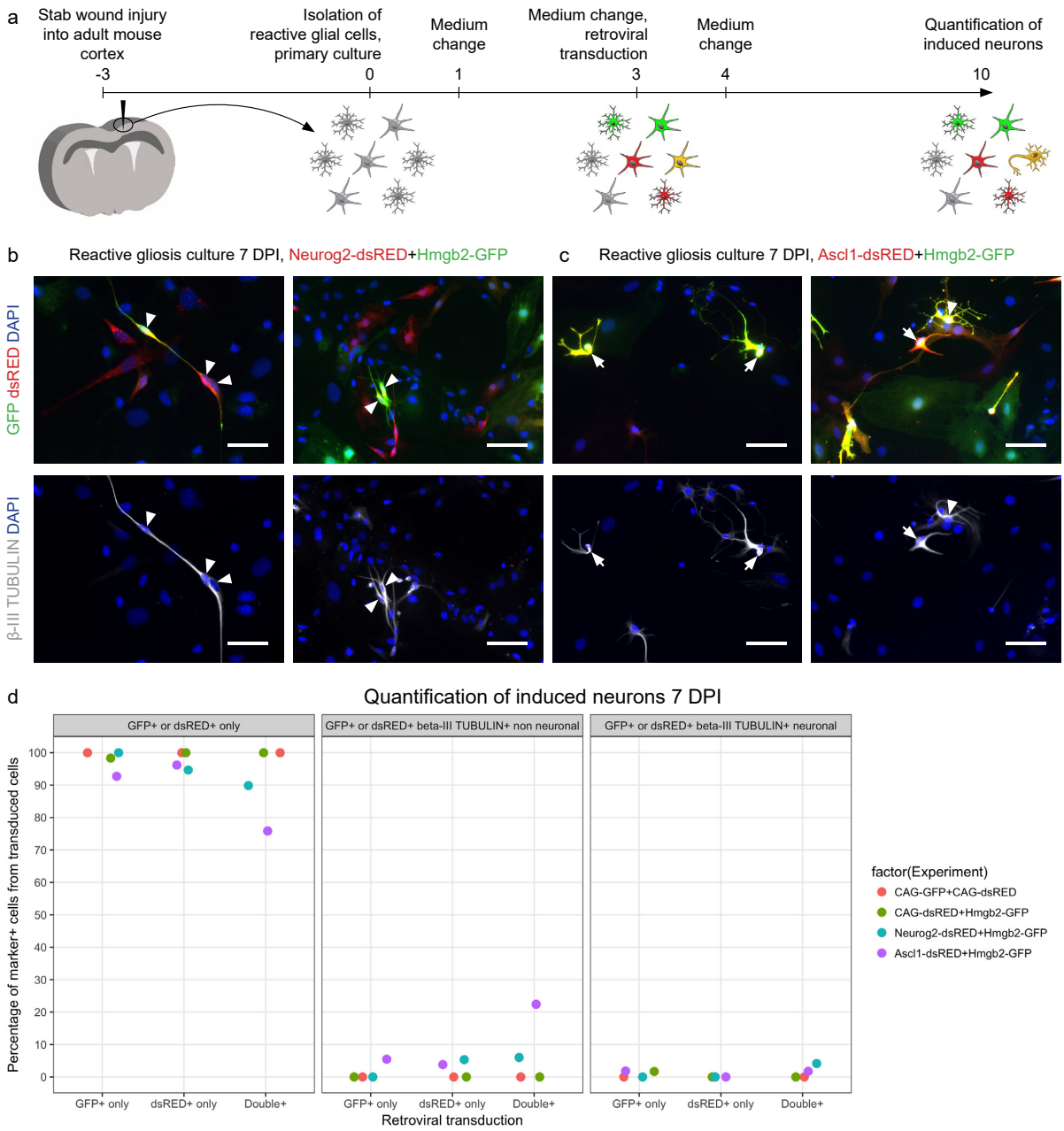

Figure 23: Simultaneous overexpression of HMGB2 in combination with NEUROG2 or ASCL1 induces the reprogramming of the adherent reactive astroglia in vitro.

(a) Scheme presenting the preparation of the adherent reactive gliosis culture after the brain injury and the reprogramming protocol. (b) Example pictures of some reprogrammed cells 7 days post transduction with Hmgb2 and Neurog2. Arrowheads show the examples of the cells that were quantified as reprogrammed “neuronal” cells. (c) Micrographs depicting some transduced cells 7 DPI in ASCL1+HMGB2 condition that express β-III TUBULIN+ already, but do not show proper neuronal-like morphology (labelled with arrows). (d) Dot plots showing the quantification of β-III TUBULIN+ “non-neuronal” cells (arrows in c) or “neuronal” cells (arrowheads in b,c)

as a proportion of transduced cells. Abbreviation: DPI, days post induction. Each of the single dots represents one condition shown in the legend on the right. Scale bars (b,c) 50 µm.

3.6 Reprogramming of reactive glial cells in vivo

Previous attempts of in vivo reprogramming by overexpression of NEUROG2 alone demonstrated its insufficiency to promote the conversion of reactive glia into neurons upon the stab wound injury, when molecules alleviating oxidative stress (BCL-2, vitamin D or E) are not provided (Gascón et al., 2016; Grande et al., 2013). Besides metabolic barriers, other roadblocks like chromatin and epigenetic states might play a role in maintaining a stable cell identity and consequently do not allow the fate transition. We identified a chromatin-associated protein HMGB2 as a possible candidate to overcome these barriers. In vitro results indicate the involvement of the HMGB2 protein in neuronal reprogramming and suggest its potent effect in the cultures where the neuronal program is difficult to obtain, including the reactive gliosis culture in vitro. Promising results from these cultures motivated us to address the question whether elevated levels of HMGB2 could help to reprogram the reactive astrocytes directly at the injury site in vivo.

3.6.1 Preparation and testing the construct for the simultaneous overexpression of HMGB2 and NEUROG2 in vivo

To test whether the HMGB2 role in vitro could be exerted also in vivo, we performed test experiments injecting the mixture of two retroviruses Neurog2-dsRED and Hmgb2-GFP upon the cortical stab wound injury in the adult mouse brain. These first attempts, however, resulted in a minimum amount of co-transduced cells. Already in the astroglial cultures in vitro, the amount of double transduced cells with both retroviruses was rather limited, suggesting that this approach is rather challenging to access the simultaneous overexpression of both factors in vivo. We, therefore, prepared a new retroviral construct containing both factors Neurog2 and Hmgb2 (Fig. 24a). They are separated by T2A “self-cleaving peptide” that makes the ribosome to skip the synthesis of a peptide bond at the C-terminus of a 2A peptide, which leads to separation between the end of the 2A sequence and the next peptide downstream (Kim et al., 2011). We also included the dsRED reporter separated by IRES (see Materials and methods) in order to visualize transduced cells (Fig. 24a). We first tested our construct in vitro in our standard EGF+FGF and FGF cultures (Fig. 24b,c),

to ensure that both proteins are functional, especially NEUROG2 that has a few additional residues from T2A added to the end. We quantified the amount of the induced neurons one week after transduction and compared the numbers to the overexpression of NEUROG2 alone and HMGB2+NEUROG2 delivered by two separated retroviruses. We also performed the immunostaining for HMGB2 protein and observed clear overexpression in dsRED+ cells (Fig. 23b). In the EGF+FGF culture, we observed comparable amount of reprogrammed cells with all 3 combinations of retroviruses, with Neurog2-dsRED 58.95±13.70%, with Neurog2-dsRED+Hmgb2-GFP 58.60±6.44% and with Neurog2-T2A-Hmgb2-dsRED 54.88±9.41%, respectively (Fig. 24c). Most importantly, we also confirmed the increase in the conversion efficiency of the FGF culture using double construct, reaching even higher levels of reprogramming compared to the transduction with two separate viruses (Fig. 24c). The Neurog2 alone induced 21.11±10.23% of neurons, Neurog2+Hmgb2 delivered by two retroviruses 36.09±12.69% and double construct 44.91±5.91%. We confirmed that the newly generated vector is functional since it can induce the neuronal fate in vitro and can be also used for the simultaneous overexpression of NEUROG2 and HMGB2 in vivo.

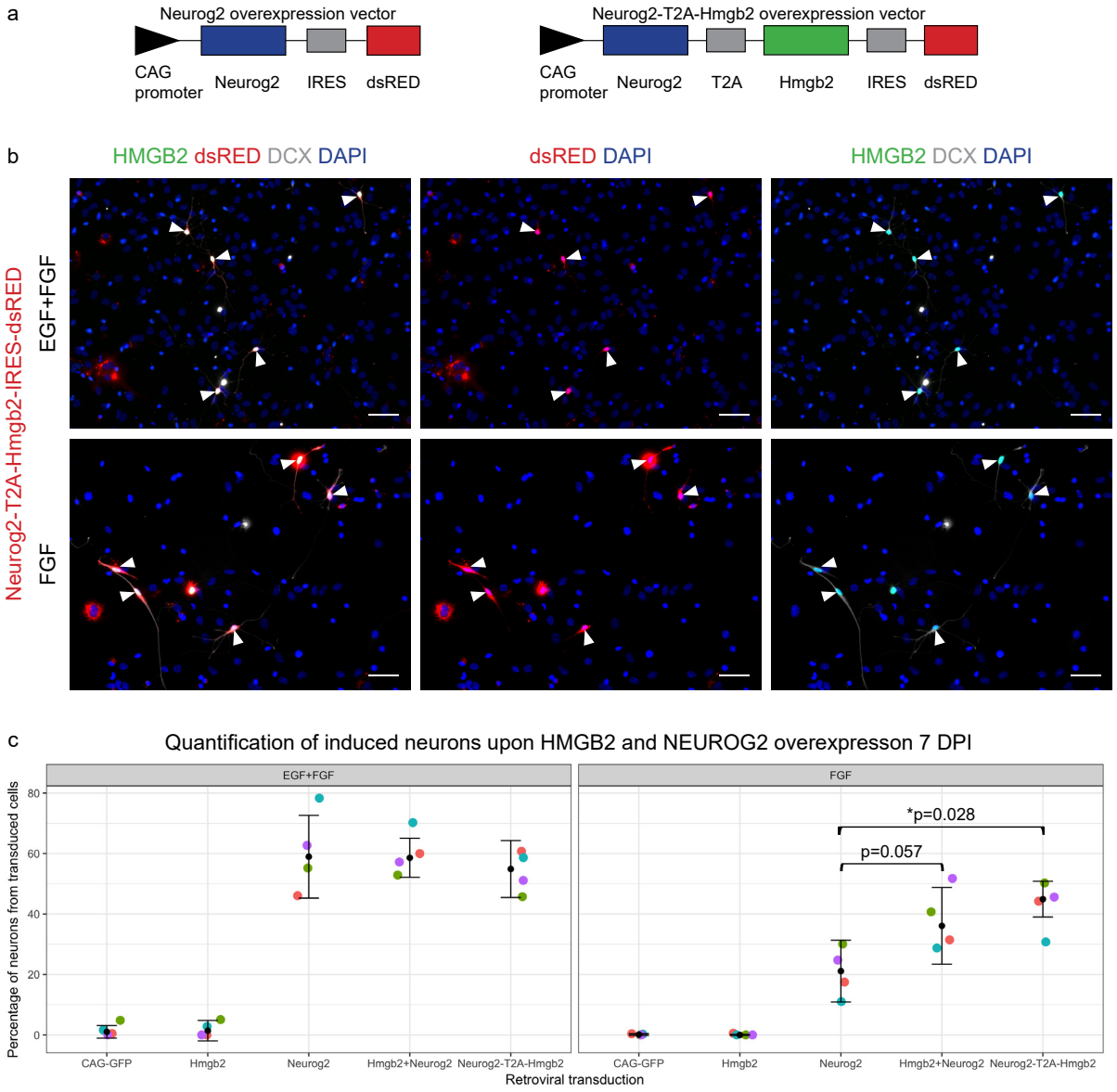

Figure 24: Testing the construct encoding for both Hmgb2 and Neurog2 in astroglial cultures in vitro.

(a) Schematic representation of the retroviral vector for NEUROG2 overexpression alone (left) or together with HMGB2 in the newly generated retroviral construct pCAG-Neurog2-T2A-Hmgb2-IRES-dsRED (right). (b) Micrographs showing astroglia transduced with double construct depicted in (a), 7 days post transduction in both culturing conditions. White arrowheads point to cells reprogrammed into DCX+ induced neurons that also show the efficient overexpression of HMGB2 protein. (c) Quantification of reprogramming efficiency after the overexpression with a retrovirus encoding for both Hmgb2 and Neurog2 and compared to Neurog2 alone or Hmgb2+Neurog2 delivered by two separated retroviruses. Abbreviations: IRES, internal ribosomal entry site; DPI, days post induction. Data are shown as median±IQR; each of the single dots represents independent biological replicate;

significance was tested by non-parametric Mann-Whitney U test. Scale bars (b) 50 µm.

3.6.2 The simultaneous overexpression of NEUROG2 and HMGB2 in reactive glial cells in vivo is not sufficient to facilitate the neuronal reprogramming

After confirming that double construct is sufficient to promote the conversion of astroglia into neurons in vitro, we performed the stab wound injury in the adult mouse brain and applied the retrovirus to the injury site to investigate whether elevated levels of HMGB2 can help NEUROG2 in the acquisition of the neuronal phenotype from reactive glial cells in vivo. The stab wound injury was performed in the grey matter of somatosensory cortex, as previously described (Buffo et al., 2005; Heinrich et al., 2014). Three days after the surgery, the same animals were injected with a retroviral suspension in the injured cortex within the stab wound area (Fig. 25a). By using the retrovirus we stably transduce only actively dividing cells at the injury site that are mostly NG2+OLIG2+ oligodendrocyte precursor cells (OPCs), GFAP+ reactive astrocytes and IBA1/CD45+ microglia as shown previously (Heinrich et al., 2014). With this approach, we exclude the transduction of endogenous neurons that would represent the false positive cells when quantifying the amount of reprogrammed induced neurons. 10 days after the injections, animals were perfused, brain tissue was cut into coronal sections and immunostained for the dsRED to identify the transduced cells (Fig. 25a). Some of the sections were also stained with HMGB2 antibody to confirm its overexpression in the cells transduced with retrovirus encoding for Neurog2-T2A-Hmgb2-IRES-dsRED (Fig. 25b). To investigate whether transduced dsRED+ cells converted into induced neurons, we performed the immunohistochemistry for NeuN, commonly used marker for mature neurons (Fig. 25c-f).

In the control condition, we injected the retrovirus encoding Neurog2 alone to confirm that overexpression of this single neurogenic transcription factor does not result in any appearance of induced neurons as published previously (Gascón et al., 2016; Grande et al., 2013). 10 days post injection many dsRED+ cells were found at the injury site, however, the majority of them maintained the glial morphology (Fig. 25c). Nevertheless, we quantified the proportion of dsRED and NeuN double positive cells

in order to determine the conversion rate. As expected, the number of induced neurons out of all transduced cells upon NEUROG2 overexpression was less than 3% (Fig. 25f). Next, we injected the retrovirus 3 days after they injury encoding for both factors, Neurog2 and Hmgb2. In 3 out of 5 injected animals, we observed very similar results to the overexpression of NEUROG2 alone (Fig. 25d). Most of the dsRED+ cells did not change their identity and only a small proportion (2.07±1.09%), displayed a detectable NeuN signal (Fig. 25d,f). Interestingly, in 2 animals transduced with both factors, Neurog2 and Hmgb2, we observed quite some cells having small round soma and long thin processes. Almost all of them were also positive for NeuN, suggesting that these could be reprogrammed neurons (Fig. 25e). We quantified the number of such cells having neuronal-like features and observed even up to 25% of induced neurons out of all dsRED+ transduced cells (Fig. 25f). Trying to understand this discrepancy between experiments, we looked more carefully at the injury site and observed that in both animals with the higher amount of neuronal-like cells, the injury was much deeper, touching the underlying white matter (WM) (Fig. 25e). On the other side, in the first 3 animals where we did not observe any improvement of the reprogramming compared to the NEUROG2 overexpression alone, the injury was only in the grey matter of the cortex (GM) (Fig. 25d). In previous in vivo reprogramming experiments (Buffo et al., 2005; Gascón et al., 2016; Heinrich et al., 2014), the stab wound injury was limited to the upper layers of the cortical gray matter, avoiding the deep layers in order to minimise the risk of migration of neural progenitors from the underlying white matter. Since we observed the presence of neuronal-like cells only in the GM+WM injury paradigm and induced neurons were mostly located at the border of the white matter (Fig. 25e), we would conclude that we transduced the neuronal progenitors that differentiated and migrated up to the cortical grey matter. Taken together, these data show that the forced expression of HMGB2 does not increase the yield of NEUROG2-mediated conversion of reactive glial cells into neurons after the grey matter stab wound injury, but it might induce differentiation and migration of neuronal progenitors to the injury site from the underlying white matter.

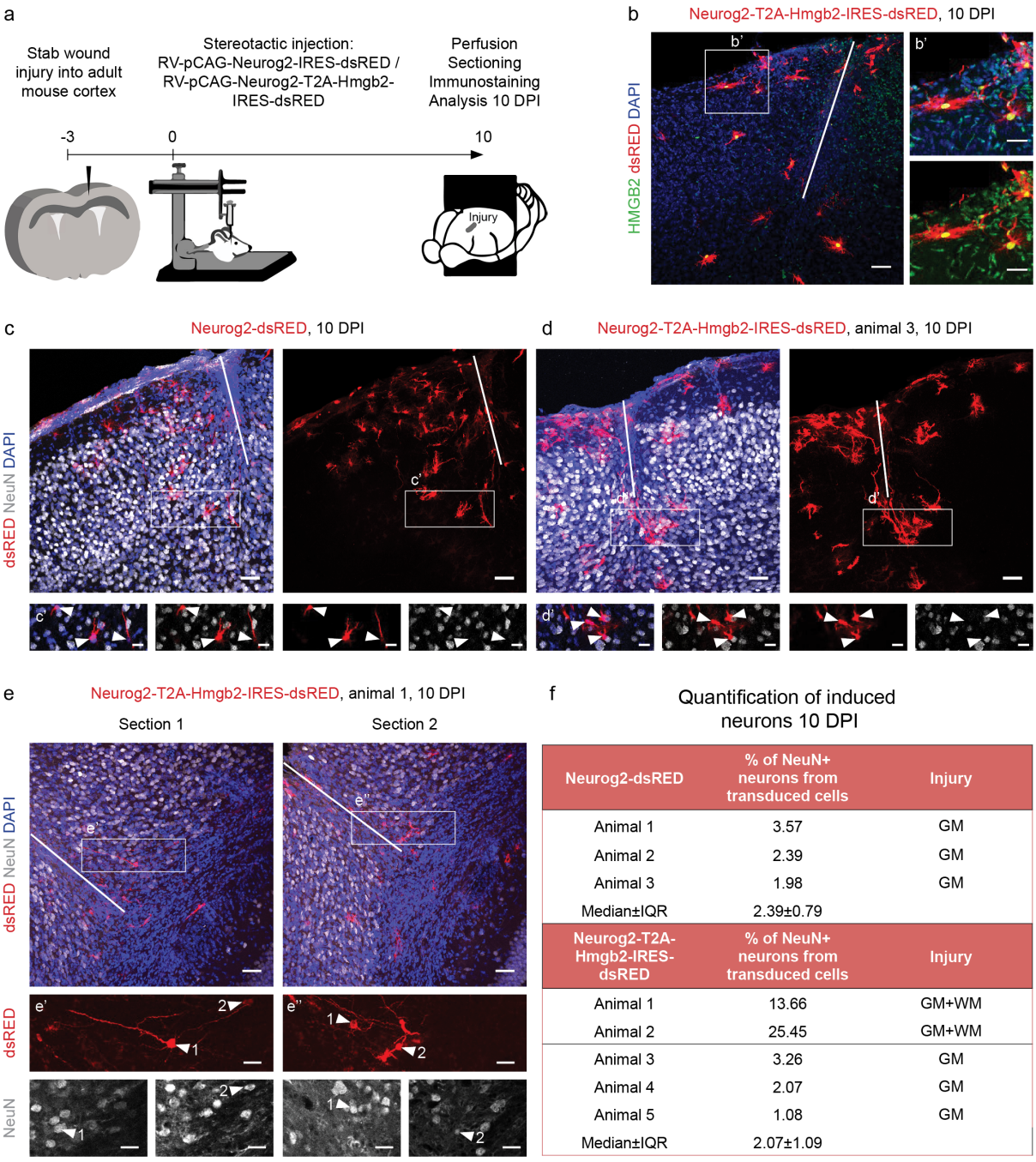

f

Quantification of induced neurons 10 DPI

Neurog2-dsRED	% of NeuN+ neurons from transduced cells	Injury
Animal 1	3.57	GM
Animal 2	2.39	GM
Animal 3	1.98	GM
Median±IQR	2.39±0.79	
Neurog2-T2A-Hmgb2-IRES-dsRED	**% of NeuN+ neurons from transduced cells**	**Injury**
Animal 1	13.66	GM+WM
Animal 2	25.45	GM+WM
Animal 3	3.26	GM
Animal 4	2.07	GM
Animal 5	1.08	GM
Median±IQR	2.07±1.09	

Figure 25: Hmgb2 is not sufficient to increase the reprogramming efficiency after the grey matter stab wound injury.

(a) Scheme of the protocol for in vivo reprogramming in the injured cortex of the adult mouse brain. (b) Confocal micrograph showing the brain section with stab-wound injury (labelled with a white line) with an injection of retrovirus encoding for Neurog2-T2A-Hmgb2-IRES-dsRED, immunostained for dsRED and HMGB2 at 10 DPI. Adjacent panels (b') represent a high-magnification view of the area boxed in (b). (c, d, e) Confocal micrographs depicting the injury site with Neurog2-IRES-dsRED transduced cells (c) or Neurog2-T2A-Hmgb2-IRES-dsRED transduced cells (d, e) at

10 DPI. White lane is marking the position of the injury. Boxed areas correspond to the higher magnifications in the adjacent panels (c', d', e', e''). In c' and d' they show examples of NeuN negative transduced cells with glial morphology (white arrowheads). Higher magnifications in e' and e'' are pointing out transduced NeuN positive neuronal-like cells labelled with the arrowheads and numbers. (f) The table summarizing the proportion of NeuN+ dsRED+ cells out of all transduced cells 10 days after NEUROG2 overexpression only or together with HMGB2 and corresponding injury paradigm. All fluorescent images are full Z-projections of confocal Z-stack, except in pictures (c', d') and NeuN staining in (e', e''), which are single plane pictures. Abbreviations: DPI, days post injection; GM, gray matter; WM, white matter. Scale bars (b-e) 50 μm, (b', e', e'') 25 μm, (c', d') 20 μm.

3.6.3 Endogenous HMGB2 expression is increased at the lesion site after the stab wound injury

Although HMGB2 was not sufficient to help NEUROG2 to induce neuronal reprogramming in vivo, we made an interesting observation while looking for the overexpression of HMGB2 in Neurog2-T2A-Hmgb2-IRES-dsRED transduced cells at the injury site (Fig. 25b). Immunostaining against HMGB2 in the injured and injected brain did not reveal its expression only in the transduced cells but also its high abundance in the injured cortex 10 days post transduction (Fig. 25b). This finding was quite unpredictable since we previously never observed any HMGB2 expression outside the two neurogenic niches in the uninjured brain. We, therefore, first asked when after the injury this HMGB2 up-regulation appears and until when it persists. To address this point, we immunostained the sections for HMGB2 and GFAP to recognize the lesion site from the animals sacrificed at different time points (1, 5, 7 and 14 days) after the injury (Fig. 26a-d). We compared its levels to the levels in the hippocampus or subventricular zone in the same brain section and also looked to the contralateral side as a negative control. On the first day after the injury, we observed some sparse HMGB2+ cells at the lesion site (Fig. 26a). On the contrary, at 5 DPI there was a huge increase in the amount of the cells that up-regulated HMGB2. The intensity of the signal was, however, considerably weaker than in the cells expressing HMGB2 in the subgranular zone of hippocampus (Fig. 26b). The HMGB2 expression declined 7 days post injury and the amount of the cells expressing it was much lower (Fig. 26c). Some positive cells still could be found even 14 days after the injury (Fig. 26d). As we observed the most abundant expression at day 5 after the injury, when

the peak of the proliferation of the reactive astrocytes takes place, we next explored whether GFAP+ reactive astrocytes up-regulate HMGB2 and we could detect some colocalisation of both proteins. We observed some double positive cells (Fig. 26e), however, there were many more cells positive for the HMGB2 only. We also used Ki67+ proliferation marker to label dividing cells at 5 DPI and observed that all Ki67+ cells express HMGB2 (Fig. 26e), but not the other way around, since only a subpopulation of HMGB2 appeared to be Ki67+ positive. Unfortunately, the antibody combination did not allow us to simultaneously label HMGB2 together with the markers for other main populations that react after the injury such as for OPC and microglia. Taken together, HMGB2 protein is up-regulated after the injury in the adult mouse cortex, reaches the peak of expression at 5 DPI that slowly declines until 14 DPI. It was detected in all proliferating cells, some reactive astrocytes and is possibly enriched in many other different populations involved in the response to the injury such as OPCs, astroglia microglia, and macrophages.

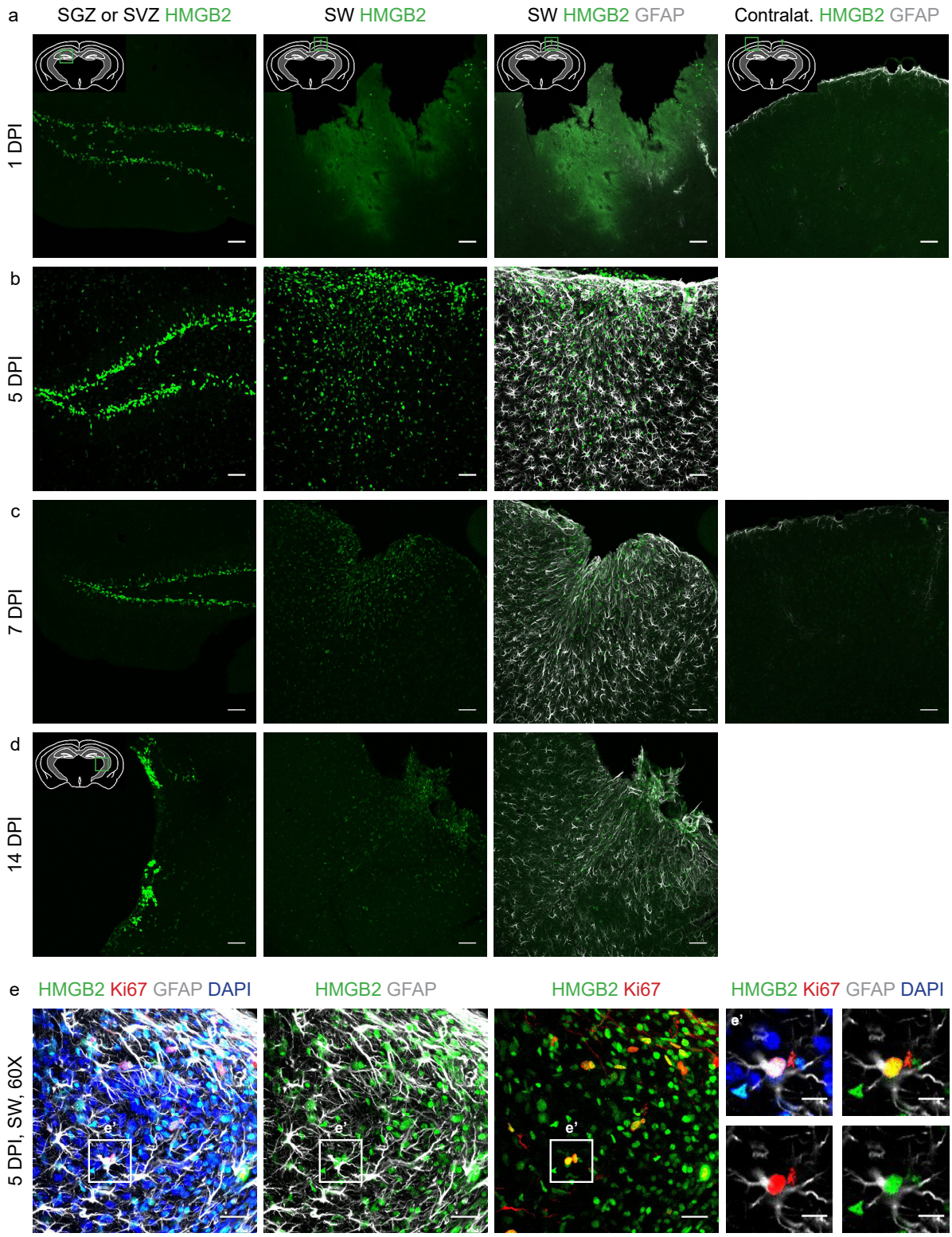

Figure 26: HMGB2 is up-regulated in the reactive glial cells upon the cortical stab wound injury.

(a-d) Micrographs depicting HMGB2 expression at the injury site at different time points after the injury. The lesion site was recognized by GFAP staining that labels reactive astrocytes. Expression levels were compared to the HMGB2 expression in

neurogenic niches SGZ or SVZ. The contralateral site at 1 and 7 DPI is shown as a negative control with no HMGB2 expression. The schemes of the coronal sections in the upper left edges of (a) are depicting the position in the brain where the picture was taken. (e) Higher magnification picture (60X) of HMGB2 expression at the injury site 5 DPI and its colocalisation with GFAP and Ki67 positive cells. e' represents the zoomed picture of the boxed area in e. All fluorescent images are full Z-projections of confocal Z-stack, except of high magnifications in (e'). Abbreviations: SGZ, subgranular zone; SVZ, subventricular zone; Contralat.; contralateral; DPI, days post injection; SW, stab wound. Scale bars (a-e) 50 µm, (e') 10 µm.

3.7 Molecular changes induced by HMGB2 overexpression to reprogram the cell fates

In vitro experiments demonstrated the involvement of HMGB2 protein in the transition from gliogenic to neuronal cell fate, but underlying molecular mechanisms still remain to be addressed. HMGB2 is a nuclear protein that belongs to one of the two major groups of the “chromatin architectural proteins”. Architectural proteins are defined as structural proteins, lacking enzymatic activity, but are able to bind to nucleosomes without DNA sequence specificity and change the local and global architecture of chromatin (Postnikov and Bustin, 2016). During the neuronal reprogramming, neurogenic transcription factors have to efficiently bind to their binding sites in order to induce the transcription of the neuronal program. However, for the ones that do not exhibit pioneer activity, this might be rather difficult when these sites are embedded in the closed chromatin. The dynamic interaction of HMGB2 protein with its chromatin targets could influence the ability of these regulatory factors to access their genomic binding sites. Recently it became very clear that not only induction of the neurogenic transcriptional network is crucial for the efficient reprogramming, but also the repression of the endogenous program in the glial cells and inhibition of alternative fates that might emerge during the reprogramming process (Mall et al., 2017).

Based on this knowledge, we developed three hypotheses how HMGB2 could act on the molecular level. In the first place, we propose the less permissive chromatin states in the FGF culture due to the lower levels of chromatin-associated proteins, which would interfere with NEUROG2 binding to its target sites. The HMGB2 protein might open these sites and enable binding of NEUROG2 that can finally induce the neurogenic program. Secondly, we hypothesize that forced expression of NEUROG2 in the FGF culture still can induce neurogenic fate, however, the insufficient repression of the gliogenic or alternative programs leads to the impaired acquisition of neuronal phenotype. We, therefore, speculate the involvement of HMGB2 in facilitating the repressor binding or opening the repressor binding sites that would exhibit the repression of the endogenous or alternative fates. Based on the fact, that transcriptional gene regulation does not only depend on promoters and nearby cis-regulatory elements, but also on distal regulatory elements, which are often located

far away from the genes they control, we developed our third hypothesis. The HMGB2 protein might elaborate opening or closing chromatin at the distal regulatory regions that represent binding sites of transcription factors involved in the reprogramming process.

To test these different possibilities, we established the ATAC-sequencing in our lab, promising method to identify regions of increased chromatin accessibility and nucleosome positioning, described by (Buenrostro et al., 2013, 2015). First, we aimed to identify the changes in the chromatin states upon EGF removal that are responsible for maintaining the astrocytes in the glial lineage even after neurogenic transcription factor overexpression. Next, we asked how does the chromatin accessibility change when overexpressing HMGB2 and NEUROG2 and planned to identify the regions that open or close via HMGB2 remodeling. Furthermore, we tried to correlate the chromatin-induced changes with the changes on the transcriptome level and therefore performed RNA-seq analysis. We looked at the gene expression in the control transduced cells and transcriptional changes induced by NEUROG2 overexpression, in order to explain the limited efficiency in neuronal conversion in the FGF culture. Next, we examined the gene expression changes by simultaneous overexpression of both, HMGB2 and NEUROG2 and tried to extract the ones that were missing before. This could explain how HMGB2 rescued the impaired acquisition of the neuronal program. Comparing both, ATAC-seq and RNA-seq datasets will give new insights into the chromatin-associated roadblocks and consequently transcriptional barriers in the process of direct reprogramming and molecular mechanism by which HMGB2 protein acts to overcome these barriers.

3.7.1 Collection of the transduced cells for the ATAC-seq and RNA-seq

For both sets of experiments, we cultured the astroglial cells for 10 days in two different growth factor conditions as previously described for the reprogramming. At day 10, cells were replated and transduced either with control retrovirus CAG-GFP, retroviruses encoding for Hmgb2-GFP or Neurog2-dsRED or both viruses simultaneously (Fig. 27a). 48 hours after transduction we used FACS (fluorescence activated cell sorting) in order to enrich for transduced cells only (Fig. 27b-d). After excluding dead cells and doublets, we set the gates using untransduced cells (Fig.

27b). We then collected all GFP+, dsRED+ or double positive cells from both conditions (Fig. 27c,d) and separated them into two batches. 50000 cells were used for the ATAC-sequencing library preparation and the rest to prepare RNA-seq libraries. We finally sequenced these libraries using the Illumina Next Generations Sequencing (NGS) approach (Fig. 27a).

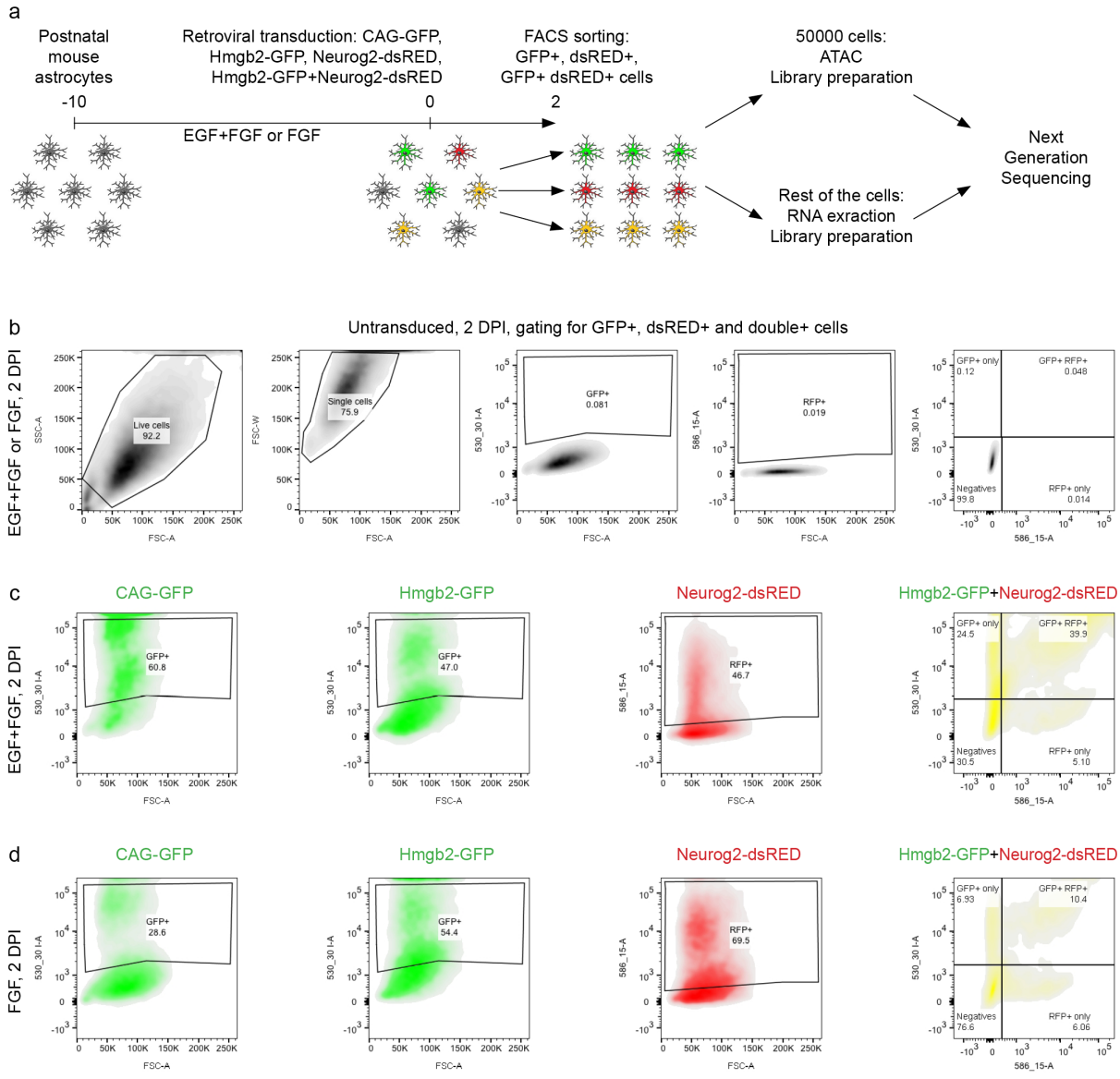

Figure 27: Astroglia collection after HMGB2 and NEUROG2 overexpression for the ATAC-seq and RNA-seq.

(a) Schematic representation of the protocol for the astroglia transduction, sorting and library preparation for the ATAC-seq and RNA-seq. (b) FACS plots showing the gates set up using untransduced cells to sort out the debris (first left), doublets (second left) and to sort GFP+, dsRED+ and double+ cells. (c,d) FACS plots

depicting the sorting strategy of transduced cells 48h DPI in EGF+FGF culture (c) and FGF culture (d). Abbreviations: DPI, days post induction; FACS, fluorescence activated cell sorting, ATAC, assay for transposase accessible chromatin; SSC-A, side scatter area; FSC-A forward scatter area; FSC-W forward scatter width.

3.7.2 ATAC-sequencing

ATAC-sequencing, assay for transposase accessible chromatin with high throughput sequencing, is a method to study the accessible sites of chromatin. The assay is based on direct in vitro transposition of sequencing adaptors into native chromatin using hyperactive Tn5 transposase, that has an ability to integrate into regions of opened chromatin, while less accessible sites make such transposition less probable. With this simple method, we can generate the amplifiable DNA fragments suitable for the high-throughput sequencing and the sequencing reads can then be used to identify regions of increased accessibility. Despite current methods for assaying chromatin structure and composition that require a couple of millions of cells as input material, the major advantage of this method is that it can be carried out with a sample size only of 50000 cells (Buenrostro et al., 2015). This was especially advantageous due to the limited amount of the sorted cells that we collected with the FACS after the retroviral transduction.

After establishing this novel method in our lab, we first performed the ATAC sequencing of the astroglia cultured for 10 days with growth factors EGF+FGF or FGF, transduced with the control virus (CAG-GFP) and collected 48 h after transduction. Next, we overexpressed HMGB2, NEUROG2 or both proteins in the astroglial cells for 48 h and prepared the chromatin for the sequencing. Following the sequencing of at least three biological replicates from each condition, the analysis was performed in collaboration with the Maren Büttner and Aaron Taudt (Institute of Computational Biology, Helmholtz Zentrum München). Quality control of the raw sequencing data showed good quality of the sequencing, but the remarkably high content of duplicates. The insert size distribution of sequenced fragments had a characteristic nucleosome-associated periodicity of approximately 200 bp, as shown in the original paper (Buenrostro et al., 2013, 2015). Confirming the required quality of the sequencing data, the BAM files were processed using the chromstaR software

(Taudt et al., 2016), followed by peak calling and differential peak analysis between different conditions (details described in Materials and methods).

First, we investigated the number of specifically enriched peaks comparing two control conditions. We aimed to pick up some differences in opened chromatin sites that might explain their different responsiveness to the reprogramming factors. In the CAG-GFP transduced cells grown in the EGF+FGF condition, we detected 283 peaks that were not present in the FGF condition (Fig. 28a). About 25% of these peaks were positioned at the promoters, therefore we created a list of the associated genes and looked for their functional annotation using David Gene Ontologies tool (Huang et al., 2009a, 2009b). Interestingly, the opened promotes in the EGF+FGF culture were enriched for the GO terms biological processes associated with nervous system development and neurogenesis (Fig. 28b). These genes were, for example, Ascl1, Sox2, Neurog2, which was quite surprising for the astroglial cells transduced with the control virus and not with any of neurogenic transcription factors. On the other hand, we also found GFAP promoter opened in this culture, suggesting that these astrocytes are somehow more plastic, having opened neurogenic promoters in parallel to gliogenic genes. Focusing on the FGF culture, we found 160 peaks specifically enriched in this condition, from which only 7 were located at the promoters with the rest assigned to the distal intragenic regions as annotated using the ChIPseeker tool (Yu et al., 2015a) (Fig. 28a). Next, we investigated the Neurog2 transduced cells and searched for the peaks significantly changed by the condition. Upon NEUROG2 overexpression there were 16 peaks present in the EGF+FGF culture and 109 in FGF only (Fig. 28a), suggesting that the cells do not equality respond to the forced neurogenesis on the chromatin levels due to their differences in the initial chromatin states. However, these differences between the two cultures are completely abolished upon HMGB2 overexpression. We did not find any specifically enriched peaks in one or the other condition anymore (Fig. 28a). These results suggest, that FGF cultured astrocytes with elevated HMGB2 levels and EGF+FGF astroglia become more homogenous regarding the chromatin states. A similar outcome was also observed after the simultaneous overexpression of both factors, where we detected only 12 specific peaks in the EGF+FGF culture and 17 in the FGF treated astroglia, respectively (Fig. 28a).

Observing this interesting function of HMGB2 making the chromatin states similar in both cultures, we next asked the question, what are the HMGB2 induced changes. To this aim, we performed the pairwise comparisons of the cells transduced with Hmgb2 and control transduced cells for both conditions. HMGB2 opens some regions, 391 in EGF+FGF and 263 in FGF (Fig. 28c) that are mostly located in the distal intragenic regions. However, investigating the 17 opened promoters in the FGF culture, revealed the opening of Ascl1, Sox2, and Neurog2, genes that were exactly the ones that were closed in the FGF culture, but opened in the EGF+FGF culture. This finding points out the important role of HMGB2 in opening the neurogenic regions. Interestingly, we observed that HMGB2 mostly functions in making chromatin more fluidic, since there were almost no peaks that would get closed upon HMGB2 overexpression (Fig. 28c). In the next step, we asked what are the NEUROG2-induced changes in both cultures. Compared to the HMGB2 overexpression, the number of newly opened or closed peaks was much higher. In the EGF+FGF culture, NEUROG2 opens 2722 peaks, while 575 peaks get closed (Fig. 28c). In the FGF culture, there were 2071 enriched peaks compared to the control and 206 closed peaks in the control (Fig. 28c). Only a few percents of these peaks are located at the gene promoters while the others can be found in noncoding regions. We closely investigated the peaks at the promoters opened upon NEUROG2 overexpression, looked at the proportion of their overlap in both cultures using the BioVenn tool (Hulsen et al., 2008) and performed the GO term analysis. 46 peaks at the promoters specific for EGF+FGF culture were related to the GO terms retina development and regulation of phosphorylation (Fig. 28d). Interestingly, the 39 FGF specific peaks were assigned to the genes related to neurogenesis (Fig. 28d). Similarly to the HMGB2 function, also NEUROG2 opens the promoters of neurogenic genes such as Ascl1, Sox2, and Neurog2 that were previously closed in this culture. Overlapping 19 genes did not show any GO terms enrichment due to their very different functions in metabolism, phosphorylation, apoptosis, regulation of transcription, transcription factor binding, and many others. Similarly, the promoters closed in both cultures show very little overlap and no enrichment for specific GO terms. Lastly, we investigated the chromatin changes induced by simultaneous overexpression of both, HMGB2 and NEUROG2. The numbers of differentially expressed opened peaks were very similar to the Neurog2-induced ones (2910 in EGF+FGF and 2024 in FGF), resulting also in a very similar number of opened

promoters (71 in EGF+FGF and 53 in FGF) (Fig. 28c). We looked for their overlap in both cultures and corresponding GO terms as we did before, and observed completely comparable results to the Neurog2-induced peaks, showing the specific enrichment of neurogenic promoters opened in the FGF culture (Fig. 28e). Since the GO terms were completely comparable, we asked the question how big is the overlap of the peaks at the promoters when overexpressing NEUROG2 alone or in combination with HMGB2. This overlap was basically 100%, pointing out that the addition of HMGB2 does not result in any additionally opened peaks, at least not at the promoters. However, there was a big decrease in the number of closed peaks upon the simultaneous expression of both factors, we found only 32 in EGF+FGF cultured cells and 33 in FGF astroglia (Fig. 28e). This shows again that HMGB2 does not participate in any closure of the chromatin and actually even opens the sites that were closed by NEUROG2. To summarize the ATAC-sequencing data, we found a surprising difference between two cultures with EGF+FGF culture having opened promoter of the neurogenic genes that might explain the more efficient reprogramming. HMGB2 protein makes these two cultures more similar by opening exactly these promoters and possibly erases the other differences in chromatin compaction in the distal intragenic regions. However, NEUROG2 on its own is also able to open these promoters in the FGF culture, but this might delay the whole reprogramming process, which can more efficiently start if these regions are already opened. The simultaneous overexpression of both factors has a comparable effect to the NEUROG2 alone, due to the fact that HMGB2 works similarly and might only complement the role of the NEUROG2. This is important in the FGF culture, where the neurogenic promoters are closed and by adding HMGB2 the opening might happen faster and more efficient. In the next step, we decided to investigate how the changes in the chromatin states influence the transcriptional program of both cultures and therefore performed the RNA-seq analysis from the same sample conditions.

a Differential peak analysis in EGF+FGF culture compared to FGF culture transduced by different retroviruses

Comparison		Peaks		Peaks at the promoters	
		Up in E+F	Up in F	Up in E+F	Up in F
CAG-GFP	EGF+FGF vs FGF	283	160	74	7
Neurog2	EGF+FGF vs FGF	16	109	2	3
Hmgb2	EGF+FGF vs FGF	0	2	0	0
Hmgb2+Neurog2	EGF+FGF vs FGF	12	17	4	0

b

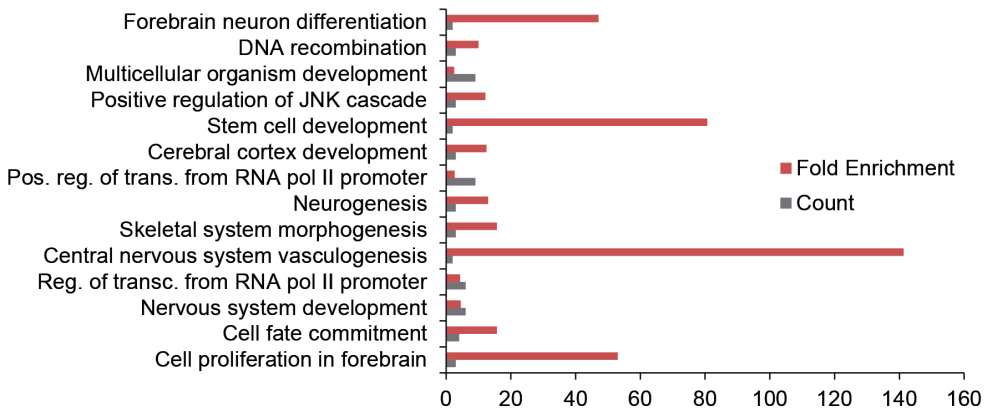

c Differential peaks induced by HMGB2 or NEUROG2 overexpression in both cultures

Comparison		Peaks		Peaks at the promoters	
		Open in Hmgb2	Open in CAG-GFP	Open in Hmgb2	Open in CAG-GFP
EGF+FGF	Hmgb2 vs CAG-GFP	391	4	12	1
FGF	Hmgb2 vs CAG-GFP	263	5	17	1
		Open in Neurog2	Open in CAG-GFP	Open in Neurog2	Open in CAG-GFP
EGF+FGF	Neurog2 vs CAG-GFP	2722	575	65	24
FGF	Neurog2 vs CAG-GFP	2071	206	58	11
		Open in double	Open in CAG-GFP	Open in double	Open in CAG-GFP
EGF+FGF	Hmgb2+Neurog2 vs CAG-GFP	2910	32	71	0
FGF	Hmgb2+Neurog2 vs CAG-GFP	2024	33	53	5

d Regions at the promoters opened upon NEUROG2 OE

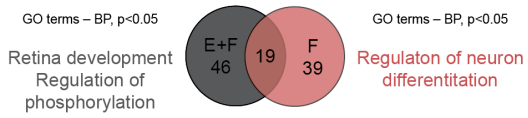

e Regions at the promoters opened upon HMGB2+NEUROG2 OE

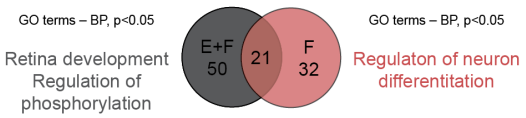

Figure 28: ATAC-seq analysis of two cultures to explore the chromatin-related changes.

(a) The summary of differential peaks analysis done by ChromstaR software comparing EGF+FGF culture versus FGF culture upon transduction with the control CAG-GFP virus or overexpression of HMGB2, NEUROG2 or both together. Highlighted 74 peaks at the promoters were used as an input in GO terms analysis in (b). (b) Bar chart depicting GO terms related to 74 peaks at the promoters enriched in

EGF+FGF culture in the control conditions. (c) The table summarizing the number of opened or closed peaks upon overexpression of HMGB2, NEUROG2 or both compared to the control transduced cells in both cultures. (d-e) Venn diagram presenting the overlap of peaks at the promoters in both cultures and their associated GO terms upon induction of Neurog2 (d) or Hmgb2+Neurog2 (e). Abbreviations: E+F, EGF+FGF; F, FGF; GO, gene ontology; BP, biological process; OE, overexpression.

3.7.3 Transcriptome analysis of the EGF+FGF and FGF cultured astroglial cells upon transduction with different retroviruses

3.7.3.1 Transcriptome of the CAG-GFP transduced cells

In order to explore the transcriptional changes induced during the reprogramming process, we isolated the mRNA from the cells overexpressing NEUROG2, HMGB2 or both factors and performed transcriptome analysis. First, we performed the comparison of the control-transduced cells cultured in two different conditions, in order to address the question whether we could identify some intrinsic differences between the cultures that are possibly responsible for their different reprogramming capacity. Surprisingly, we observed a relatively high number of genes that were enriched specifically in one or the other culture, suggesting that culturing the cells in different growth factor conditions induces quite some differences at the transcriptome level. We detected 234 genes (fold change>2, $p<0.05$) specifically enriched in EGF+FGF cultured cells 48 h after transduction with the CAG-GFP control virus. This set of EGF+FGF enriched genes was related to many different gene ontology (GO) terms (fold enrichment>2, $p<0.05$) in the category biological processes (Huang et al., 2009a, 2009b), such as cellular response to different stimuli, metabolic processes, and regulation of protein functions (Fig. 29a). In the FGF cultured cells, we detected 329 enriched genes that have a significantly higher expression when compared to EGF+FGF culture. Interestingly, the most represented GO terms biological processes were related to oligodendrocyte cell fate specification (Fig. 29b), but there were also some genes associated with the terms such as nervous system development, regulation of transcription and metabolic processes (Fig. 29b). Taken together, due to the high number of deferentially expressed genes between two culturing conditions it is rather difficult to determine which of them might be involved in limited

reprogramming capacity of the FGF culture. However, there were many genes specific for the FGF culture, which are related to the oligodendrocyte differentiation suggesting the enrichment of oligodendrocytic population in this growth condition. This subpopulation might be resistant to neurogenic transcription factor induction and would not undergo the fate transition. To test this hypothesis, we next explored the Neurog2 induced changes in both cultures.

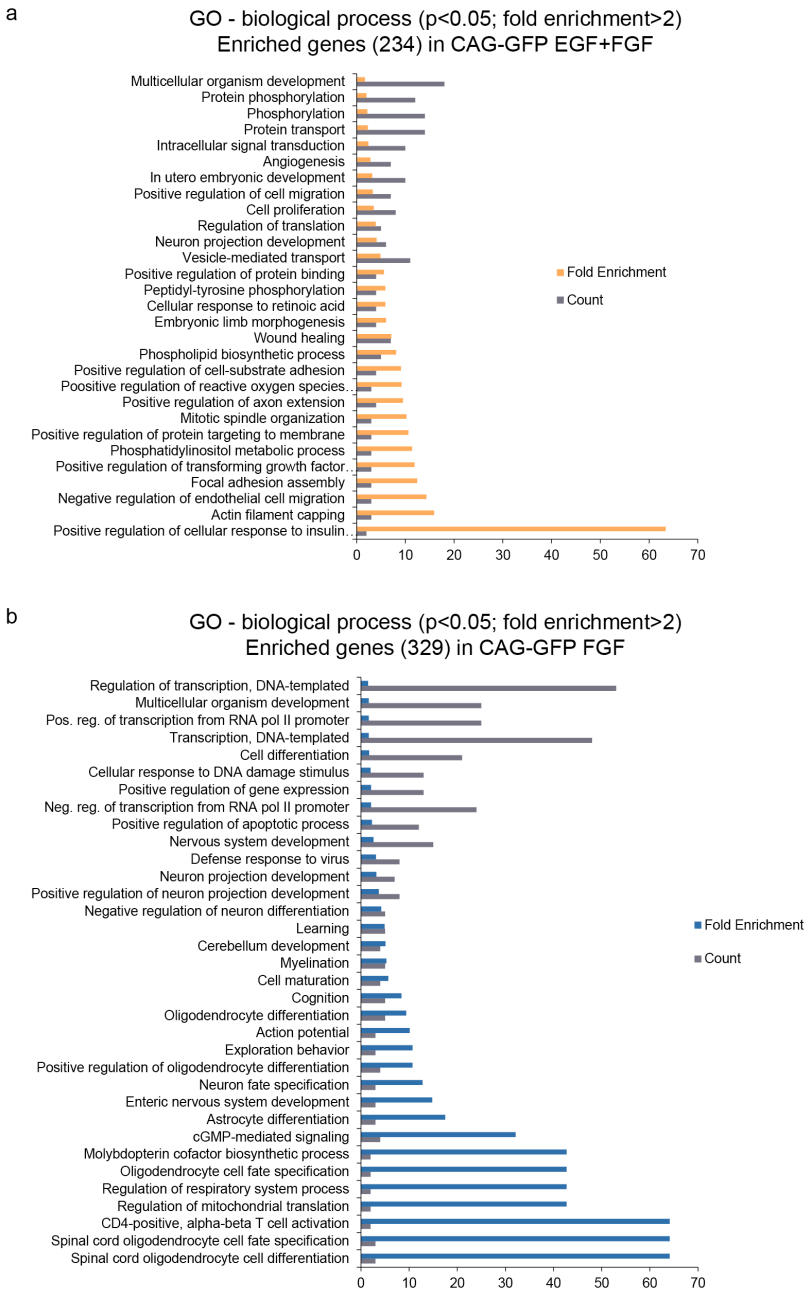

Figure 29: EGF+FGF and FGF cultured astroglia transduced with the control virus exhibit differences in their transcriptional programs.

(a,b) Bar charts depicting GO terms biological processes assigned to the 234 genes specifically enriched in the EGF+FGF culture (a) and to the 329 genes specific for the FGF culture (b). Abbreviations: GO, gene ontology.

3.7.3.2 Transcriptional changes induced by NEUROG2 overexpression

Following the comparison of two control conditions, we analyzed the transcriptome of Neurog2 transduced astroglial cultures grown with EGF+FGF or FGF. Based on lower reprogramming capacity of FGF culture, one of the hypotheses was that overexpression of NEUROG2 in this culture might not efficiently induce neuronal program at the transcriptional level. In order to address this point, we carefully investigated the genes enriched in both conditions upon NEUROG2 overexpression and their overlap. Activation of NEUROG2 after 48 hours changed the expression of 596 genes in EGF+FGF culture and 711 in FGF culture compared to the CAG-GFP transduced control in each condition (fold change>2, $p<0.05$). Inspecting the top 25 genes with the highest fold enrichment compared to control in both cultures revealed induction of quite some genes that were present in both conditions (Fig. 30a). We, therefore, looked at the proportion of the overlapping genes in both cultures that were significantly enriched after NEUROG2 overexpression using the BioVenn tool (Hulsen et al., 2008) and found 283 genes common for both cultures (Fig. 30b). This set of common regulated genes was significantly enriched for the gene ontology (GO) terms biological processes (Huang et al., 2009a, 2009b) associated with neuronal differentiation and regulation of neurogenesis (Fig. 30b,c). Interestingly, most of the published NEUROG2 downstream targets like NeuroD1, Rnd2, Dll1, Dll3 (Castro et al., 2006; Gohlke et al., 2008; Henke et al., 2009; Ochiai et al., 2009; Schuurmans and Guillemot, 2002; Seo et al., 2007) or previously reported NEUROG2 induced genes in the reprogramming of the astrocytes like Hes6, Insm, Prox1, Sox11, Trnp1 and Cnr1 (Masserdotti et al., 2015) were up-regulated in both cultures. This suggests the ability of NEUROG2 to induce its targets regardless of the culture condition. As this does not explain why the FGF cultured cells do not turn into the neurons although they have induction of the neurogenic transcriptional program similar to the EGF+FGF culture, we investigated whether the levels of induction are lower and not sufficient to promote neurogenesis (Fig. 30d). This was not the case, as we observed similar enrichment of NEUROG2 targets expression when compared

to the control in both cultures for most of the investigated genes (Fig. 30d). The next hypothesis would be the emergence of a competing alternative program that would not allow the cell to acquire neurogenic fate. However, we found genes that are related to the GO terms linked to the alternative fate commitment of mesodermal origin in both cultures (Fig. 30b). NEUROG2 induces the different sets of genes in both cultures but most of them are related to the similar alternative program. In addition, in both cultures, NEUROG2 induces the changes in transcription rate. Searching for the GO terms present specifically in the EGF+FGF culture revealed that forced expression of NEUROG2 resulted in the high expression of genes involved in the regulation cell cycle (Fig. 30b). On the other side the genes that are specific for the FGF culture are involved in different signaling pathways (Fig. 30b). To sum it up, we found a subset of NEUROG2 genes specific for the culture condition and subset of commonly induced genes that are enriched for GO terms related to neurogenesis. Since these genes are in both cultures induced to the same level, we can also confirm that there is not only a subpopulation in the FGF culture that would respond to forced neurogenesis. Induction of the neurogenic transcriptional program and the partial emergence of the alternative program are similar in both cultures and therefore cannot account for the differences in the reprogramming efficiency.

Induced reprogramming does not only require the induction of the neurogenic genes but also silencing of transcriptional program defining the starting cell population and the alternative fates that might be induced in parallel. By investigating the genes down-regulated in both cultures and their overlap, we tried to address the question whether the gliogenic fate in the FGF culture was not efficiency silenced and this resulted in the reprogramming failure. In general, we found much less down-regulated genes as up-regulated. In the EGF+FGF culture, the total amount of down-regulated genes compared to the control was 257, while in the FGF culture 362 (fold change>2, $p<0.05$) (Fig. 30e). 100 overlapping genes were enriched for the GO terms biological processes associated with the development of alternative fate mesodermal origin (angiogenesis, cartilage development, muscle development) or signaling pathways (BMP, protein kinase signaling) (Fig. 30e). Genes specifically down-regulated in the EGF+FGF culture were related to the regulation of transcription, while the ones in the FGF culture to the alternative fate of mesodermal and endodermal origin and signaling pathways (Wnt and FGF) (Fig. 30e).

Interestingly, the NEUROG2 overexpression stimulates the genes of the alternative program, which cells possibly try to repress at the same time to keep their identity. As we could not find any astrocyte markers down-regulated in the subset of significantly repressed genes, we manually looked for their expression levels compared to the control. While glutamate transporter 1 (Slc17a7 gene) was not detected, there were many transcript variants of GLAST (encoded by Slc1a3 gene) and glutamine synthetase (Glul), however not showing any differences upon NEUROG2 overexpression. We investigated some further markers for the astroglia, such as GFAP, S100β, Aldh1l1, Aqp4, Acsbg1, and Gjb6 - Connexin30 (Cahoy et al., 2008) (Fig. 30f). In the EGF+FGF culture, GFAP, some transcript variants of Acsbg1 and connexin30 showed a slight decrease already, while in the FGF culture, only the GFAP and one variant of Acsbg1 were down-regulated compared to the control (Fig. 30f). These changes were not significant, however, they show the trend in repression of the endogenous program. In contrary to neurogenic genes induction, that appears very rapidly, the silencing of the endogenous cell program might be slower as a consequence of the neuronal fate acquisition. In order to address the question, whether this can be done efficiently in both cultures, we would need to investigate the transcriptional changes at the later time point. This might help us to interpret the differences in the reprogramming capacity of the EGF+FGF and FGF cultures since they cannot be explained by transcriptional changes observed at 48 h after NEUROG2 overexpression.

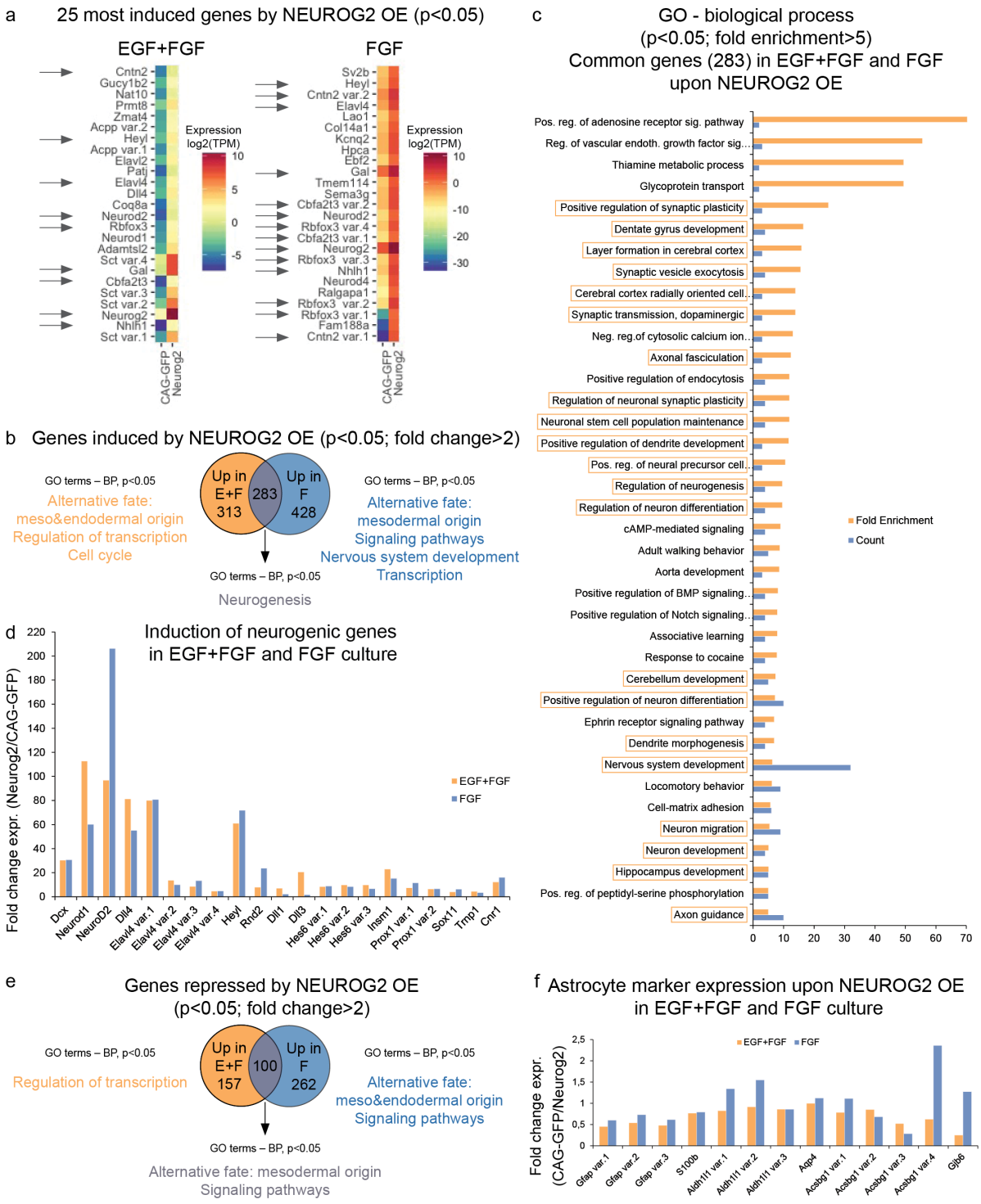

Figure 30: Transcriptional changes induced or repressed by NEUROG2 overexpression.

(a) Heatmap showing the expression of 25 most induced genes after NEUROG2 overexpression compared to the control in EGF+FGF and FGF culture. The arrows are pointing out the genes that are commonly induced in both cultures. (b) Venn diagram showing the number of the Neurog2-induced genes in both cultures, their overlap and corresponding GO terms biological processes. (c) Bar chart depicting

GO terms related to the commonly induced genes after NEUROG2 overexpression. Boxed areas are labeling the GO terms associated with neurogenesis. (d) Graph showing fold change enrichment of neurogenic genes compared to control in both conditions. (e) Venn diagram presenting the numbers of down-regulated genes in both cultures their overlap with associated GO terms. (f) Bar chart showing the fold change differences in expression of astrocyte markers compared to the control in EGF+FGF and FGF culture. Abbreviations: OE, overexpression; TPM, transcripts per million; E+F, EGF+FGF; F, FGF; GO, gene ontology; BP, biological process; expr., expression.

3.7.3.3 HMGB2-related changes in the gene expression in the EGF+FGF and FGF cultures

Next, we investigated the transcriptional changes introduced by HMGB2 overexpression in EGF+FGF and FGF cultures cells. We aimed to elucidate the ones enabling better reprogramming and improved neuronal yield of the FGF culture. HMGB2 overexpression induced an independent set of genes in both cultures (111 in EGF+FGF and 102 in FGF), with very little overlap (9 genes) (Fig. 31a). However, the GO terms biological processes assigned to the differentially expressed genes are similar in both culturing conditions indicating the involvement of HMGB2 in the regulation of transcription (Fig. 31a). Specifically, in the EGF+FGF culture, HMGB2 facilitates the DNA repair and regulates apoptotic signaling pathways. In the FGF culture, it promotes the expression of different kinases involved in protein phosphorylation (Fig. 31a). The 9 commonly regulated genes in both cultures are related to the regulation of transcription and regulation of the neuronal differentiation (Fig. 31a). Interestingly, the most up-regulated gene in the EGF+FGF culture upon HMGB2 overexpression is Neurog2, which is also in the FGF culture one of the top 10 up-regulated ones. In addition, we discovered up-regulation of some known Neurog2 targets like Heyl, Dll4, and Elavl4, which might be induced by HMGB2 directly or as a consequence of Neurog2 up-regulation. These results suggest that HMGB2 induces Neurog2 expression and possibly enhances its function during the reprogramming process. Similarly as described above, we found a specific subset of down-regulated genes in each of the cultures upon HMGB2 overexpression with only 6 common ones (Fig. 31b). These 6 genes are involved in different processes like DNA repair, cell cycle regulation, apoptosis, and phosphorylation. Genes specifically down-regulated in the EGF+FGF culture are assigned to the GO term regulation of

transcription and DNA damage checkpoint (Fig. 31b). Similarly, also the FGF culture specific genes that were lower in their expression are related to the regulation of transcription and DNA repair (Fig. 31b).

To sum up, despite most of the significantly up and down-regulated genes being different in both cultures upon HMGB2 overexpression, the majority of them play a role in the gene expression regulation and response to the DNA damage. Importantly, HMGB2 induced transcriptional changes that stimulate Neurog2 and its targets expression, which might enhance the reprogramming process in the FGF culture where NEUROG2 alone is not sufficient to do so. In addition, HMGB2 promotes changes in the transcripts involved in the DNA repair that might become very relevant when the cells undergo the reprogramming. During the metabolic switch from the glycolysis to the oxidative phosphorylation in the conversion process from the astroglial cells to the neurons, there is an excessive production of the reactive oxidative species (ROS) (Gascón et al., 2016; Quadrato et al., 2016) that can cause a lot of endogenous DNA damage. Therefore HMGB2 induced DNA repair mechanisms might be very beneficial after overexpression together with NEUROG2, to help the cells survive and properly acquire a neuronal identity.

3.7.3.4 Simultaneous overexpression of HMGB2 and NEUROG2 and its related transcriptional changes

To explore more about the transcriptional changes stimulated by simultaneous overexpression of NEUROG2 and HMGB2, we investigated the genes up and down-regulated (fold change>2, $p<0.05$) 48 h after the viral transduction with both factors (Fig. 31c,d). The number of differentially up-regulated genes was similar to the NEUROG2 overexpression alone, showing a subset of genes induced specifically in EGF+FGF culture (378 genes), FGF culture (367 genes) and around one third of genes being commonly up-regulated (254 genes). The GO term analysis of biological processes ($p<0.05$) gave a quite similar outcome to the one with NEUROG2 overexpression only (Fig. 30b; Fig. 31c). Commonly enriched genes were related to neurogenesis, while in each of both cultures there were some specific genes related to the alternative fate induction and regulation of transcription (Fig. 31c). The analysis of the gene repression upon NEUROG2 and HMGB2 overexpression showed many

more genes down-regulated when compared to NEUROG2 alone in the EGF+FGF culture and also more commonly down-regulated genes (Fig. 30e; Fig. 31d). In both cultures, we observed repressed genes associated to the alternative fate, as well as endogenous gliogenic fate in the EGF+FGF culture (Fig. 31d), with down-regulation of astrocytic marker S100β for 2-fold. Interestingly, when HMGB2 is overexpressed together with NEUROG2, many genes repressed in both cultures were related to the GO term metabolic processes (Fig. 31d). In the EGF+FGF culture, these were lipid metabolic processes and glycogen metabolic processes, while in FGF culture in addition to lipid metabolic processes there were genes down-regulated as a response to oxidative stress. HMGB2 proteins seem to work at the different levels, for example enhancing the transcription, facilitating DNA repair and together with NEUROG2 participating in changes in metabolic states.

To elucidate which of these processes are the most relevant for the conversion, we decided to overlay differentially expressed genes in the conditions where reprogramming works efficiently (EGF+FGF upon NEUROG2 overexpression, FGF upon NEUROG2+HMGB2 overexpression) and exclude the genes showing differences in the inefficient reprogramming paradigm (FGF upon NEUROG2 overexpression) (Fig. 31e,f). With this approach we found 36 common up-regulated genes having functions in chromatin remodeling, regulation of gene expression, and transcription factors binding (Fig. 31e). The examination of commonly down-regulated genes from 3 conditions revealed only 15 genes related to alternative fate repression, for example, cardiac muscle cell development (Fig. 31f). All in all, HMGB2 incudes transcriptional changes in the FGF culture possibly by his chromatin remodeling function. Although NEUROG2 manages to induce its targets in both cultures, this seems not to be enough for the efficient reprogramming in the FGF cultures. Therefore, additional transcriptional changes also need to take place and can be induced by higher levels of HMGB2 in the culture. On the other side, HMGB2 also helps to more efficiently down-regulate the emerging alternative program leading to muscle cells differentiation mostly likely by enabling the access to some repressor complexes via chromatin remodeling.

To summarize the transcriptome analysis results, we observed considerable differences in the global gene expression that are influenced by different growth

factors conditions. NEUROG2 is able to induce neurogenic program in both cultures and to repress genes specific for each of the condition, however, having a role in similar biological processes. HMGB2 shows its involvement mostly in the regulation of transcription including the induction of Neurog2 levels and DNA damage response. Synergistic effect of both factors results in a similar outcome as with Neurog2 alone when investigating the up-regulated genes, however, it reveals more repressed genes related to the metabolic changes that were not regulated upon the overexpression of NEUROG2 alone.

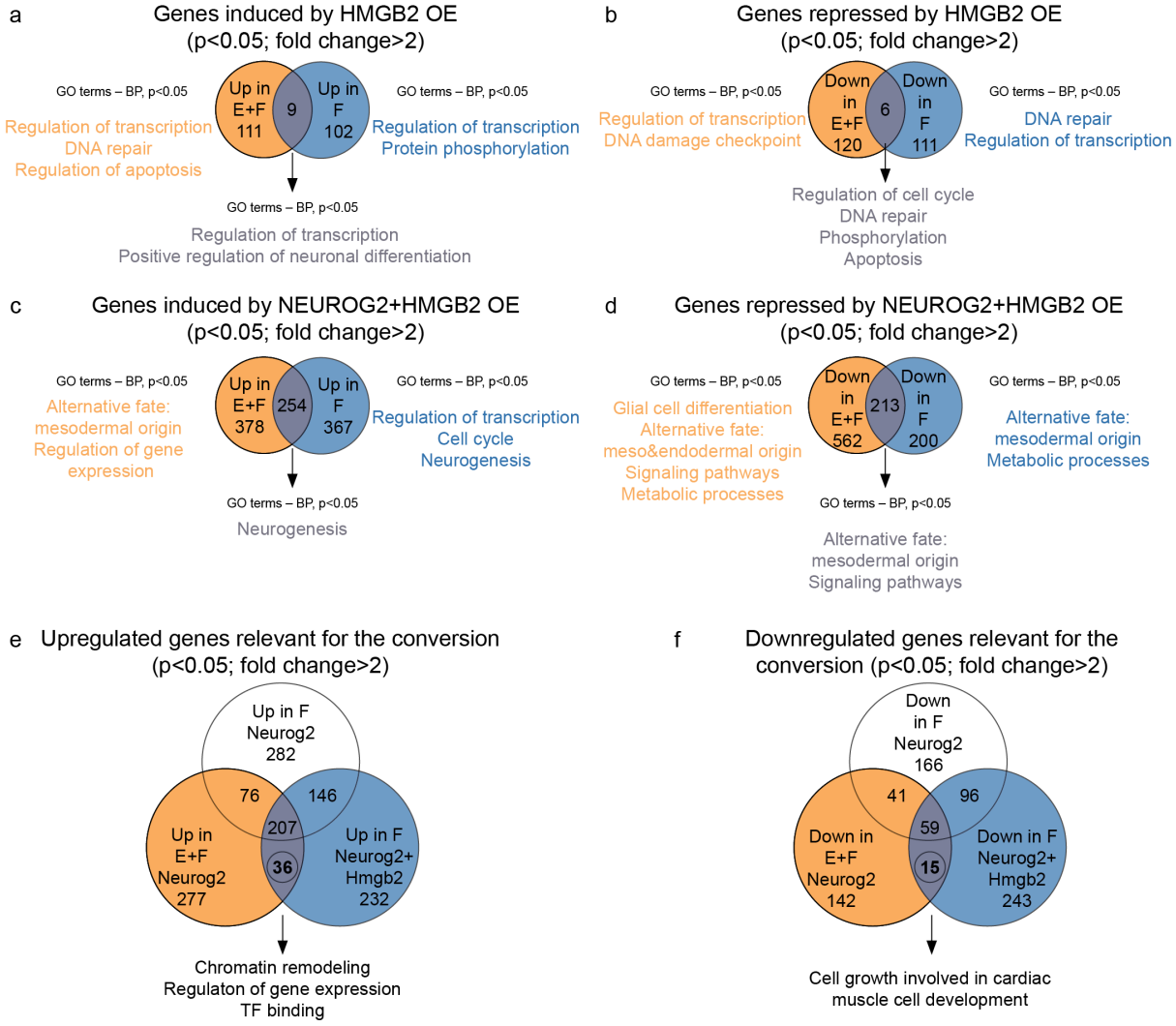

Figure 31: Transcriptional changes induced by HMGB2 overexpression and simultaneous overexpression of HMGB2 and NEUROG2.

(a-d) Venn diagrams showing up or down-regulated genes in both cultures, their overlap and corresponding GO terms biological processes after transduction with the

retrovirus encoding for Hmgb2 only (a,b) or Neurog2 and Hmgb2 together (c,d). (e) Venn diagrams overlaying the up-regulated genes from three different conditions, showing 36 genes relevant for the conversion and their functional annotations. (f) Venn diagram showing 18 down-regulated genes and corresponding GO term that is important to enable efficient reprogramming identified by overlapping the conditions of the cultures with a good neuronal yield.

4 Discussion

Our ability to manipulate cell fate depends very much on our understanding of the underlying molecular mechanisms specifying or maintaining particular cell fate. In order to study the molecular changes and hurdles of the direct reprogramming, we first developed a new in vitro model that revealed the influence of extrinsic factors on the capacity of the cells to undergo the fate transition. I will first discuss how we developed this model and what we have learned from comparing the two paradigms with good and impaired reprogramming capacity. I will then focus on chromatin-associated changes and the role of architectural protein HMGB2, which is largely responsible for increasing the efficiency of reprogramming in the cells that are otherwise difficult to convert in vitro. I will continue the discussion with the main principles of NEUROG2 and HMGB2 transcriptional regulation during direct neuronal conversion, trying to pinpoint the changes that are sufficient to silence the programs of the starting cells and to activate those of the target cells. Finally, I will conclude by summarizing the newly gained knowledge on the molecular mechanism of the reprogramming and raised some questions that still remain to be addressed.

4.1 New in vitro model suitable to study challenging reprogramming conditions and identify possible barriers in the cell fate transition

The knowledge about the cellular and molecular mechanisms and possible hurdles of glial to neuronal cell fate transition can be only gained by analysing the less efficient reprogramming paradigms, similar to the in vivo environment conditions. To better recapitulate in vivo environment after the brain injury and establish more challenging model for molecular studies in vitro, we adjusted growth factors composition and cultured postnatal astrocytes in the medium lacking EGF, as its levels rapidly decrease after the injury. At the lesion site, 3-4 days post injury when neurogenic transcription factors are applied to induce the neuronal reprogramming, EGF levels already reach their baseline (Addington et al., 2015) and rather limited number of neurons from adult glial cells by forced expression of single neurogenic factor NEUROG2 can be achieved (Gascón et al., 2016). The removal of EGF from the culturing medium, similarly to the in vivo conditions, rendered the astroglia into the

cell types resistant to the reprogramming by the overexpression of neurogenic transcription factors in vitro. Therefore, we established a new in vitro model, consisting of the cells cultured with two growth factors EGF+FGF, having a good reprogramming capacity and the cells with limited conversion rate cultured with FGF growth factor only. Next, we performed different sets of experiments to compare the molecular features of the cells prone and resistant to reprogramming to identify the ones that enable efficient acquisition of neuronal fate and the ones that inhibit this process.

4.2 EGF+FGF and FGF cultured astroglia are not different based on their markers identity but differ in their cell cycle properties

We first investigated similarities between two cultures based on their cellular markers expression, to exclude the influence of the growth factors on the culture composition. It was important to prove that the removal of the EGF from the culturing medium does not result in the enrichment of some specific populations during the expansion phase, which would respond differently to the neurogenic transcription factor overexpression. Since the astroglial cells are obtained directly from the piece of postnatal cortical tissue, different cell types such as astrocytes, oligodendrocytes, pericytes, microglia, and neurons can be co-isolated. However, using published protocol (Heinrich et al., 2011), we enrich mostly for the GFAP+ astrocytes. The purity of the EGF+FGF culture was previously confirmed with various astrocyte markers and genetic fate mapping (Berninger et al., 2007; Heinrich et al., 2010; Heins et al., 2002), where they also proved that these cells do not have any intrinsic neurogenic potential or contamination with β-III TUBULIN+ neurons. Importantly, we demonstrated that the withdrawal of the EGF does not change the characteristics of the culture, as the majority of cells remained S100β+ and GFAP+ in both conditions. However, most of the cells were also OLIG2+ regardless of the growth factor composition. Previous studies indicated the OLIG2 expression in immature developing astrocytes and its role in astrocyte development in the brain (Cai et al., 2007; Marshall et al., 2005), therefore it is not surprising that we detected it in our postnatal astroglial cells. Despite expecting a low proportion of contaminating oligodendrocyte progenitor cells in both cultures, we would need to use other

markers that would exclusively label OPCs, such as SOX10 or PDGFRα to properly quantify the abundance of this population.

Based on tested markers we concluded that the different growth factor composition doesn't affect the starting population, yet, it also doesn't account for their different reprogrammability. We, therefore, asked whether the observed differences in the proliferation rate could explain the lower neuronal yield in the FGF culture. Most of the published data suggest that proliferative behavior and direct fate conversion of the cells are not necessarily directly linked. Many cell types can switch their cell fate into neurons without cell division (Fishman et al., 2015; Heinrich et al., 2010; Karow et al., 2012; Marro et al., 2011). Live cell imaging of postnatal astrocytes during reprogramming process revealed that most of the astrocytes directly converted into neurons without dividing after the retroviral transduction (Gascon et al., 2015). Based on this observation from previous studies we assumed, that the better conversion efficiency of EGF+FGF culture is not a consequence of its higher proliferation activity.

All in all, we observed that culturing the cells with or without EGF growth factor does not affect heterogeneity of the cultures apart from observed differences in the cell cycle. However, this analysis was based on a few commonly used cellular markers. To investigate the composition of the cultures at the single cell level, recent advances in single cell transcriptomics might provide valuable insights into cellular heterogeneity. We performed first pilot experiments using Fluidigm single cell RNA-sequencing approach on untransduced astrocytes 10 days after the culturing with EGF+FGF of FGF growth factors, which present the starting point of the reprogramming. The preliminary PCA analysis suggested that most of the cells of both cultures cluster together, however it revealed the subpopulation in the FGF culture that formed a separate cluster. We would speculate that this might be the population that favors astrocytes lineage commitment over neurogenesis, but the analysis is still ongoing and will hopefully give more insights into the heterogeneity of our starting cultures. In the meantime, we investigated the intrinsic differences between two cultures more into details using the proteome analysis. With immunostaining, we were able to test only for few markers that did not reveal the

differences, which would explain the altered reprogramming capacity of FGF culture. With this aim, we investigated the global protein expression in both cultures.

4.3 Changes in metabolic states and chromatin compaction could be responsible for different reprogramming capacity of two cultures

The proteome analysis did not reveal the major differences between two cultures what was not completely unexpected since the majority of cells exhibited the astrocyte features and showed similar expression of tested cellular markers regardless of the culture condition. Still, we identified some proteins specifically enriched in the each of the cultures and carefully investigated them in order to identify the molecular features that could explain the differences in the reprogramming capacity. The GO terms assigned to the proteins enriched specifically in the FGF culture suggest some morphological differences of these cells and the enrichment of the cell populations with the muscle cell identity. The only source of such cells in the culture could be vascular smooth muscle cells and pericytes. Published data reported that many different FGF growth factors, including FGF2, induce vascular smooth muscle cells proliferation in vitro (Yang et al., 2015). Nevertheless, comparing EGF+FGF and FGF cultures, we did not observe any differences in αSMA marker, which should label both of the above-mentioned populations. Furthermore, the percentage of transduced cells expressing smooth muscle actin was so low that it cannot account for different reprogramming capacity of two cultures. As we did not identify any other features in the FGF culture that would maintain these cells in the glial lineage after the overexpression of neurogenic transcription factors, we decided to investigate the proteins enriched in the EGF+FGF culture with the aim to identify the factors necessary for the efficient reprogramming.

Proteins highly enriched in the EGF+FGF culture were mostly related to the metabolism and chromatin remodeling. The importance of the metabolic transition in the neuronal reprogramming was recently published in our lab (Gascón et al., 2016). The astrocytes mostly rely on anaerobic glycolysis and β-oxidation (Tsacopoulos and Magistretti, 1996) but during reprogramming, they need to switch to an oxidative

metabolism, which is required by neurons. This can lead to an excessive oxidative stress (Gascón et al., 2016; Quadrato et al., 2016), that results in the cell death and interferes with the successful reprogramming. The proteins identified to be specific for the EGF+FGF culture are mostly components of the electron transport chain in oxidative phosphorylation. Higher expression of these proteins in the EGF+FGF cultured astrocytes could allow them to acquire the most appropriate metabolism more efficiently than FGF cultured cells. The metabolic transition might occur more smoothly as these cells already have the necessary components that FGF astrocytes still need to gain. However, to test this hypothesis we would need to perform the Seahorse analysis (Agilent) that enables measurement of the two major energy pathways (mitochondrial respiration and glycolysis) in live cells in real time. We would expect that EGF+FGF astrocytes exhibit higher mitochondrial respiration and rely less on the glycolysis compared to the FGF cultured cells.

Along with the enrichment of proteins related to the respiratory chain, the proteome analysis revealed the abundance of the chromatin-associated proteins in the EGF+FGF culture. This raised an important question about the role of the chromatin status of the starter cell in modulating reprogramming. While the differences in the chromatin compaction in both cultures were addressed using ATAC-sequencing and will be discussed later on, we first focused on the candidates that were identified in the EGF+FGF culture based on the proteome analysis. One of the candidates enriched in the culture more prone to be reprogrammed was chromatin-associated protein HMGB2. Due to its high and specific expression in neuronal progenitors similarly to the other neurogenic transcription factors, we speculated that it might help to instruct the neuronal fate from the astroglial cells. Moreover, some recent studies reported about its role in the regulation of adult hippocampal neurogenesis (Kimura et al., 2018), although its molecular mechanism is yet to be elucidated. Therefore it is not only the potential candidate to be tested in the reprogramming paradigm, but we might also reveal how it works on the molecular level and what are its related changes in the chromatin architecture. Interestingly, HMGB2 was not the only member of HMGB protein family enriched in the EGF+FGF culture. HMGB1 also showed higher levels in the culture with better conversion rate. However, HMGB1 shows completely different expression in the adult brain, it is much more abundant in the whole brain and not specifically enriched in neuronal progenitors. This would

suggest different function of both proteins in different brain cell types. In addition to the HMGB proteins, we also found two members of the second major family of the chromatin structural proteins, linker histones H1. This was quite surprising since these two families play the opposite role at the chromatin level. In general, H1 proteins stabilize the compacted chromatin structures, while HMG proteins promote chromatin decompaction and higher accessibility. All HMGs compete with H1 for chromatin binding sites in a dose-dependent fashion but each HMG family member has interactions with specific variants of H1 members (Postnikov and Bustin, 2016). Therefore, the histone variants that are highly expressed in the EGF+FGF culture might not be the ones that directly compete with HMGB1 or HMGB2. An alternative explanation for their simultaneous enrichment in the EGF+FGF culture could be that their expression has to be tightly regulated and cannot allow much higher enrichment of one or the other family since this could result in completely disrupted balance in the chromatin structure.

The observed enrichment of HMGB proteins in the cells cultured with EGF+FGF, lead to the question whether the expression of this proteins could be directly induced by the EGF signaling. Although we did not find any literature reporting about this, there might be some evidence supporting this hypothesis (Holth et al., 1997; Müller et al., 2004). HMGB1 gene is transcriptionally controlled by steroid hormones, probably by the cytokine-activated JAK/STAT signaling pathway (Müller et al., 2004). JAK/STAT pathway is also signaling cascade initiated by EGF growth factor (Henson and Gibson, 2006; Kisseleva et al., 2002), therefore it is not completely exclusive that it has an effect on the Hmgb1 (possibly also Hmgb2) transcription. The second study reported that the treatment of a human mammary epithelial cancer cell line with EGF induces transcription of the HMGA1 gene (Holth et al., 1997). There are no direct indications about Hmgb2 being regulated by EGF signaling pathways but based on the studies with the other HMG members, this might not be completely unexpected (Holth et al., 1997; Müller et al., 2004). However, searching for the upstream regulators of the HMGB2 would be a new project on its own and in this study, we rather focused on its downstream effects.

4.4 HMGB2 enhances the neuronal conversion in the cultures less prone to be reprogrammed

To test the importance of the proteins involved in the chromatin rearrangement during the reprogramming process, we overexpressed the HMGB2 protein alone or together with NEUROG2 in the EGF+FGF and FGF culture and investigated its role in facilitating the cell fate transition. HMGB2 on its own is not neurogenic and also did not change the glial cell identity. However, it plays an important role in the process of forced neurogenesis, specifically in the cells that are otherwise difficult to reprogram. The number of induced neurons was not increased in the EGF+FGF culture, where the NEUROG2 allows the acquisition of a neuronal phenotype very efficiently. We would speculate that this culture already reached its reprogramming capacity and we would correlate this to the number of GFAP+ cells at the starting point. We observed about 60% of GFAP+ cells from transduced cells and the comparable number of induced neurons upon NEUROG2 overexpression, suggesting that only the GFAP+ cells can be converted. Although also the FGF culture contains a similar number of GFAP+ cells, only the small percentage of them can undergo the cell fate transition. One of the reasons might be the lower level of HMGB2 protein. Indeed, elevated expression of HMGB2 together with NEUROG2 induced neurogenesis in the FGF culture almost to the levels that can be reached in the EGF+FGF culture. Interestingly, HMGB2 does not only help the NEUROG2 but it also seems to have the similar effect together with the BRN2. Although the other neurogenic factors might be tested, such as ASCL1 or SOX11, we would conclude that HMGB2 does not work as a specific co-factor of NEUROG2.

We next asked whether the presence of HMGB2 is crucial for the cells undergoing the fate transition. The experiments in the astrocytes isolated from Hmgb2-/- animals showed that HMGB2 is not necessary for the reprogramming since cells can still convert, however with limited efficiency. This brings up a question, how much can other members of the HMGB family compensate for its loss, especially due to the fact that they are structurally very similar and based on the enrichment of HMGB1 along with HMGB2 in the EGF+FGF culture. On the other hand, HMGB1 did not facilitate NEUROG2-mediated reprogramming in the FGF culture in wild-type astrocytes,

suggesting that HMGB1 does not resemble the function of HMGB2 in the astroglial cells and reprogramming process. Nevertheless, the situation might be different if the HMGB2 protein is not expressed from the beginning on likewise in Hmgb2-/- astrocytes. In this case, the partial redundant functions are suggested since the complete absence of HMGB2 is not lethal for the animals, while Hmgb1-/- animals die immediately after the birth (Bianchi and Agresti, 2005). The Hmgb2-/- animals are smaller in size, males are sterile, but in general phenotypically do not differ to the wild-type animals (Bronstein et al., 2017), therefore the redundancy with the other family members is not excluded. To test this in our reprogramming paradigm, we would need to knock down the HMGB1 protein in Hmgb2-/- astrocytes and test the reprogramming capacity of the cells or create the inducible line for the Hmgb2 deletion. It would be also interesting to see whether the reprogramming efficiency in the FGF cultured astrocytes from Hmgb2-/- animals would be limited even further. Many questions still remain to be explored, however, based on the reprogramming of Hmgb2-/- astrocytes we can conclude that HMGB2 protein is not necessary for the neuronal conversion but is it definitely involved in this process and it is sufficient to enhance the neuronal conversion in the cultures with a limited acquisition of the neuronal program. This is also supported by the results from the reprogramming of the reactive glial cells isolated after the injury, where HMGB2 also showed a promising outcome in inducing the reprograming together with NEUROG2 and ASCL1.

4.5 HMGB2 does not increase the efficiency of the reprogramming in vivo but is abundantly expressed after the brain injury

Promising results from in vitro experiments motivated us to test whether the role of HMGB2 could be exerted also in vivo, by helping NEUROG2 to acquire neuronal program in reactive glial cells after the brain injury. The simultaneous overexpression of both factors was not sufficient to facilitate the reprogramming after the injury limited to the cortical gray matter, however, some induced neurons emerged when the injury was deeper, reaching the white matter. The retroviral injection does not exclude the transduction of neural progenitors in the white matter, therefore, the observed induced neurons possibly originate from these progenitors that migrated

from the white matter up to the gray matter where they finally differentiated. It would be interesting to explore, whether this phenotype is related to the HMGB2 induction or it can be also triggered by the overexpression of the NEUROG2 alone. To address this point, deeper GM+WM injury needs to be performed, followed by the injection of the retrovirus encoding for Neurog2 and quantification of the NEUN+ induced neurons in comparison to the GM injury. Comparable numbers upon NEUROG2 overexpression regardless of the injury type would indicate the involvement of HMGB2 in differentiation and migration of the neuronal progenitors to the injury site. Although HMGB2 helped NEUROG2 and other neurogenic transcription factors to overcome the barriers of reprogramming in vitro, the other roadblocks (like oxidative stress) are most possibly still present in vivo. Therefore, some additional strategies are acquired to ameliorate the final acquisition of a neuronal program in the reactive glial cells after the brain injury.

Despite being insufficient to allow the conversion of reactive glial cells to neurons in vivo, HMGB2 still might be involved in the response to the injury. The high abundance of HMGB2+ cells at the injury site suggested its up-regulation associated to the several cell types. To prove this hypothesis, the investigation of the HMGB2 colocalisation with the markers for different populations that react upon the injury – NG2 glia, reactive astrocytes, microglia, and macrophages, is required. The response of HMGB2 seems to be very similar to the previously described HMGB1 secretion at the injury site (Parker et al., 2017). HMGB1 gets highly up-regulated already 12 h after the injury and then gradually decreases until day 10 when it reaches its basal levels (Parker et al., 2017). HMGB2 expression dynamics appeared to be slightly delayed. 1 day after the injury there were only a few HMGB2+ cells at the injury site, with their highest numbers at day 5 post injury and their decline up to 14 days after the injury. Despite delayed response, the question how similar is the role of HMGB2 compared to the HMGB1 in response to injury, remains elusive. HMGB1 gets activated under inflammatory conditions, translocates to the cytoplasm and is released into the extracellular space by innate immune cells, such as macrophages and dendritic cells as well as from damaged and necrotic neurons where it exhibits the chemoattractant activity for inflammatory cells (Parker et al., 2017). It would be very interesting to investigate the possible translocation of the HMGB2, similar to the HMGB1 and the cells types involved. In line with this

hypothesis, we observed some HMGB2 staining surrounding DAPI labelled nuclei. Additionally supporting this observation, there is a study reporting the secretion of the HMGB2 from cultured monocytes, promoting proliferation and migration of endothelial cells (Pusterla et al., 2009). These functions of HMGB2 are exerted via binding to the receptor for advanced glycation endproducts (RAGE) that is also activated by HMGB1 (Pusterla et al., 2009). Overall, this publication indicates the same biological properties of extracellular HMGB2 and HMGB1, suggesting that they might play a similar role after the injury. This role, however, might not only be in promoting the inflammation but might also have some beneficial effects during the recovery stage of brain injury. Likewise, the HMGB1 promotes neurovascular remodelling by recruiting endothelial progenitor cells and increasing their proliferation (Li et al., 2014), the HMGB2 shows the similar role in promoting the proliferation and migration of endothelial cells in vitro (Pusterla et al., 2009). It would be extremely interesting to test the beneficial or detrimental effect of HMGB2 protein in our injury paradigm using our Hmgb2-/- mouse model, exploring the reaction of different cell populations in and investigating whether the glial scar formation would be rather induced or inhibited when HMGB2 protein is not present. It might be necessary to target HMGB1 at the same and knock it down in parallel, but due to such a high abundance of HMGB2, it is rather difficult to believe that HMGB1 can completely take over its function. Taken together, we could not confirm the involvement of HMGB2 in facilitating the in vivo reprogramming, but we discovered its up-regulation at the lesion site suggesting its involvement in response to the injury that still remains to be explored and would be very interesting follow up of the project.

4.6 ATAC-sequencing revealed permissive chromatin states in the EGF+FGF culture and the role of HMGB2 in defining such states

Proteome analysis revealed the enrichment of chromatin structural proteins in the culture more prone to be reprogrammed, which could enable more permissive chromatin states for the efficient glia to neuron conversion. Using the ATAC-sequencing method, we confirmed this hypothesis, observing a higher number of opened regions in EGF+FGF culture when compared to FGF culture, many of them being located at the promoters. Interestingly, most of these promoters were assigned

to the neurogenic genes. This result suggests that EGF+FGF culture is more “plastic” in regard to chromatin states having neurogenic genes already opened that can get immediately transcribed upon induction. This might explain why the EGF+FGF culture is more prone to be reprogrammed. In addition, we identified the peaks located at the noncoding sites, which could represent the binding sites for the distal regulatory elements. The importance of these regions still remains elusive. To investigate which regulatory factors would bind there, we plan to perform the transcription factor binding site analysis and to evaluate whether they might be involved in the transition from gliogenic to neurogenic fate. In the FGF culture, we were able to extract much less information from the opened regions, as they were almost exclusively intergenic. Nevertheless, regardless where these sites are located, HMGB2 protein erases the differences between two cultures and opens specifically the neurogenic promoters that were closed in the FGF culture. We identified the required chromatin rearrangements to elicit the proper neuronal program the FGF culture and thereby the novel mechanism of the HMGB2 facilitating the reprogramming. However, when looking into the NEUROG2 induced changes, we observed that even on its own, this factor is able to open the closed neurogenic promoters due to its pioneering activity. To explain why these astrocytes still exhibit the limited reprogramming capacity, we developed two different hypotheses. One hypothesis would be that the required opening of neurogenic regions delays the whole process and thereby affects the efficiency of the reprogramming. In the EGF+FGF culture, the transcription of the neuronal program can immediately start upon NEUROG2 induction, while in the FGF culture NEUROG2 needs to first open this sites before the neurogenic transcription program can be applied. Exactly at this point involvement of the HMGB2 might be essential, resembling the role of NEUROG2, opening the same target sites of neurogenic genes and leading to the faster and more efficient induction of neurogenic fates. This explains also very well why we did not see any improvement of reprogramming in the EGF+FGF culture upon simultaneous expression of both factors. In this culture, the target sites of HMGB2 are already opened so the chromatin rearrangement of these regions via HMGB2-mediated remodeling is not needed. It would be very interesting to explore the spatial dynamics of the chromatin opening in the FGF culture comparing the NEUROG2 induced changes to the NEUROG2+HMGB2 induced ones, trying to confirm that HMGB2 can enhance this process. We would expect that such changes

take place very rapidly as reported for ASCL1 in the fibroblast reprogramming, where the first changes appear as early as 12 h after induction (Wapinski et al., 2017). However, this study discovered that the majority of the accessibility changes occur at day 2-5, therefore, we would also like to test whether the HMGB2 might be important during the later stages of the reprogramming and not only at the starting point.

The second hypothesis how the HMGB2 could help NEUROG2 in facilitating the neuronal reprogramming at the chromatin level comes from another study of the fibroblasts reprogramming. Similarly to our FGF culture, NEUROG2 was reported to show limited reprogramming capacity in human fibroblasts (Smith et al., 2016). To induce the reprogramming of fibroblasts, NEUROG2 required the help of the small molecules forskolin (FK) and dorsomorphin (DM) that induced the Sox4 expression and consequentially SOX4 dependent chromatin remodeling. While NEUROG2 on its own induced only a modest increase in open chromatin, the Sox4 expression enhanced NEUROG2 chromatin occupancy that activated the expression of neuronal transcription factors, leading to a new neuronal cell fate (Smith et al., 2016). SOX4 and HMGB2 have one common feature, HMG box binding domain (Dy et al., 2008), therefore it could very well be that HMGB2 plays a similar role in the FGF culture as reported for SOX4 in the fibroblast reprogramming. It would be also interesting to address whether HMGB2 physically interact or HMGB2 only sets up the chromatin states for the NEUROG2 binding.

4.7 HMGB2 and NEUROG2 induced changes at the transcriptome level

In the last aim of this study, we addressed the differences between the EGF+FGF and FGF cultures at the transcriptional level, explored the changes in the transcription upon NEUROG2 and HMGB2 overexpression and tried to correlate them to the changes in the chromatin dynamics. Examination of the differences in the control transduced cells resulted in a quite surprising finding of a high number of differentially expressed genes between two cultures, that was unexpected due to small differences in the proteome and high similarities based on the cellular marker expression. This analysis unraveled some specific characteristics of both cultures, but it could not answer why only a subset of cells can successfully complete the

reprogramming process. However, one observation was very clear, namely the high enrichment of genes related to the oligodendrocyte fate specification in the FGF culture. This was again quite unexpected since we proved that the majority of the transduced cells express astrocyte markers in both cultures. As discussed above, the oligodendrocyte progenitor cells need to be labeled with additional markers, but the proportion of this population is expected to be rather low with the remainder of the cells being astrocytes in both culturing conditions.

Next, we investigated the NEUROG2 induced changes and found a lot of genes differentially expressed compared to the control, however, only about one-third of these genes were commonly induced in both cultures. The larger the differences between the transcriptomes of the starting population were, the more different changes had to be implemented in two cultures. The common genes were exclusively related to neurogenesis meaning that NEUROG2 induced neuronal transcriptional program in both cultures. Therefore, the explanation for the different reprogramming capacity of two conditions remained elusive. We speculate that at the 48 h upon NEUROG2 induction, we do see the same transcriptional levels of neurogenic genes, but at the earlier time point, they might differ due to the fact that NEUROG2 still needs to open their closed chromatin sites (as seen on the ATAC-seq). Transcriptional changes have to take place very rapidly, and if this is not efficient the reprogramming might be impaired and delayed. To prove this hypothesis, the earlier investigation of the changes in the transcriptome is required - the earliest time point to be able to select for the transduced cells would be 24 h upon the transduction. In agreement with the hypothesis of delayed reprogramming would be the also fact that the non-reprogrammed Neurog2 transduced cells were not positive for GFAP in the FGF culture. They could be still a transition phase, being somewhere between the astrocytes and induced neurons and will start expressing neuronal markers at the later time point. Some of them might do so already, but cannot be considered as induced neurons due to non-neuronal morphology. This question might be addressed keeping the cultures longer in reprogramming process and quantifying their reprogramming efficiency a week or two later.

The next hypothesis to explain the different reprogramming efficiency would suggest that forced expression of NEUROG2 in the FGF culture still can induce neurogenic

fate, however, the insufficient repression of the gliogenic or alternative programs leads to the impaired acquisition of neuronal phenotype. We observed different genes being differentially expressed and related to the similar alternative fates in both cultures, suggesting their efficient down-regulation regardless of the culture condition. However, we did not observe the clear repression of the endogenous program in any of the two cultures. We would need to investigate further in one of the later time points in order to explore whether this can to be the major efficiency limits of direct reprogramming. The initial transcriptional response to induce neurogenic program is triggered very rapidly, instead, the down-regulation of starting cell program might take more time.

In the next step, we investigated the HMGB2 functions as a transcriptional activator through the modulation of chromatin structure. Due to big differences in the starting populations, also HMGB2 induces a very different transcriptional response in both cultures. However, the assigned GO terms are similar in the EGF+FGF and FGF condition, related to gene expression regulation and response to the DNA damage. This fits well to the previously published role of HMGB2 protein, being known to affect many DNA dependent processes such as transcription, replication, and the repair of damaged DNA (Postnikov and Bustin, 2016). In agreement with ATAC-seq data, we also detected transcriptional changes at the Neurog2 locus, where HMGB2 stimulates Neurog2 and its target genes expression. Interestingly, in the subset of genes induced by NEUROG2 overexpression, we also found Hmgb2 gene as differentially expressed when compared to the control. However, this was only in the EGF+FGF culture, meaning that it is probably a consequence of the changing cell identity when the cells start acquiring the neuronal phenotype. This is another proof of the importance of the HMGB2 in the neuronal transition since only the cells that can efficiently reprogram to the neurons up-regulate its levels.

Looking at the simultaneous overexpression of both factors showed that the induced genes do not greatly differ to the ones induced by NEUROG2 alone, however, there were many more genes down-regulated with the help of HMGB2. These genes are related to the GO term metabolism, which is already a well-known regulator of the reprogramming. In addition to its previously discussed functions, HMGB2 seems to help the NEUROG2 to navigate through the metabolic switch. Since HMGB2 on its

own does not close any chromatin regions, we speculate that its effect in the down-regulation might be achieved by opening the repressor binding sites. In addition to repression of some metabolic genes, HMGB2 improves the repression of the myogenic cell fate, which seems to be the reprogramming hurdle also in the astrocytes and not only in the fibroblasts as previously reported (Mall et al., 2017). We confirmed this role of the HMGB2 protein by a pilot experiment, trying to reprogram the astrocytes into the muscle cells by forced expression of MyoD1. While MYOD1 on its own induced myogenic fate in some cells, in combination with HMGB2 all cells died, which would fit with the hypothesis that HMGB2 inhibits the muscle cell fate.

We tried to further correlate the observed transcriptional changes upon the simultaneous overexpression of both factors with the HMGB2 induced chromatin rearrangements. Based on the observed opening of the regions at the neurogenic promoters, we proposed that HMGB2 enhances the acquisition of neuronal program induced by NEUROG2 overexpression. This could result in a shortened time of the metabolic transition and consequently reduce the levels of the oxidative stress that is a major hurdle in the cell fate transition. Overcoming these barriers rapidly, might enhance the survival of the cell during conversion and thereby improve the reprogramming capacity.

4.8 Summary and conclusions

The present work highlights the importance of the chromatin status of the starting cells by measuring the chromatin accessibility that is influenced by different growth factors and results in heterogeneous responsiveness to the activation of the neurogenic factors. The chromatin architectural factor HMGB2 plays a role in modulating the conversion susceptibility of differentiated cells at the different levels. With the help of HMGB2, astrocytes undergo the transition to a more plastic cell state by undergoing chromatin rearrangements, which makes them more permissive to fate specifying transcription factors and results in the acquisition of a new neuronal identity. We showed that this happens at the promoters of neuronal genes and

possibly at some distal regulatory regions, that contain the binding motives for the repressors of myogenic cell fate.

In vivo situation seems to be more complicated due to many more environmental influences that might additionally inhibit the NEUROG2 pioneering activity. We believe that the chromatin remodeling is apart from the metabolic switch the second hurdle for the efficient reprogramming in vivo that was until now very much neglected since it happened in parallel with the effect on the metabolism. It would be interesting to explore the chromatin states of the reactive glial cells upon the injury using ATAC-sequencing and the specific regions that need to undergo the chromatin rearrangements in order to acquire the new cell identity. It would be also crucial to find the specific candidates that can perform these rearrangements in vivo. With this project, we provided new insights into the mechanisms maintaining the glial cell identity and explored the new approaches to overcome such blocks to improve the reprogramming in vitro. Understanding the molecular basis of the reprogramming process is of fundamental importance when it comes to translating this approach to the clinic, either for disease modeling, drug screening or cell therapies. Although there is a lot to be explored, we still hope that our study contributed a piece of knowledge to this important field.

5 Materials and methods

5.1 Materials

5.1.1 Chemicals and reagents

2-mercaptoethanol, Merck
Acetic acid, Merck
Acetone, Millipore
Acrylamide, 30%, Roth
Agarose, Biozym
Amersham ECL Western Blotting Detection Reagent, GE Healthcare
Ammonium peroxide disulphate (APS), Sigma-Aldrich
Ammonium persulfate, Thermo Fischer Scientific
Ampicillin, Roth
AMPure XP beads, Beckman Coulter
Aqua Poly/Mount mounting medium, Polyscience
Bacto-Tryptone, BD Biosciences
BD Difco™ Dehydrated Culture Media: LB Agar, Miller (Luria-Bertani), A. Hartenstein
BD FACSFlow™, BD Biosciences
Bromphenol Blue, Sigma-Aldrich
Buffer EB, Qiagen
cOmplete™ Protease Inhibitor Cocktail, Roche
DAPI (4',6-diamidino-2-phenylindole), AppliChem
DNA Polymerase I, Large (Klenow) Fragment, NEB
Ethanol (EtOH), Merck
Ethylene glycol, Sigma-Aldrich
Ethylenediaminetetraacetic acid (EDTA), Merck
Gateway™ LR Clonase™ II Enzyme mix, Thermo Fisher Scientific
GeneRuler 1 kb DNA Ladder, Thermo Fisher Scientific
Glycerol, Sigma-Aldrich
Glycine, Sigma-Aldrich
Glycogen, Molecular Biology Grade, Roche
Hydrochloric acid (HCl), 37%, Merck

IGEPAL CA-630, Sigma-Aldrich

Immersion oil 518N, Zeiss

Isopropanol, Merck

Kanamycin sulphate, Roth

Ketavet, 100 mg/ml, Pfizer

Magnesium chloride (MgCl2), Sigma-Aldrich

Methanol, Merck

Milk powder, Roth

Mineral oil, Sigma-Aldrich

NaCl 0.9%, B. Braun

NEBNext High-Fidelity 2X PCR Master Mix, New England Biolabs

NEBuffer 2 (10X), New England Biolabs

NEBuffer 2.1 (10X), New England Biolabs

NEBuffer 3.1 (10X), New England Biolabs

Normal goat serum (NGS), Vector Laboratories

Orange G, Sigma-Aldrich

Paraformaldehyde (PFA), Merck

PCR dNTP Mix (25 mM), Fermentas (Thermo Fisher Scientific)

Pierce Ripa buffer, Thermo Fischer Scientific

Potassium chloride (KCl), Sigma-Aldrich

Potassium phosphate monobasic (KH2PO4), Sigma-Aldrich

Proteinase K, Roche

Restriction enzymes, New England Biolabs

Ringer-Infusionslösung, B. Braun

Rompun, 2%, Bayer

SeeBlue™ Plus2 Pre-stained Protein Standard, Invitrogen (Thermo Fisher Scientific)

Sodium azide (NaN3), Merck

Sodium bicarbonate, 7.5%, Invitrogen (Thermo Fisher Scientific)

Sodium chloride (NaCl), Merck

Sodium citrate (C6H5Na3O7), Merck

Sodium dodecyl sulphate (SDS), Roth

Sodium hydroxide (NaOH), Roth

Sodium phosphate dibasic (Na2HPO4), Sigma-Aldrich

SYBR™ Green I Nucleic Acid Gel Stain, Invitrogen (Thermo Fisher Scientific)
SYBR™ Safe DNA Gel Stain, Invitrogen (Thermo Fisher Scientific)
T4 DNA Ligase Buffer (10X), New England Biolabs
T4 DNA Ligase, New England Biolabs
TE Buffer (pH 8.0), Qiagen
TEMED, Sigma-Aldrich
Tris Base, Sigma-Aldrich
Tris-HCl, Roth
Triton-X-100, Roth
Tween 20, Sigma-Aldrich
Yeast extract, Sigma-Aldrich

5.1.2 Tissue culture reagents

B27 serum-free supplement (50X), Gibco (Thermo Fischer Scientific)
Bovine basic fibroblast growth factor - bbFGF, Roche
D-(+) Glucose solution, Sigma-Aldrich
DMEM, high glucose, Gibco (Thermo Fischer Scientific)
DMEM/F-12, no glutamine, Gibco (Thermo Fischer Scientific)
DMEM/F12+GlutaMAX, Gibco (Thermo Fischer Scientific)
DPBS (1X), Gibco (Thermo Fischer Scientific)
Epidermal growth factor – EGF, Roche
Fetal Bovine Serum - FBS, heat inactivated, Gibco (Thermo Fischer Scientific)
Fetal calf serum - FCS, PAN-Biotech
Geneticin (G418 Sulfate), Gibco (Thermo Fischer Scientific)
GlutaMAX™ Supplement, Gibco (Thermo Fischer Scientific)
HBSS with calcium and magnesium (10X), Gibco (Thermo Fischer Scientific)
HBSS with calcium and magnesium (1X), Gibco (Thermo Fischer Scientific)
HEPES, 1M, Gibco (Thermo Fischer Scientific)
Horse serum, PAN-Biotech
Hyaluronidase from bovine testes, Sigma-Aldrich
Lipofectamine® 2000 Transfection Reagent, Invitrogen (Thermo Fisher Scientific)
Opti-MEM, Gibco (Thermo Fischer Scientific)
Penicillin/Streptomycin (10000 U/ml), Gibco (Thermo Fischer Scientific)

Poly-D-Lysine (PDL), Sigma-Aldrich
Puromycin Dihydrochloride, Gibco (Thermo Fischer Scientific)
Tetracycline, Sigma-Aldrich
Trypsin from bovine pancreas, Sigma-Aldrich
Trypsin-EDTA (0.05%), Gibco (Thermo Fischer Scientific)

5.1.3 Kits

Agilent High Sensitivity DNA Kit, Agilent
Agilent RNA 6000 Pico Kit, Agilent
ApopTag Red In Situ Apoptosis Detection Kit, Millipore
BigDye Terminator v3.1 Cycle Sequencing Kit, Applied Biosystems (Thermo Fisher Scientific)
Dye Ex 2.0 Spin Kit, Qiagen
MicroPlex Library Preparation kit v2, Diagenode
MinElute PCR Purification Kit, Qiagen
Nextera DNA Library Prep Kit, Illumina
Nextera Index Kit, Illumina
PicoPure RNA Isolation Kit, Thermo Fisher Scientific
Pierce™ BCA Protein Assay Kit, Thermo Fisher Scientific
Qiagen Plasmid Maxi kit, Qiagen
QIAprep Spin Miniprep Kit, Qiagen
QIAquick Gel Extraction Kit, Qiagen
QIAquick PCR Purification Kit, Qiagen
Qubit™ dsDNA HS Assay Kit, Invitrogen (Thermo Fisher Scientific)
SensiMix™ SYBR® No-ROX Kit, Bioline
SMART-Seq® v4 Ultra® Low Input RNA Kit for Sequencing, Clontech Laboratories
Taq DNA Polymerase Kit, Qiagen

5.2 Methods

5.2.1 In vivo methods

5.2.1.1 Experimental animals

The described experiments were conducted on both, female and male animals, which were either wild types (C57BL/6J mice) or transgenic Hmgb2-/- animals. Hmgb2-/- breeding pairs on a C57BL/6 background were obtained from Dr. Lorenza Ronfani (Core Facility for Conditional Mutagenesis, San Raffaele Scientific Institute, Milan, Italy). The Hmgb2 deficient mouse line was generated by replacing the Hmgb2 coding sequence with the ble-lacZ coding sequence, using homologous recombination in ES cells, starting from the ATG translation start site in exon 2 to exon 4. Hmgb2 gene has in total 5 exons, from which the first one is not translated (Ronfani et al., 2001). The Hmgb2-/- animals are smaller in size, homozygous null males are viable, but in general, they phenotypically do not differ to the wild-type animals (Ronfani et al., 2001).

For all in vitro experiments, animals at postnatal stage P5-P6 were used, except for reactive gliosis culture that was prepared from adult mice (8-10 weeks old). For the reprogramming experiments with Hmgb2 deficient astrocytes, heterozygous females were crossed with heterozygous males to obtain the pups of all 3 possible genotypes (see “Genotyping” section). In vivo reprogramming experiments were performed in adult 8-10 weeks old animals.

Animals were kept under standard conditions with access to water and food ad libitum. All animal experimental procedures were performed in accordance with the German and European Union guidelines and were approved by the Institutional Animal Care and Use Committee (IACUC) and the Government of Upper Bavaria under license number: AZ 55.2-1-54-2532-171-2011 and AZ 55.2-1-54-2532-150-11. All efforts were made to minimize animal suffering and to reduce the number of animals used.

5.2.1.2 Surgical Procedures

5.2.1.2.1 Stab wound injury

Prior to every surgery, mice were deeply anesthetised by intra-peritoneal injection of sleep solution (10 µl per g body weight) that was provided by the Research Unit Comparative Medicine (Helmholtz Zentrum München). After the injection of the anaesthesia, mice were checked for pain reactions by pinching their tail and toes. The fur on top of the head was removed with a small electric razor and Bepanthen (Bayer) was administered to the eyes to prevent their dryness. The animals were then fixed in a stereotaxic frame and the skin of the head was cut following the midline with a scalpel to expose the skull surface. Stab wound injury was performed in the somatosensory cortex, as previously described (Buffo et al., 2008; Heinrich et al., 2014). For the in vivo reprogramming experiments, the injury was performed only in one hemisphere, while for the reactive gliosis culture, both hemispheres were injured in order to obtain a higher amount of reactive glial cells. To perform the injury, bregma was searched using the forceps by pressing gently on the skull bones. Once bregma was found, the stereotactic apparatus was set to coordinate zero. Next, a small circular cranial window (diameter of ~3 mm) was drilled above the cerebral cortex with the high-speed rotary micromotor (Foredom) and the cranial window was collected in a drop of a Ringer solution. Following coordinates below, 1 mm long stab wound was performed in the cortical grey matter parenchyma by moving the V-lance shaped knife (Alcon) back and forth.

medio-lateral (x): ±1.8 from bregma
rostro-caudal (y): -1.6 to -2.5 from bregma
dorso-ventral (z): -0.6 from the meninges

Importantly, the depth of the cut was restricted to 0.6 mm to avoid the deeper cortical layers and underlying white matter and therefore minimise the risk of migrating neuroblasts into the injured cortex. At the end of the procedure, the cranial window was placed back to protect the wounded area and the skin covering the skull was closed by Vicryl suture (Ethicon) with at least three stitches. Anaesthesia was

antagonized with an intra-peritoneal injection of awake solution (10 µl per g body weight), pre-prepared by Research Unit Comparative Medicine (Helmholtz Zentrum München), and the mice were kept on a pre-warmed pad until they were awake and recovered from the surgery.

5.2.1.2.2 Injection of retroviral suspension at the injury site

Three days after the stab wound injury in the retroviruses encoding for Neurog2-IRES-RFP or Neurog2-T2A-Hmgb2-IRES-dsRED were injected at the lesion site. Mice were anesthetised and fixed in the stereotaxic frame as described before. The skin was opened along the previous cut, cranial window was removed and stored in a Ringer solution. Next, glass capillary was filled with the mineral oil and then with the viral suspension. After determining the injury site, 1 µl of retrovirus was injected with a glass capillary using Sys-Micro4 Controller for Micro Syringe Pumps (World Precision Instruments) at the z position -0.5 from the brain surface. The starting infusion speed was very low with 30 nl/min and was gradually increased to 50 nl/min, in order to avoid retroviral leakiness on the brain surface and allow the tissue to absorb the viral suspension. The capillary was retracted after 5 minutes when the injection was completed to avoid reflux along the needle tract. The bone flap was put back in place to cover the injured area followed by the procedures described above.

5.2.1.3 Perfusion

Prior to perfusion, animals were deeply anesthetized with a cocktail of Ketamin Rompun (20 µl per g body weight). Subsequently, they were transcardially perfused first with 1X PBS, followed by fresh ice-cold 4% PFA in PBS, which was left to circulate in the organism for about 20 minutes. The brain was then carefully removed from the skull and post-fixed in the same fixative overnight at 4°C.

Ketamin-Rompun anaesthetic
0.5 ml 100 mg/ml Ketavet
0.5 ml 2% Rompun
9 ml NaCl 0.9%

10X Phosphate Buffered Saline (PBS)

400 g NaCl

10 g KCl

10 g KH2PO4

58.75 g Na2HPO4

Final pH=7.4. Dissolve in 5 l in Milli-Q water, autoclave and dilute 1:10 in autoclaved Milli-Q water to obtain 1X PBS.

4% PFA

40 g PFA

3 NaOH pellets

100 ml of 10X PBS

900 ml Milli-Q water

Dissolve 40 g PFA in 800 ml MilliQ water by gentle heating while stirring with the addition of 3 NaOH pellets to enable the PFA powder to dissolve. Cool down the solution to the room temperature and adjust the pH with the HCl extremely slowly drop by drop. When the pH drops dramatically to 1-3, quickly add 100 ml of 10X PBS. Adjust the pH to 7.2-7.3 and add Milli-Q water to final volume 1 l. Filter the solution through a paper filter and store at 4°C.

5.2.2 Methods in cell biology

5.2.2.1 Vibratome sectioning

To perform vibratome sectioning, brain tissue was washed in PBS and allowed to dry. Both olfactory bulbs and cerebellum were removed and the brain was placed in an embedding mold (Polysciences) with the rostral part facing the bottom. A solution of 3% (w/v) agarose in 1X PBS was then poured into the mold and left to polymerize at the room temperature. Subsequently, brain tissue was cut into 70-80 µm thick coronal sections and collected in PBS. For long-term preservation, vibratome sections were kept in storing solution at -20°C.

10X Phosphate Buffered Saline (PBS)

400 g NaCl
10 g KCl
10 g KH2PO4
58.75 g NaH2PO4
Final pH=7.4. Dissolve in 5 l in Milli-Q water, autoclave and dilute 1:10 in autoclaved Milli-Q water to obtain 1X PBS.

Storing solution
30 ml Glycerol
30 ml Ethylene glycol
10 ml 10X PO4 buffer
30 ml ddH2O
Store at 4°C.

10X PO4 buffer
13.8 g NaH2PO4 x 2H2O
3.0 g NaOH
40 ml ddH2O
Final pH=7.2-7.4.

5.2.2.2 Preparation of PDL-coated glass coverslips

Glass coverslips are first washed with acetone and boiled for 30 min in ethanol containing 0.7% (v/v) HCl. After two washing steps in 100% ethanol, coverslips are dried at the RT and autoclaved for 2 h at 180°C. To each well of a 24-well plate, one sterilized cover slip was added and pre-wetted with DPBS. Next, DPBS was replaced by 1X poly-D-lysine (PDL) solution and plates were incubated for at least 2 h at 37°C. Wells were washed three times with autoclaved ultrapure water and dried in the laminar flow before being transferred to the fridge and stored at 4°C until needed.

50X poly-D-lysine (PDL)
Poly-D-lysine powder 1 mg/ml in ddH2O
Filter-sterilize, aliquot and store at -20°C for up to 6 months. Dilute to 1X poly-D-lysine (PDL) in ddH2O water before use.

5.2.2.3 Primary culture of postnatal cortical astroglial cells

Postnatal cortical astroglia were isolated and cultured as described previously (Heinrich et al., 2011). Following decapitation of postnatal (P5-P6) wild-type C57BL/6J mice, the skin and the skull were carefully removed and the brain was extracted avoiding any tissue damage and placed into the dissection solution. After separating the two hemispheres, the meninges was removed and a piece of cerebral cortex was dissected using fine forceps and collected in a tube with astrocyte medium. After the mechanical dissociation with a 5 ml pipette, cells were placed into uncoated plastic flasks for expansion in astrocyte medium supplemented with two growth factors EGF+FGF or with the FGF only. Usually, the dissociated tissue from 2 P5-P6 pups (4 pieces of cortex) was placed into one T75 culture flask. After 4-5 days, the medium was exchanged and supplied with the fresh growth factors. After 10 days of culturing, cultured cells were rinsed with DPBS and contaminating oligodendrocyte precursor cells were removed by brusquely shaking the culture flasks several times. Astroglial cells were then detached from the flask by trypsinization and seeded onto poly-D-lysine (PDL)-coated glass coverslips (see protocol above) at a density of $8x10^4$ cells per well in a 24-well plate with astrocyte medium. Alternatively, for the ATAC-seq and RNA-seq experiments, cells were plated to T75 flasks with the seeding density $3x10^6$ cells per flask. At 2-4 h after the seeding, the cells were transduced with different retroviral vectors (see section "Expression plasmids and retroviral production"), usually in ratio 1 µl of virus per 1 ml of medium to prevent the toxicity of the virus. On the next day, astrocyte medium was changed to differentiation medium containing no growth factors for the reprogramming experiments. For the ATAC-seq and RNA-seq experiments, the cells were kept in the astrocyte medium.

Cells were kept in the reprogramming process for 1 week and were then fixed an immunostained as described below (see chapter "Immunocytochemistry and immunohistochemistry"). To access the cellular identity and proliferation of the EGF+FGF and FGF cultured cells, they were fixed at the earliest possible time point (24 h after the transduction). Astrocytes in the T75 culture flasks were collected 48 h

after transduction, prepared for the FACS and sorted for the following ATAC-seq and RNA-seq experiments (see chapters below).

The astroglial cultures from the Hmgb2-/- transgenic animals were prepared following the same protocol, however, the cortical tissue from each of the animal was kept separately and placed into the small T25 flask. In addition, the tips of the tails were collected to perform the genotyping (see chapter “Genotyping of Hmgb2 transgenic animals”). The cultures from Hmgb2-/- transgenic mouse line were grown only in the double growth factor condition EGF+FGF.

Dissection solution
500 ml 1X HBSS
5 ml 1 M HEPES (10 mM final concentration)

Astrocyte medium
5 ml Fetal calf serum-FCS (10% (v/v) final concentration)
2.5 ml Horse serum-HS (5% (v/v) final concentration)
0.5 ml 45% glucose (3.5 mM final concentration)
1 ml 50X B27 supplement (1X final concentration)
0.5 ml Penicillin/Streptomycin (final dilution 1:100)
Up to 50 ml DMEM/F12+GlutaMAX

Growth factors are added freshly prior to the culturing in dilution 1:1000.
Epidermal growth factor-EGF (10 ng/ml final concentration)
Basic bovine fibroblast growth factor-bbFGF (10 ng/ml final concentration)

Differentiation medium
0.5 ml 45% glucose (3.5 mM final concentration)
1 ml 50X B27 supplement (1X final concentration)
0.5 ml Penicillin/Streptomycin (final dilution 1:100)
Up to 50 ml DMEM/F12+GlutaMAX

5.2.2.4 Reactive gliosis culture

To prepare the adherent reactive gliosis culture, cells from the lesioned area were isolated 3 days after the stab wound injury performed in the cortical grey matter of the adult wild-type animals (see chapter “Surgical procedures, Stab wound injury”). After removing the meninges, the cortical tissue around the lesion site from both injured hemispheres was carefully isolated avoiding any white matter contamination and cut into small pieces in the dissection solution. Pieces were collected into 15 ml falcon tube and centrifuged for 5 min at 1400 rpm. Dissection solution was replaced by pre-warmed Trypsin+Hyaluronidase mix and the tissue was gently homogenized following by 5 min incubation at 37°C. In the next step, the tissue was homogenized strongly by 1 ml pipette and incubated again for 5 min at 37°C. This step was repeated once more and then stopped by addition of the FBS. To remove the dissociation mix, cells were centrifuged for 5 min at 1400 rpm and finally resuspended in basis medium without EGF or FGF growth factors. Cells were plated on poly-D-lysine coated coverslips (see protocol above), placing the cells from one injured hemisphere into one well of a 24-well plate and transferred into low oxygen incubator with 5% CO2 and 5% O2. The basis medium was exchanged with the fresh medium already 24 h after the plating. After 3 days of culturing the cells, the medium was changed again prior to the retroviral transduction. Subsequently, the cells were transduced with different combinations of retroviruses (see the chapter “Expression plasmids and retroviral production”) and 24 h after transduction the medium was changed again and replaced with basis medium without FBS. 7 days after the transduction cells were fixed and immunostained as described below (see section “Immunocytochemistry and immunohistochemistry”).

Dissection solution
500 ml 1X HBSS
5 ml 1M HEPES (10 mM final concentration)

Trypsin+Hyaluronidase mix
3.4 mg Trypsin
3.5 mg Hyaluronidase
5 ml Solution 1

Solution 1

50 ml 10X HBSS (1X final concentration)
9 ml 45% glucose (0.81% final concentration)
7.5 ml HEPES (15 mM final concentration)
Up to 500 ml ddH2O
Adjust pH to 7.5 with 7.5% (w/v) sodium bicarbonate and sterilize by filtration with 0.22 µm PVDF filter.

Basis medium
500 ml DMEM/F-12, no glutamine
5 ml Penicillin/Streptomycin (final dilution 1:100)
5 ml 45% glucose (3.5 mM final concentration)
50 ml Fetal bovine serum-FBS (10% (v/v) final concentration)
10 ml 50X B27 supplement (1X final concentration)
5 ml GlutaMAX™ Supplement (final dilution 1:100)

5.2.2.5 Immunocytochemistry and immunohistochemistry

Immunostaining was performed on a cell culture samples or on free-floating sections. Cells were first fixed in 4% PFA in 1X PBS for 20 min at the room temperature and washed 3x 10 min in PBS. Sections stored in the storing solution were washed well with PBS prior to immunostaining. Meanwhile, antibodies were diluted in 0.5% Triton-X-100 in 1X PBS with 10% normal goat serum (NGS) to reduce non-specific binding. Antibodies were used in different combinations; all the details about primary antibodies used are listed below. Antigen labelling was performed overnight at 4°C or 2 hours at the RT, followed by 3x 10 min washing steps in PBS. In order to visualize primary antibody binding, samples were exposed to appropriate species and/or subclass specific secondary antibodies conjugated to Alexa Fluor 488, 546 or 647 (Invitrogen). They were diluted 1:1000 in 0.5% Triton-X-100 in 1X PBS with 10% NGS and incubated with the specimen for about 90 min at the room temperature in the dark. Nuclei were visualized with DAPI (4',6-diamidino-2-phenylindole) that was added to the mix of secondary antibodies in dilution 1:1000. Following extensive washing steps with PBS, coverslips or sections were mounted with Aqua Poly/Mount (Polysciences), a glycerol-based mounting medium that enhances and retains fluorescent stains.

Antigen	Company, ordering number	Dilution
Chick-anti-GFP	Aves Lab, GFP-120	1:1000
Rabbit-anti-RFP	Rockland, 600-401-379	1:500
Mouse IgG1-anti-GFAP	Sigma-Aldrich, G3893	1:500
Rabbit-anti-GFAP	DakoCytomation, Z0334	1:1000
Mouse IgG1κ-anti-S100β	Sigma-Aldrich, S2644	1:500
Rabbit-anti-OLIG2	Millipore, AB9610	1:500
Mouse IgG2a-anti-αSMA	Sigma-Aldrich, A2547	1:400
Rabbit-anti-Ki67	Abcam, 15580	1:200
Rat-anti-Ki67	DakoCytomation, M7249	1:200
Rabbit-anti-PH3 (Ser10)	Millipore, 06-570	1:200
Guinea pig-anti-DCX	Millipore, AB-2253	1:1000
Mouse IgG2b-anti-β-III-TUBULIN	Sigma-Aldrich, T8660	1:500
Mouse IgG1-anti-NEUN	Chemicon, MAB377	1:250
Rabbit-anti-HMGB2	Abcam, ab67282	1:1000
Mouse IgG2aκ-anti-HMGB2	Sigma-Aldrich, 07173-3E5	1:500*
Rabbit-anti-HMGB1	Abcam, ab18256	1:1000

* Heat-mediated antigen retrieval with citrate buffer required

4% PFA

40 g PFA

3 NaOH pellets

100 ml of 10X PBS

900 ml Milli-Q water

Dissolve 40 g PFA in 800 ml MilliQ water by gentle heating while stirring with the addition of 3 NaOH pellets to enable the PFA powder to dissolve. Cool down the solution to the room temperature and adjust the pH with the HCl extremely slowly drop by drop. When the pH drops dramatically to 1-3, quickly add 100 ml of 10X PBS. Adjust the pH to 7.2-7.3 and add Milli-Q water to final volume 1 l. Filter the solution through a paper filter and store at 4°C.

10X Phosphate Buffered Saline (PBS)

400 g NaCl
10 g KCl
10 g KH2PO4
58.75 g NaH2PO4
Final pH=7.4. Dissolve in 5 l in Milli-Q water, autoclave and dilute 1:10 in autoclaved Milli-Q water to obtain 1X PBS.

5.2.2.6 Heat-mediated antigen retrieval with citrate buffer

For some nuclear stainings, sections had to be pre-treated to enable primary antibody binding, for example, mouse-anti-Hmgb2. To perform heat-mediated antigen retrieval, free-floating sections were transferred into 1.5 ml tubes filled with 1X citrate buffer and cooked for 15 min at 95°C. Following the treatment, they were stained using the protocol described above.

10X citrate buffer
29.4 g sodium citrate
1000 ml ddH2O
Adjust pH to 6.0 and dilute 1:10 in ddH2O to obtain 1X citrate buffer.

5.2.2.7 Cell death assay

To assess the cell death in cultured astroglial cells, the cultures were prepared as described before (see section “Primary culture of postnatal cortical astroglial cells”). 24 h after re-plating the cells into 24-well PDL-coated plate, they were fixed in 4% PFA for 20 min at the room temperature and washed 3x 10 min in PBS. To detect the apoptotic cells, the ApopTag Red In Situ Apoptosis Detection Kit was used according to the manufacturer’s instructions. Afterward, the immunostaining for GFAP was performed to label the astrocytes following the standard protocol described above (see chapter “Immunocytochemistry and immunohistochemistry”).

4% PFA
40 g PFA
3 NaOH pellets

100 ml of 10X PBS
900 ml Milli-Q water
Dissolve 40 g PFA in 800 ml MilliQ water by gentle heating while stirring with the addition of 3 NaOH pellets to enable the PFA powder to dissolve. Cool down the solution to the room temperature and adjust the pH with the HCl extremely slowly drop by drop. When the pH drops dramatically to 1-3, quickly add 100 ml of 10X PBS. Adjust the pH to 7.2-7.3 and add Milli-Q water to final volume 1 l. Filter the solution through a paper filter and store at 4°C.

10X Phosphate Buffered Saline (PBS)
400 g NaCl
10 g KCl
10 g KH2PO4
58.75 g NaH2PO4
Final pH=7.4. Dissolve in 5 l in Milli-Q water, autoclave and dilute 1:10 in autoclaved Milli-Q water to obtain 1X PBS.

5.2.2.8 FACS analysis and sorting

To enrich for the transduced cells that were further used for the ATAC-seq and RNA-seq, we performed the fluorescence activated cell sorting (FACS). Primary cortical astrocytes were isolated and cultured as described above (see section “Primary culture of postnatal cortical astroglial cells”). They were collected by trypsinization 48 h after retroviral transduction, washed, resuspended in DPBS and transferred to the FACS tubes. Next, they were analyzed using a FACS Aria II instrument (BD Biosciences) in the FACSFlow™ medium. Debris and aggregated cells were gated out by forward scatter area (FSC-A) and side scatter area (SSC-A). Forward scatter area (FSC-A) vs. forward scatter width (FSC-W) was used to discriminate doublets from single cells. To set the gates for the sorting, untransduced astrocytes were recorded. Sorted cells were collected in the DPBS, counted and divided into two batches: 50000 cells were immediately processed for the ATAC-seq and the remainder of the cells was collected for the RNA-seq library preparation (see chapters “ATAC-sequencing” and “Preparation of libraries for RNA-sequencing”).

5.2.3 Methods in molecular biology

5.2.3.1 Genotyping of Hmgb2 transgenic animals

For DNA extraction, mouse ear punches or tips of the tails were collected and incubated in 0.5 ml lysis buffer with proteinase K (100 µg/ml final concentration), shaking overnight at 55°C. On the next day, hairs and tissue residues were removed by centrifugation at 12000 rpm for 20 minutes. The supernatant was transferred to a new 1.5 ml tube and DNA was precipitated by adding 0.5 ml isopropanol, mixing well and centrifuging 20 min at the maximum speed. The supernatant was removed from the pellet and tubes were dried upside down at the room temperature. Dried DNA was dissolved in 150 µl of H2O, followed by 1-2 hours incubation at 55°C in the shaker. The DNA was kept at 4°C until PCRs were performed. Primers, solutions, and cycling conditions used in the PCR to characterise the genotype of transgenic mice are listed below.

Lysis buffer
100 ml 1 M Tris-HCl pH=8.5 (100 mM final concentration)
10 ml 0.5 M EDTA (5 mM final concentration)
20 ml 10% SDS (0.2% (v/v) final concentration)
200 ml 1 M NaCl (200 mM final concentration)
660 ml ddH2O

Primers:
Hmgb2 forward primer 5’ CGGACAGCTAGGAGCTTTGAAGTC 3’
Hmgb2 reverse primer 5’ GCGATGGGTTCGTTAGTTCTCAG 3’
LacZ forward primer 5’ GCTGGCGTAATAGCGAAGAGG 3’
LacZ reverse primer 5’ ATGCGCTCAGGTCAAATTCAGAC 3’

PCR reaction mix:
10x CoralLoad PCR buffer (Qiagen): 2.5 µl
dNTPs: 0.5 µl
10 µM Hmgb2 forward primer: 0.5 µl
10 µM Hmgb2 reverse primer: 0.5 µl

10 µM LacZ forward primer: 0.5 µl
10 µM LacZ reverse primer: 0.5 µl
Taq Polymerase (homemade): 0.2 µl
DNA: 1 µl
H2O: up to 25 µl

The DNA was amplified under following cycling conditions:

3 min 95°C (hotstart)	
45 sec 95°C	
30 sec 60°C	35x
30 sec 72°C	
5 min 72°C	

The product was loaded on 2% agarose gel (see chapter “Gel electrophoresis” below). Expected band sizes were: WT allel-236 bp and LacZ allel-413 bp.

5.2.3.2 Gel Electrophoresis

To prepare 1-2% (w/v) gel, depending on product size, the appropriate amount of agarose was dissolved in 1X TAE buffer by boiling in a microwave. After the solution cooled down, SYBR™ Safe DNA Gel Stain was added (1:25000) and the gel was poured in a prepared electrophoretic chamber. After the gel solidified, DNA samples were mixed with 6X loading dye and loaded into the wells, along with a 1 kb DNA ladder. Electrophoresis was performed at 100-150V. Finally, the band sizes were imaged at the Biorad Gel Doc™ XR+ System.

For the cloning of Neurog2-T2A-Hmgb2-IRES-dsRED construct, DNA fragments with the right size were cut under UV light at the Biorad Gel Doc™ XR+ System, transferred into a 1.5 ml tube and purified with the QIAquick gel extraction kit according to the manufacturer’s instructions.

50X TAE Buffer
242 g Tris base

57.1 ml Acetic acid
100 ml 0.5 M EDTA (50 mM final concentration)
Dissolve in 800 ml autoclaved H2O, adjust pH to 8.0 with HCl and fill up to 1 l with autoclaved H2O. Dilute 1:50 in autoclaved H2O to obtain 1X TAE Buffer.

5.2.3.3 ATAC-sequencing

Assay for Transposase Accessible Chromatin with high-throughput sequencing (ATAC-seq), a method to detect chromatin accessibility genome-wide, was performed following the published protocol (Buenrostro et al., 2013, 2015). Briefly, right after the FACS sorting, 50000 cells were lysed and centrifuged. Extracted nuclei were resuspended in transposase reaction mix, following by transposition reaction for 30 minutes at 37°C. To stop the transposition reaction, samples were purified using a Qiagen MinElute PCR purification kit according to the instructions provided with the kit. Library fragments were first amplified for 5 cycles and then for additional 7-8 cycles, as determined by RT-qPCR reaction, using the combination of primer Ad1_noMX and one of the Nextera Index Kit primers listed below. Finally, the libraries were purified using a Qiagen MinElute PCR purification kit and their quality was assessed using the Agilent Bioanalyzer High-Sensitivity DNA kit according to the manufacturer's instructions. The concentration was measured by Qubit using provided protocol and the maximum of 6 libraries was pooled together in order to obtain 20 ng of each library. Prior to the sequencing, pooled libraries were additionally purified with AMPure beads (ratio 1:1) to remove contaminating primer dimers and quantified using Qubit and Agilent Bioanalyzer High-Sensitivity DNA kit. Single pools were combined into one lane, and 50-bp paired-end deep sequencing was carried out on HiSeq 4000 (Illumina) at the Next Generation Sequencing facility at the Helmholtz Zentrum München.

Ad1_noMX primer (Buenrostro et al., 2013)
5' AATGATACGGCGACCACCGAGATCTACACTCGTCGGCAGCGTCAGATGTG 3'
Nextera Index Kit (Illumina) primers N701-N706

Transposase reaction mix
25 µl 2x TD buffer (Illumina)

2.5 µl Transposase (Illumina)
22.5 µl nuclease free water

5.2.3.4 ATAC-sequencing analysis

Next Generation Sequencing facility at the Helmholtz Zentrum München demultiplexed the sequenced data, which were subsequently transferred for the analysis to the Institute of Computational Biology (ICB) at the Helmholtz Zentrum München. In collaboration with Maren Büttner (ICB), reads were aligned to the mouse genome mm10 using Bowtie (Langmead et al., 2009). For all data files, the data quality control was performed using FastQC*. Duplicates and mitochondrial reads were removed using Picard** and SAMtools (Li, 2011; Li et al., 2009).

* https://www.bioinformatics.babraham.ac.uk/projects/fastqc/
**https://broadinstitute.github.io/picard/

ATAC-seq peaks were called with chromstaR 1.5.1 (Taudt et al., 2016) in collaboration with Aaron Taudt (ICB) with the following parameter settings: binsize=100bp, stepsize=100bp, prefit.on.chr=chr1 and default settings otherwise. For the pairwise comparisons, peaks were called in a multivariate analysis using samples "CAG-GFP", "Neurog2", “Hmgb2" and “Hmgb2+Neurog2" in both “EGF+FGF” and “FGF” conditions. The multivariate analysis was performed with setting “mode=differential” for comparisons between conditions EGF+FGF and FGF, and “mode=combinatorial” for comparisons between "CAG-GFP", "Neurog2", “Hmgb2" and “Hmgb2+Neurog2”. Pairwise differential peaks were extracted by requiring a maximum posterior difference (maxPostInPeak) between bins of greater or equal to 0.99999. The genomic distribution of peaks was annotated with the annotatePeak function from ChipSeeker 1.12.1 (Yu et al., 2015a).

5.2.3.5 Preparation of libraries for RNA-sequencing

Astroglial cells that were FACS sorted 48 h after transduction with different retroviruses, were counted and centrifuged to collect them in the 1.5 ml tube. The pellet was resuspended in 100 µl of extraction buffer from PicoPure RNA isolation kit

and the RNA was extracted according to the manufacturer's protocol. The Agilent 2100 Bioanalyzer was used to assess RNA quality and concentration. For the RNA-seq library preparation, only high-quality RNA with the RIN value >8 was used. cDNA was synthesized from 10 ng of total RNA using SMART-Seq v4 Ultra Low Input RNA Kit for Sequencing, according to the manufacturer's instructions. The total number of amplification cycles was determined by RT-qPCR side reaction described below.

Primer:
PCR_SMARTer II A primer 5' AAGCAGTGGTATCAACGCAGAGT 3'

RT-qPCR reaction mix:
4 cycles amplified cDNA: 5 µl
5 µM PCR_SMARTer II A: 1 µl
SensiMix™ SYBR® 2x PCR Master Mix: 7.5 µl
H2O: up to 15 µl

Cycling conditions:

10 min 95°C (hotstart)	
10 sec 98°C	
30 sec 65°C	20x
3 min 68°C	
10 min 72°C	

The Ct corresponding to ¼ of the maximum fluorescence represented the total amount of cycles needed for cDNA amplification. Additional cycles were performed to complete the cDNA amplification and PCR-amplified cDNA was purified by immobilization on AMPure XP beads. Prior to generating the final library for the sequencing, the Covaris AFA system was used to perform the cDNA shearing in Covaris microtubes (microTUBE AFA Fiber Pre-Slit Snap-Cap 6x16mm), resulting in 200-500 bp long cDNA fragments that were subsequently purified by ethanol precipitation. The quality and concentration of the sheared cDNA were assessed on Agilent 2100 Bioanalyzer before proceeding to library preparation using MicroPlex Library Preparation kit v2 following user manual. Final libraries were evaluated using

an Agilent 2100 Bioanalyzer and the concentration was measured with Qubit Fluorometer (Thermo Fischer Scientific). The uniquely barcoded libraries were multiplexed onto one lane and 100-bp paired-end deep sequencing was carried out at the Next Generation Sequencing facility at the Helmholtz Zentrum München on HiSeq 4000 (Illumina) that generated ~20 million reads per sample.

5.2.3.6 RNA-sequencing analysis

The RNA-seq analysis was performed by Prof. Dr. Jovica Ninkovic. Kallisto pipeline (Bray et al., 2016) was used for the read mapping and the Sleuth pipeline (Pimentel et al., 2017) was used for the statistical analysis. The cut-off for the differentially regulated genes was based on the expression fold change (>2 fold) and p value adjusted for the 10% false discovery rate (q value<0.05). The genes having less than 1 TPM in both compared conditions were excluded. Gene Ontology enrichment analyses were analyzed using DAVID 6.8 Gene Ontologies tool (p value<0.05, fold change>2) (Huang et al., 2009a, 2009b).

5.2.3.7 Protein isolation and Western blot

Postnatal cortical astroglia were isolated and cultured as described above. After 10 days of culturing with growth factors EGF+FGF or FGF, they were detached from the flask by trypsinization, washed and counted. Around $0.5x10^6$ cells were centrifuged to obtain the pellet, which was either frozen at -80°C or dissolved in RIPA buffer containing protease inhibitors in dilution 1:25, when proceeded with the protein isolation immediately after. During the 30 min lysis performed on ice, samples were homogenized by passing five times through 27 G needle syringe. Lysed samples were then centrifuged at 13000 rpm for 10 min at 4°C to remove cell debris and the supernatant was transferred to a new tube. Protein concentration was measured by Pierce BCA Protein Assay Kit following the manufacturer's instructions. Finally, the samples were mixed with the 5X sample buffer in ratio 5:1, denatured for 4 min at 95°C, cooled down to room temperature and frozen at -20 °C till use.

Western blot was performed using the Mini-PROTEAN Tetra Cell System (Biorad). Gels were polymerised in the corresponding gel casting system. First, the separating

gel (15% acrylamide) was prepared and covered by a thin layer of isopropanol in order to prevent air bubbles. When separating gel had set, isopropanol was discarded, the gel was rinsed with deionised water and the loading gel was poured on top followed by insertion of a comb to create the wells for the samples. The chamber was filled with the running buffer and a total amount of 20-25 µg protein per lane was loaded. Protein samples and coloured protein ladder were run for approximately 1 h with a constant current at 25 mA (voltage set at 200 V). Finishing the run, loading gel was cut off and the separating gel was equilibrated for 10 min in transfer buffer.

In the next step, the proteins were transferred to a PVDF membrane (Millipore) that was first activated with methanol and washed in transfer buffer. The separating gel was placed on top of the equilibrated membrane and this gel-membrane sandwich was positioned between a stack of six Whatman filter papers. The entire stack covered by transfer buffer was placed into the semi-dry Trans-Blot® Turbo™ Transfer System (Biorad) and the transfer was performed using the preprogramed protocol for mixed molecular weight proteins.

For the protein detection, the membrane was pre-incubated in blocking buffer for 1 h at RT and subsequently overnight at 4°C with a primary antibody directed against HMGB2 (1:5000) and α-ACTIN (1:10000), both diluted in blocking buffer. On the next day, the membrane was first washed three times in TTBS and then incubated for 90 min with an HRP-coupled secondary antibody (dilution 1:20000 in TTBS) at RT. Proteins were detected by Amersham ECL Western Blotting Detection Reagent and visualized on the Biorad Gel Doc™ XR+ System.

25X protease inhibitors

Dissolve one cOmplete Protease Inhibitor tablet in 2 ml ddH2O and store at -20°C.

5X sample buffer

12.5 ml 1 M Tris-HCl pH=6.8 (250 mM final concentration)
5 g SDS (10% (w/v) final concentration)
15 ml glycerol (30% (v/v) final concentration)
0.15 g Bromphenol Blue (0.3% (w/v) final concentration)

2.5 ml 2-mercaptoethanol (5% (v/v) final concentration)
20 ml Milli-Q water

Separating gel buffer
90.8 g Tris-HCl (1,5 M final concentration)
20 ml 10% SDS (0.4% (w/v) final concentration)
500 ml Milli-Q water
Final pH=8.8.

Separating gel, 15%
4.5 ml water
2.5 ml separating gel buffer (pH=8.8)
4.9 ml 30% Acrylamide
0.1 ml 10% SDS
75 µl 10% APS
7.5 µl Temed

Loading gel buffer
30.3 g Tris-HCl (0.5 M final concentration)
20 ml 10% SDS (0.4% (w/v) final concentration)
500 ml Milli-Q water
Final pH=6.8.

Loading gel
3.46 ml water
625 µl loading gel buffer (pH=6.8)
833 µl 30% Acrylamide
50 µl 10% SDS
25 µl 10% APS
5 µl Temed

10X Running buffer
30.3 g Tris Base (250 mM final concentration)
144.2 g Glycine (1.92 M final concentration)

1000 ml Milli-Q water

Dilute 1:10 in Milli-Q water and add 10% SDS in 1:100 dilution (0.1% final concentration) to obtain 1X Running buffer.

10X Transfer buffer

30.3 g Tris Base (250 mM final concentration)

144.2 g Glycine (1.92 M final concentration)

1000 ml Milli-Q water

Mix 100 ml 10X Transfer buffer, 200 ml Methanol (20% (v/v) final concentration) and 700 ml Milli-Q water to obtain 1X Transfer buffer.

10X TBS

24.2 g Tris Base

80 g NaCl

1 l Milli-Q water

Adjust pH to 7.6 with HCl.

TBS Tween washing buffer (TTBS)

100 ml 10X TBS

10 ml 10% Tween 20 (0.1% (v/v) final concentration)

1 l Milli-Q water

Blocking buffer

10 g Milk powder

200 µl TTBS

Antibodies for WB	Company, ordering number	Dilution
Rabbit-anti-HMGB2	Abcam, ab67282	1:5000
Mouse-anti-α-ACTIN	Millipore, MAB1501	1:10000
HRP-coupled anti-mouse IgG1	GE Healthcare, NA931	1:20000
HRP-coupled anti-rabbit IgG	Jackson ImmunoResearch, 111-036-045	1:20000

5.2.3.8 Quantitative mass spectrometry

Preparation of astroglial cultures from the postnatal mouse cortex for the proteome analysis was performed as described above (see chapter “Primary culture of postnatal cortical astroglial cells”). The cells were collected after 10 days of culturing with EGF+FGF or FGF growth factors and prior to viral transduction. They were detached from the flask by trypsinization, centrifuged and resuspended in fresh medium. We submitted them to our collaborator Dr. Stephanie Hauck at the Research Unit Proteome Science (Helmholtz Zentrum München) for the label-free LC-MSMS based protein quantification. The collaborators also quantified detected proteins, performed statistical analysis and prepared the final list of the detected proteins including significantly enriched ones in EGF+FGF and FGF culture.

5.2.3.9 Expression plasmids

In order to overexpress different neurogenic transcription factors in the astroglial cells in vitro and in vivo, different constructs were used to produce Moloney murine leukemia virus (MMLV)-derived retroviral vectors. These factors were expressed under the regulatory control of a strong and silencing-resistant pCAG promoter together with GFP or dsRED reporter proteins that followed an internal ribosomal entry site (IRES) allowing simultaneous reporter expression. For control experiments, we used a retrovirus encoding for the fluorescent proteins (GFP or dsRED) behind the IRES driven by the same CAG promoter. Most of the plasmids are commonly used in our lab and are listed below. The Hmgb2 overexpression construct was kindly prepared by Dr. Alexandra Lepier. The vector preparation for the simultaneous overexpression of Neurog2 and Hmgb2 was part of this PhD project, as well as cloning of Hmgb1 overexpression vector (see following chapters). All the constructs with different genes and reporters that were used for the overexpression are listed below.

pCAG-IRES-GFP
pCAG-IRES-dsRED
pCAG-Neurog2-IRES-dsRED

pCAG-Brn2-IRES-dsRED
pCAG-Sox11-IRES-GFP
pCAG-Ascl1-IRES-dsRED
pCAG-Hmgb2-IRES-GFP
pCAG-Neurog2-T2A-Hmgb2-IRES-dsRED
pCAG-Hmgb1-IRES-GFP

5.2.4 Cloning the pCAG-Neurog2-T2A-Hmgb2-IRES-dsRED construct for simultaneous overexpression of NEUROG2 and HMGB2

In order to prepare the retroviral construct encoding for both, Neurog2 and Hmgb2 in a single vector, we ordered the cDNA sequences of both genes separated by T2A (Neurog2-T2A-Hmgb2) at the Genscript. The construct was designed with the BamHI restriction site upstream of the Neurog2 and EcoRV restriction site downstream of the Hmgb2 in order to clone it into the pENTR1A entry vector containing both restrictions sites. The synthesized sequence was delivered in the pUC57 vector, therefore, we first digested both vectors with the BamHI and EcoRV, expecting 1350 bp long product of Neurog2-T2A-Hmgb2 and 2262 bp long linearized pENTR1A entry vector. The restriction reaction was prepared as described below:

15 µl (3 µg) pUC57 plasmid or 10 µl (5.5 µg) pENTR1A plasmid
5 µl 10X reaction buffer 3.1 (NEB)
1 µl restriction enzyme BamHI (NEB)
1 µl restriction enzyme EcoRV (NEB)
Up to 50 µl H2O

The reaction was incubated at 37°C overnight and the DNA digestion was assessed on the next day by gel electrophoresis on the 1% agarose gel as described in the chapter “Gel electrophoresis”. The bands of proper size were purified with the QIAquick Gel Extraction Kit according to the manufacturer’s instructions and their concentration was measured with Nanodrop spectrophotometer (Thermo Fischer Scientific). Next, the insert was ligated into the opened pENTR1A plasmid with the ratio insert:vector 3:1 in a ligation reaction performed 4 h at the RT using T4 DNA Ligase according to the manufacturer’s instructions. The ligation reaction was

followed by the transformation of 50 µl DH5-α E. coli competent cells. Briefly, the cells were first thawed on ice and then about the half of the ligation reaction was added to the competent cells and incubated for 30 min on ice. The mixture was heat shocked for 30 sec at 42°C and immediately placed on ice for 5 min. 250 µl of pre-warmed LB medium was added to the transformation reaction mixture and the cells were then allowed to recover for 1 hour at 37°C in the shaking incubator. Finally, the cells were plated on LB-kanamycin agar plates and incubated overnight at 37°C.

LB medium
0.5% (w/v) NaCl
1% (w/v) Bacto-Tryptone
0.5% (w/v) Yeast extract
20 mM Tris-HCl pH 7.5
ddH2O
Adjust pH to 7.0 with NaOH and sterilize by autoclaving.

LB agar plates
Add 15 g/l agar to the LB medium before autoclaving. After autoclaving cool down, add proper antibiotic (see below), and pour into Petri dishes.

Ampicillin stock (100 mg/ml): use 1:1000
Kanamycin stock (50 mg/ml): use 1:1000

On the next day, single colonies from the agar plate were inoculated into 5 ml of LB medium, supplemented with the kanamycin and incubated overnight at 37°C under vigorous shaking. Plasmid DNA was then isolated with QIAprep Spin Miniprep Kit according to the instructions of the manufacturer. To test whether ligation of the Neurog2-T2A-Hmgb2 sequence into the pENTR1A entry vector worked properly, we performed the restriction reaction of purified plasmid with two restriction enzymes cutting inside the insert and checked the band sizes by the gel electrophoresis.

Obtaining the expected results, we proceeded with the recombination reaction to shuttle the insert into the final retroviral destination vector pCAG-IRES-dsRED. This was accomplished through the Gateway cloning method (Invitrogen). Since both,

entry and destination vector contain the gateway cassette, the insert was transferred by site-specific recombination using Gateway LR Clonase II Enzyme Mix according to the manufacturer's instructions. Next, the transformation of DH5-α E. coli competent cells was performed as described above and transformed bacteria were plated on LB-ampicillin agar plates. The colonies were picked and inoculated on the next day into LB medium supplemented with the ampicillin and grown overnight at 37°C. Plasmids were isolated with the QIAprep Spin Miniprep Kit and sequenced to confirm the proper recombination and correct sequence of the insert.

To perform sequencing of destination plasmid with the Neurog2-T2A-Hmgb2 insert, BigDye Terminator v3.1 Cycle Sequencing Kit was used including the primer S32 recognizing the sequence in front of the insert and IRES primer located after the insert. Sequencing PCR was performed by preparing the reaction mix and cycling conditions as described below.

S32 primer 5' TAGAGCCGCCGGTCACACG 3'
IRES primer 5' GCTTGGAATAAGGCCGGTG 3'

PCR reaction mix:
Big Dye Terminator: 1 µl
5X Big Dye Buffer: 1 µl
S32 primer or IRES primer (from 100µM stock): 0.5 µl
Miniprep plasmid: 2.5 µl

Cycling conditions:

1 min 96°C	
10 sec 96°C	
5 sec 50°C	35x
4 min 60°C	
∞ 16°C	

The sequencing PCR was then purified using Dye Ex 2.0 Spin Kit according to the protocol of the manufacturer and filled in a sequencing plate. The sequencing was performed at the Genome Analysis Center of the Helmholtz Zentrum München.

For the retroviral production, the plasmid was amplified using large-scale bacterial cultures and isolated with Qiagen Plasmid Maxi kit following the manufacturer's protocol.

5.2.4.1 Cloning the pCAG-Hmgb1-IRES-GFP construct

In order to overexpress the HMGB1, its cDNA (source Genscript) was cloned into the pENTR1A entry vector. The Hmgb1 construct was delivered in the pUC57 vector with the restriction site BamHI upstream and HindIII downstream of the Hmgb1 sequence. As the pENTR1A does not contain the HindIII restriction site, it was digested with BamHI and EcoRV and the blunt ligation at the EcoRV site was required. To do so, the cloning strategy described below was applied. First, the pUC57+Hmgb1 vector was linearized using HindIII restriction enzyme in the following restriction reaction:

80 µl (4.5 µg) pUC57+Hmgb1 plasmid
10 µl 10X reaction buffer 2.1 (NEB)
3 µl restriction enzyme HindIII (NEB)
Up to 100 µl H2O

The digestion reaction was incubated for 2 h at 37°C and the plasmid linearization was assessed by gel electrophoresis as described in the chapter "Gel electrophoresis". Next, to create the blunt ends, Klenow fragment was used in the following reaction mix:

12 µl 10X Klenow buffer (NEBuffer 2)
5 µl dNTP mix (2 mM)
3 µl Klenow fragment
97 µl linearized DNA from the restriction reaction mix
Up to 120 µl H2O

The blunting was performed for 10 min at 37°C and the reaction was terminated by heating for 10 min at 75°C. DNA was purified by QIAquick PCR Purification Kit according to the manufacturer's instructions and subsequently digested with the BamHI restriction enzyme to cut out the Hmgb1 sequence. In parallel, the double digest of pENTR1A plasmid with the BamHI and EcoRV was performed. Both digestion reaction mixes are described below.

Restriction reaction of pUC57+Hmgb1 linearized plasmid with the blunt overhangs:
30 µl pUC57+Hmgb1
5 µl 10X reaction buffer 3.1 (NEB)
1 µl restriction enzyme BamHI (NEB)
Up to 50 µl H2O

Restriction reaction of pENTR1A:
10 µl (5.5 µg) pENTR1A plasmid
5 µl 10X reaction buffer 3.1 (NEB)
1 µl restriction enzyme BamHI (NEB)
1 µl restriction enzyme EcoRV (NEB)
Up to 50 µl H2O

The restriction reaction took place for 2 h at 37°C and the bands were separated by the gel electrophoresis. Opened pENTR1A plasmid had the size of 2262 bp and Hmgb1 construct 654 bp. The bands of proper size were purified with the QIAquick gel extraction kit according to the manufacturer's instructions. The ligation reaction, bacterial transformation, inoculation and plasmid purification was performed as described in the previous chapter. To test the proper insertion of Hmgb1 into the entry vector, the plasmid was digested using the restriction site within the Hmgb1 sequence.

In the last step, the Hmgb1 cDNA was transferred to the retroviral destination vector pCAG-IRES-GFP using gateway recombination as described above. The final construct was amplified and purified from the transformed bacteria and the sequencing using the primers listed above (IRES, S32) was performed to confirm the insertion of the correct sequence.

5.2.4.2 Production of the retroviruses

The VSV-G-pseudotyped retroviruses were prepared using the HEK293-derived retroviral packaging cell line (293GPG) (Ory et al., 1996), that stably express the gag-pol genes of murine leukemia virus and vsv-g under the control of a tet/VP16 transactivator (Heinrich et al., 2011). Packaging cells were cultured in GPG medium and passaged 1:2 on a day before transfection to reach 80-90% confluency. On the next day, cells were first washed with DPBS to eliminate any traces of antibiotics and the GPG medium was replaced by 12 ml 0-medium 1-2 h prior to transfection. Meanwhile, two transfection mixes were prepared: 9 ml Opti-MEM + 360 µl Lipofectamine 2000 and 9 ml Opti-MEM + 144 µg DNA and separately incubated for 5 min at the RT. After 5 min, the diluted Lipofectamine 2000 reagent was combined with the diluted DNA, mixed well and incubated at RT for 30 min shaking gently. Next, the cells were transfected by carefully pipetting 3 ml of the transfection mix to each plate (6x 10 cm dishes in total). The following morning, transfection medium was replaced by 6 ml of 0-medium. The first medium collection was performed 3 days after transfection, followed by a second harvest 5 days after transfection and third and fourth harvest, on the day 7 and 9, respectively. To concentrate viral particles, the culture medium was filtered through a 0.45 µm PVDF filter and spun down at 50000 g for 90 min at 4°C. The supernatant was discarded and the pellet was covered by 30 µl TNE buffer and incubated at 4°C overnight. On the next day, pellet was carefully resuspended and the viral suspension was aliquoted and stored at -80°C.

GPG medium

500 ml DMEM, high glucose
50 ml Fetal calf serum-FCS (10% (v/v) final concentration)
1 ml 0.5 mg/ml Tetracycline (1 µg/ml (w/v) final concentration)
100 µl 10 mg/ml Puromycin (2 µg/ml (w/v) final concentration)
3 ml 50 mg/ml Geneticin (0.3 µg/ml (w/v) final concentration)
3 ml Penicillin/Streptomycin
3 ml 1M HEPES

0-medium

500 ml DMEM, high glucose
25 ml Fetal calf serum-FCS (10% (v/v) final concentration)
2.5 ml Penicillin/Streptomycin

TNE buffer
2.5 ml 1 M Tris-HCl pH=7.8 (50 mM final concentration)
1.3 ml 5 M NaCl (130 mM final concentration)
0.1 ml 0.5 M EDTA (1 mM final concentration)
Up to 50 ml ddH2O

5.2.5 Data analysis

5.2.5.1 Image acquisition and quantifications

Immunostainings were analysed with a fluorescent Microscope Axio Imager M2m (Zeiss) and the images from the cultured cells were acquired using the ZEN software (Zeiss) with a 20x or 40x objective. Fluorescent-labelled sections were photographed with FV1000 confocal laser-scanning microscope (Olympus), using the FW10-ASW 4.0 software (Olympus).

The quantifications of in vitro cultured cells were performed using the ZEN software (Zeiss) analysing at least 25 randomly taken pictures per coverslip depending on the number of transduced cells. These cultures were always prepared in triplicates for the same condition in the single experiment. Therefore, 3 coverslips per condition per experiment were analysed. In total, about 100-200 retroviral vector-transduced cells were quantified from randomly chosen fields on a single coverslip. The number of induced neurons was expressed as a percentage out of all transduced cells. To analyse the number of apoptotic cells, between 350-550 DAPI labelled cells were counted from 5 randomly selected fields on one coverslip. In the reprogramming experiments of the astrocytes isolated from Hmgb2+/+, Hmgb2+/- and Hmgb2-/- animals, each of the single animals was considered as a biological replicate and at least 3 coverslips were counted per animal. We analysed in total 6 litters from different time points with the different number of wild-type, heterozygous or homozygous littermates. In the reactive gliosis culture, one coverslip per condition

was analysed, by counting in total at least 100 double transduced cells from randomly chosen fields on the coverslip.

Quantitative analysis of in vivo reprogramming was done by counting all transduced cells in all the sections with the injury site from ≥3 independent biological replicates. The numbers are indicating the proportion of NEUN+ cells out of all counted RFP+ transduced cells. Quantifications were performed using Fiji software (Schindelin et al., 2012) to analyze all the individual planes of an optical Z-stack and cells were examined in orthogonal planes to verify the markers coexpression.

In order to analyse Western blot experiment, the gel analysing tool in the Fiji software was used (Schindelin et al., 2012). All lanes of interest were outlined using the rectangular selection tool and the signal intensity of each band was calculated by determining the area under the peak. The measurements of the corresponding α-ACTIN bands were used to normalize the amount of proteins loaded on the gel.

5.2.5.2 Statistical analysis

Numbers of biological replicates can be seen on the dot plots or in the figure legend in case of the bar charts. All results are presented as a median ± interquartile range (IQR). IQR was calculated in RStudio (RStudio, 2015), using the default method based on type 7 continuous sample quantile. For the reprogramming experiments, statistical analysis was performed in R (RStudio, 2015) using non-parametric Mann-Whitney U test to test for significance as indicated throughout the thesis. The statistical test was performed only in the experiments with at least 4 biological replicates. Results were considered significant with $p<0.05$ (one asterisk). Statistics performed in the proteome analysis was a log2 intensity based t-test. The statistical analysis of the RNA-sequencing data was carried out using Sleuth program (Pimentel et al., 2017).

6 Abbreviations

Acsbg1 – Acyl-CoA Synthetase Bubblegum Family Member 1
AD – Alzheimer's disease
ALDH1L1 – Aldehyde Dehydrogenase 1 Family Member L1
aNSC – Adult neural stem cell
Aqp4 – Aquaporin 4
aRG – Apical radial glial cell
ASCL1 – Achaete-Scute Family BHLH Transcription Factor 1
ATAC – Assay for Transposase Accessible Chromatin
ATP – Adenosine triphosphate
BCL-2 – B-cell lymphoma 2
BDNF – Brain-derived neurotrophic factor
bHLH – Basic helix-loop-helix
BLBP – Brain lipid-binding protein
BMP – Bone morphogenetic protein
bp – Base pair
BP – Biological process
BrdU – 5-bromo-2'-deoxyuridine
Brn2 – Brain2
CAG – Cytomegalovirus early enhancer/chicken beta-actin promoter
cDNA – Complementary DNA
CGE – Caudal ganglionic eminence
ChiP – Chromatin immunoprecipitation
CHUD – Chromatin unfolding domain
CNS – Central nervous system
CP – Cortical plate
CPN – Callosal projection neuron
CR – Cajal-Retzius cell
CSF – Cerebrospinal fluid
CThPN – Corticothalamic projection neuron
CTIP – COUP-TF-Interacting Protein 2
CUX – Cut Like Homeobox 1
DPBS – Dulbecco's phosphate-buffered saline

DAMP – Damage-associated molecular pattern

DAPI – 4’,6-diamidino-2-phenylindole

DCX – Doublecortin, x-linked lissencephaly

DG – Dentate gyrus

Dll4 – Delta-like 4

Dlx – Distal-less homeobox

Dlx2 – Distal-less gene 2

DM – Dorsomorphin

DMEM – Dulbecco’s modified Eagle’s medium

DNA – Deoxyribonucleic acid

dNTP – Deoxynucleoside triphosphate

DPI – Days post induction/injury

dsRED – Discosoma sp. red fluorescent protein

E – Embryonic day

E+F – EGF+FGF

ECM – Extracellular matrix

EDTA – Ethylene-diamine-tetra-acetic-acid

EGF – Epidermal growth factor

Elavl4 – ELAV Like RNA Binding Protein 4

Emx1/2 – Empty spiracles homeobox 1/2

EZ – Ependymal zone

F – FGF

FACS – Fluorescence activated cell sorting

FBS – Fetal bovine serum

FCS – Fetal calf serum

FGF – Basic fibroblast growth factor

FK – Forskolin

FOXG1 – Forkhead box G1

FOXP2 – Forkhead box protein P2

FSC-A – Forward scatter area

FSC-W – Forward scatter width

GABA – γ-aminobutyric acid

GCL – Granule cell layer

GE – Ganglionic eminence

GF – Growth factor
GFAP – Glial fibrillary acidic protein
GFP – Green fluorescent protein
Gjb6 – Gap junction protein beta 6
GLAST – Astrocyte-specific glutamate transporter
Glul – Glutamine synthetase
GM – Gray matter
GN – Granular neuron
GO – Gene ontology
HBSS – Hank's balanced salt solution
HEPES – 4-(2-hydroxyethyl)-1-piperazineethanesulfonic acid
Hey1 – Hairy/enhancer-of-split related with YRPW motif protein 1
hiNSC – human induced neural stem cells
HMG – High Mobility Group
IBA1 - Ionized calcium-binding adapter molecule 1
IHC – Immunohistochemistry
IP – Intermediate progenitor
IQR – Interquartile range
IRES – Internal ribosome entry site
IZ – Intermediate zone
kDa – Kilodalton
LC – Liquid chromatography
LGE – Lateral ganglionic eminence
LMX1A – LIM Homeobox Transcription Factor 1 Alpha
LV – Lateral ventricle
MAP – Mitogen-activated protein
MGE – Medial ganglionic eminence
miR – microRNA
ML – Molecular layer
MMLV – Moloney murine leukemia virus
mRNA – Messenger ribonucleic acid
MS – Mass spectrometry
MyoD – Myogenic factor 3
MYT1L – Myelin transcription factor 1-like protein

MZ –Marginal zone

n – Number of experiments, sample number

NADPH – Nicotinamide adenine dinucleotide phosphate

NB – Neuroblast

NBD – Nucleosomal binding domain

NC – Neuroepithelial cells

NE – Neuroepithelium

NEUN – Neuronal nuclear antigen

NeuroD1 – Neuronal differentiation 1

NeuroD2 – Neuronal differentiation 2

NeuroD4 – Neuronal differentiation 4

NEUROG1 – Neurogenin1

NEUROG2 – Neurogenin2

NF-κB – Nuclear factor 'kappa-light-chain-enhancer' of activated B-cells

NG2 – Neuron-glial antigen 2

NGS – Normal goat serum

nIPC – Neurogenic intermediate progenitor cell

Nkx2.1 – NK2 Homeobox 1

NLS – Nuclear localisation signal

NPC – Neural precursor/progenitor cell

NSC – Neural stem cell

NURR1 – Nuclear receptor related-1 protein

OB – Olfactory bulb

OE – Overexpression

oIPC – Oligodendrocytic intermediate progenitor cell

OLIG2 – Oligodendrocyte Transcription Factor 2

OPC – Oligodendrocyte progenitor cell

oRG – Outer radial glia

OxPhos – Oxidative phosphorylation

P – Postnatal day

Pax6 – Paired box 6

PBS – Phosphate buffered saline

PCA – Principle component analysis

PCR – Polymerase chain reaction

PDGFRα – Platelet-derived growth factor receptor Alpha

PDL – Poly-D-lysine

PEN/STREP – Penicillin/streptomycin

PFA – Paraformaldehyde

PH3 – Phospho histone 3

PSC – Pluripotent stem cell

PTB – Polypyrimidine tract binding

PVDF – Polyvinylidene fluoride

Pol – Polymerase

RT-qPCR – Quantitative reverse transcription polymerase chain reaction

RAGE – Receptor for Advanced Glycation End products

REST – RE-1 transcription factor repressor complex

RG – Radial glial cells

RMS – Rostral migratory stream

RNA – Ribonucleic acid

ROS – Reactive oxygen species

RT – Room temperature

SATB2 – SATB Homeobox 2

SCPN – Subcortical projection neuron

SDS – Sodium dodecyl sulfate

Seq – Sequencing

SGZ – Subgranular zone

SHH – Sonic hedgehog homolog

Sox – Sex determining region Y (SRY)

SP – Subplate

SPN – Subplate neuron

SSC-A – Side scatter area

SVZ – Subventricular zone

TAP – Transient amplifying progenitor

Tbr1 – T-Box, Brain 1

Tbr2 – T-Box, Brain 2

TF – Transcription factor

TLR – Toll-like receptor

TUNEL – Terminal deoxynucleotidyl transferase (TdT) dUTP Nick-End Labeling

VPA – Valproic acid
VZ – Ventricular zone
WM – White matter
WNT – Wingless-Int
αSMA – Alpha smooth muscle actin

s – second
min – minute
h – hour

µm – micrometer
mm – millimeter

ng – nanogram
µg – microgram
mg – milligram

nl – nanoliter
µl – microliter
l – liter

µM – micromolar
mM – millimolar
M – molar

v/v – volume per volume
w/v – weight per volume

7 References

Abraham, A.B., Bronstein, R., Reddy, A.S., Maletic-Savatic, M., Aguirre, A., and Tsirka, S.E. (2013). Aberrant Neural Stem Cell Proliferation and Increased Adult Neurogenesis in Mice Lacking Chromatin Protein HMGB2. PLoS One *8*, e84838.

Addington, C.P., Roussas, A., Dutta, D., and Stabenfeldt, S.E. (2015). Endogenous repair signaling after brain injury and complementary bioengineering approaches to enhance neural regeneration. Biomark. Insights *10*, 43–60.

Agresti, A., and Bianchi, M.E. (2003). HMGB proteins and gene expression. Curr. Opin. Genet. Dev. *13*, 170–178.

Alvarez-Buylla, A., Kohwi, M., Nguyen, T.M., and Merkle, F.T. (2008). The heterogeneity of adult neural stem cells and the emerging complexity of their niche. Cold Spring Harb. Symp. Quant. Biol. *73*, 357–365.

Amamoto, R., and Arlotta, P. (2014). Development-inspired reprogramming of the mammalian central nervous system. Science (80-.). *343*, 1–18.

Arenas, E., Denham, M., and Villaescusa, J.C. (2015). How to make a midbrain dopaminergic neuron. Development *142*, 1918–1936.

Arlotta, P., Molyneaux, B.J., Chen, J., Inoue, J., Kominami, R., and Macklis, J.D. (2005). Neuronal Subtype-Specific Genes that Control Corticospinal Motor Neuron Development In Vivo. Neuron *45*, 207–221.

Bardehle, S., Krüger, M., Buggenthin, F., Schwausch, J., Ninkovic, J., Clevers, H., Snippert, H.J., Theis, F.J., Meyer-Luehmann, M., Bechmann, I., et al. (2013). Live imaging of astrocyte responses to acute injury reveals selective juxtavascular proliferation.

Beckervordersandforth, R., Tripathi, P., Ninkovic, J., Bayam, E., Lepier, A., Stempfhuber, B., Kirchhoff, F., Hirrlinger, J., Haslinger, A., Lie, D.C., et al. (2010). In vivo fate mapping and expression analysis reveals molecular hallmarks of prospectively isolated adult neural stem cells. Cell Stem Cell *7*, 744–758.

Bélanger, M., Allaman, I., and Magistretti, P.J. (2011). Brain energy metabolism: focus on astrocyte-neuron metabolic cooperation. Cell Metab. *14*, 724–738.

Bergmann, O., Spalding, K.L., and Frisén, J. (2015). Adult Neurogenesis in Humans. Cold Spring Harb. Perspect. Biol. *7*, a018994.

Berninger, B., Costa, M.R., Koch, U., Schroeder, T., Sutor, B., Grothe, B., and Gotz, M. (2007). Functional Properties of Neurons Derived from In Vitro Reprogrammed

Postnatal Astroglia. J. Neurosci. *27*, 8654–8664.

Bianchi, M.E., and Agresti, A. (2005). HMG proteins: Dynamic players in gene regulation and differentiation. Curr. Opin. Genet. Dev. *15*, 496–506.

Blum, R., Heinrich, C., Sánchez, R., Lepier, A., Gundelfinger, E.D., Berninger, B., and Götz, M. (2011). Neuronal Network Formation from Reprogrammed Early Postnatal Rat Cortical Glial Cells. Cereb. Cortex *21*, 413–424.

Boldrini, M., Fulmore, C.A., Tartt, A.N., Simeon, L.R., Pavlova, I., Poposka, V., Rosoklija, G.B., Stankov, A., Arango, V., Dwork, A.J., et al. (2018). Human Hippocampal Neurogenesis Persists throughout Aging. Cell Stem Cell *22*, 589–599.e5.

Bond, A.M., Ming, G.-L., and Song, H. (2015). Adult Mammalian Neural Stem Cells and Neurogenesis: Five Decades Later. Stem Cell *17*, 385–395.

Borrell, V., and Götz, M. (2014). Role of radial glial cells in cerebral cortex folding. Curr. Opin. Neurobiol. *27*, 39–46.

Bray, N.L., Pimentel, H., Melsted, P., and Pachter, L. (2016). Near-optimal probabilistic RNA-seq quantification. Nat. Biotechnol. *34*, 525–527.

Bronstein, R., Kyle, J., Abraham, A.B., and Tsirka, S.E. (2017). Neurogenic to Gliogenic Fate Transition Perturbed by Loss of HMGB2. Front. Mol. Neurosci.

Brulet, R., Matsuda, T., Zhang, L., Miranda, C., Giacca, M., Kaspar, B.K., Nakashima, K., and Hsieh, J. (2017). NEUROD1 Instructs Neuronal Conversion in Non-Reactive Astrocytes. Stem Cell Reports *8*, 1506–1515.

Buenrostro, J.D., Giresi, P.G., Zaba, L.C., Chang, H.Y., and Greenleaf, W.J. (2013). Transposition of native chromatin for fast and sensitive epigenomic profiling of open chromatin, DNA-binding proteins and nucleosome position. Nat. Methods.

Buenrostro, J.D., Wu, B., Chang, H.Y., and Greenleaf, W.J. (2015). ATAC-seq: A Method for Assaying Chromatin Accessibility Genome-Wide. Curr. Protoc. Mol. Biol. *109*, 21.29.1-9.

Buffo, A., Vosko, M.R., Ertürk, D., Hamann, G.F., Jucker, M., Rowitch, D., and Götz, M. (2005). Expression pattern of the transcription factor Olig2 in response to brain injuries: implications for neuronal repair. Proc. Natl. Acad. Sci. U. S. A. *102*, 18183–18188.

Buffo, A., Rite, I., Tripathi, P., Lepier, A., Colak, D., Horn, A.-P., Mori, T., and Götz, M. (2008). Origin and progeny of reactive gliosis: A source of multipotent cells in the injured brain. Proc. Natl. Acad. Sci. U. S. A. *105*, 3581–3586.

Burda, J.E., and Sofroniew, M. V (2014). Reactive gliosis and the multicellular response to CNS damage and disease. Neuron *81*, 229–248.

Bustin, M. (1999). Regulation of DNA-Dependent Activities by the Functional Motifs of the High-Mobility-Group Chromosomal Proteins. Mol. Cell. Biol. *19*, 5237–5246.

Bustin, M. (2001). Revised nomenclature for high mobility group (HMG) chromosomal proteins. Trends Biochem. Sci. *26*, 152–153.

Cahoy, J.D., Emery, B., Kaushal, A., Foo, L.C., Zamanian, J.L., Christopherson, K.S., Xing, Y., Lubischer, J.L., Krieg, P.A., Krupenko, S.A., et al. (2008). A Transcriptome Database for Astrocytes, Neurons, and Oligodendrocytes: A New Resource for Understanding Brain Development and Function. J. Neurosci.

Cai, J., Chen, Y., Cai, W.-H., Hurlock, E.C., Wu, H., Kernie, S.G., Parada, L.F., and Lu, Q.R. (2007). A crucial role for Olig2 in white matter astrocyte development. Development *134*, 1887–1899.

Caiazzo, M., Dell 'anno, M.T., Dvoretskova, E., Lazarevic, D., Taverna, S., Leo, D., Sotnikova, T.D., Menegon, A., Roncaglia, P., Colciago, G., et al. (2011). Direct generation of functional dopaminergic neurons from mouse and human fibroblasts. Nature *476*.

Casarosa, S., Fode, C., and Guillemot, F. (1999). Mash1 regulates neurogenesis in the ventral telencephalon. Development *126*, 525–534.

Castro, D.S., Skowronska-Krawczyk, D., Armant, O., Donaldson, I.J., Parras, C., Hunt, C., Critchley, J.A., Nguyen, L., Gossler, A., Göttgens, B., et al. (2006). Proneural bHLH and Brn proteins coregulate a neurogenic program through cooperative binding to a conserved DNA motif. Dev. Cell *11*, 831–844.

Catena, R., Escoffier, E., Caron, C., Khochbin, S., Martianov, I., and Davidson, I. (2009). HMGB4, a Novel Member of the HMGB Family, Is Preferentially Expressed in the Mouse Testis and Localizes to the Basal Pole of Elongating Spermatids. Biol. Reprod. *80*, 358–366.

Catez, F., and Hock, R. (2010). Binding and interplay of HMG proteins on chromatin: Lessons from live cell imaging. Biochim. Biophys. Acta - Gene Regul. Mech.

Chanda, S., Ang, C.E., Davila, J., Pak, C., Mall, M., Lee, Q.Y., Ahlenius, H., Jung, S.W., Südhof, T.C., and Wernig, M. (2014). Generation of induced neuronal cells by the single reprogramming factor ASCL1. Stem Cell Reports *3*, 282–296.

Chen, G., Wernig, M., Berninger, B., Nakafuku, M., Parmar, M., and Zhang, C.-L. (2015). In Vivo Reprogramming for Brain and Spinal Cord Repair. ENeuro *2*, 1–6.

Colasante, G., Lignani, G., Rubio, A., Medrihan, L., Yekhlef, L., Sessa, A., Massimino, L., Giannelli, S.G., Sacchetti, S., Caiazzo, M., et al. (2015). Rapid Conversion of Fibroblasts into Functional Forebrain GABAergic Interneurons by Direct Genetic Reprogramming. Cell Stem Cell.

Dametti, S., Faravelli, I., Ruggieri, M., Ramirez, A., Nizzardo, M., and Corti, S. (2016). Experimental Advances Towards Neural Regeneration from Induced Stem Cells to Direct In Vivo Reprogramming. Mol. Neurobiol. *53*, 2124–2131.

Deng, T., Zhu, Z.I., Zhang, S., Leng, F., Cherukuri, S., Hansen, L., Mariño-Ramírez, L., Meshorer, E., Landsman, D., and Bustin, M. (2013). HMGN1 modulates nucleosome occupancy and DNase I hypersensitivity at the CpG island promoters of embryonic stem cells. Mol. Cell. Biol. *33*, 3377–3389.

Deng, T., Postnikov, Y., Zhang, S., Garrett, L., Becker, L., Rácz, I., Hölter, S.M., Wurst, W., Fuchs, H., Gailus-Durner, V., et al. (2017). Interplay between H1 and HMGN epigenetically regulates OLIG1&2 expression and oligodendrocyte differentiation. Nucleic Acids Res. *45*, 3031–3045.

Dennis, C. V., Suh, L.S., Rodriguez, M.L., Kril, J.J., and Sutherland, G.T. (2016). Human adult neurogenesis across the ages: An immunohistochemical study. Neuropathol. Appl. Neurobiol. *42*, 621–638.

Doetsch, F., Caillé, I., Lim, D.A., García-Verdugo, J.M., and Alvarez-Buylla, A. (1999). Subventricular Zone Astrocytes Are Neural Stem Cells in the Adult Mammalian Brain. Cell *97*, 703–716.

Drouin-Ouellet, J., Pircs, K., Barker, R.A., Jakobsson, J., and Parmar, M. (2017). Direct Neuronal Reprogramming for Disease Modeling Studies Using Patient-Derived Neurons: What Have We Learned? Front. Neurosci. *11*, 530.

Drouin Ouellet, J., Lau, S., Brattås, P.L., Rylander Ottosson, D., Pircs, K., Grassi, D.A., Collins, L.M., Vuono, R., Andersson Sjöland, A., Westergren-Thorsson, G., et al. (2017). REST suppression mediates neural conversion of adult human fibroblasts via microRNA-dependent and -independent pathways. EMBO Mol. Med. *9*, 1117–1131.

Dy, P., Penzo-Méndez, A., Wang, H., Pedraza, C.E., Macklin, W.B., and Lefebvre, V. (2008). The three SoxC proteins--Sox4, Sox11 and Sox12--exhibit overlapping expression patterns and molecular properties. Nucleic Acids Res. *36*, 3101–3117.

Enokido, Y., Yoshitake, A., Ito, H., and Okazawa, H. (2008). Age-dependent change of HMGB1 and DNA double-strand break accumulation in mouse brain. Biochem.

Biophys. Res. Commun. *376*, 128–133.

Eriksson, P.S., Perfilieva, E., Björk-Eriksson, T., Alborn, A.-M., Nordborg, C., Peterson, D.A., and Gage, F.H. (1998). Neurogenesis in the adult human hippocampus. Nat. Med. *4*, 1313–1317.

Ernst, A., and Frisén, J. (2015). Adult Neurogenesis in Humans- Common and Unique Traits in Mammals. PLOS Biol. *13*, e1002045.

Ernst, A., Alkass, K., Bernard, S., Salehpour, M., Perl, S., Tisdale, J., Possnert, G., Druid, H., and Frisén, J. (2014). Neurogenesis in the striatum of the adult human brain. Cell *156*, 1072–1083.

Falk, S., Bugeon, S., Ninkovic, J., Pilz, G.-A., Postiglione, M.P., Cremer, H., Knoblich, J.A., and Götz, M. (2017). Time-Specific Effects of Spindle Positioning on Embryonic Progenitor Pool Composition and Adult Neural Stem Cell Seeding. Neuron *93*, 777–791.e3.

Fischer, J., Beckervordersandforth, R., Tripathi, P., Steiner-Mezzadri, A., Ninkovic, J., and Götz, M. (2011). Prospective isolation of adult neural stem cells from the mouse subependymal zone. Nat. Protoc. *6*, 1981–1989.

Fishman, V.S., Shnayder, T.A., Orishchenko, K.E., Bader, M., Alenina, N., and Serov, O.L. (2015). Cell divisions are not essential for the direct conversion of fibroblasts into neuronal cells. Cell Cycle *14*, 1188–1196.

Fode, C., Ma, Q., Casarosa, S., Ang, S.L., Anderson, D.J., and Guillemot, F. (2000). A role for neural determination genes in specifying the dorsoventral identity of telencephalic neurons. Genes Dev. *14*, 67–80.

Fuentealba, L.C., Rompani, S.B., Parraguez, J.I., Obernier, K., Romero, R., Cepko, C.L., and Alvarez-Buylla, A. (2015). Embryonic Origin of Postnatal Neural Stem Cells. Cell.

Furusawa, T., and Cherukuri, S. (2010). Developmental function of HMGN proteins. Biochim. Biophys. Acta - Gene Regul. Mech.

Gascón, S., Murenu, E., Masserdotti, G., Ortega, F., Russo, G.L., Petrik, D., Deshpande, A., Heinrich, C., Karow, M., Robertson, S.P., et al. (2016). Identification and Successful Negotiation of a Metabolic Checkpoint in Direct Neuronal Reprogramming. Cell Stem Cell.

Gascón, S., Masserdotti, G., Russo, G.L., and Götz, M. (2017). Direct Neuronal Reprogramming: Achievements, Hurdles, and New Roads to Success. Cell Stem Cell 18–34.

Gavrieli, Y., Sherman, Y., and Ben-Sasson, S.A. (1992). Identification of programmed cell death in situ via specific labeling of nuclear DNA fragmentation. J. Cell Biol. *119*, 493–501.

Gerlitz, G., Hock, R., Ueda, T., and Bustin, M. (2009). The dynamics of HMG protein-chromatin interactions in living cells. Biochem. Cell Biol. *87*, 127–137.

Ghasemi-Kasman, M., Hajikaram, M., Baharvand, H., and Javan, M. (2015). MicroRNA-mediated in vitro and in vivo direct conversion of astrocytes to neuroblasts. PLoS One.

Gilbert, S.F. (2014). Developmental biology (Sinauer Associates).

Gohlke, J.M., Armant, O., Parham, F.M., Smith, M. V, Zimmer, C., Castro, D.S., Nguyen, L., Parker, J.S., Gradwohl, G., Portier, C.J., et al. (2008). Characterization of the proneural gene regulatory network during mouse telencephalon development. BMC Biol. *6*, 15.

Gonçalves, J.T., Schafer, S.T., and Gage, F.H. (2016). Adult Neurogenesis in the Hippocampus: From Stem Cells to Behavior. Cell *167*, 897–914.

Goodman, T., and Hajihosseini, M.K. (2015). Hypothalamic tanycytes—masters and servants of metabolic, neuroendocrine, and neurogenic functions. Front. Neurosci. *9*, 387.

Götz, M., and Huttner, W.B. (2005). The cell biology of neurogenesis. Nat. Rev. Mol. Cell Biol.

Götz, M., Nakafuku, M., and Petrik, D. (2016). Neurogenesis in the developing and adult brain—similarities and key differences. Cold Spring Harb. Perspect. Biol.

Grade, S., and Götz, M. (2017). Neuronal replacement therapy: previous achievements and challenges ahead. Npj Regen. Med. *2*, 29.

Grande, A., Sumiyoshi, K., López-Juárez, A., Howard, J., Sakthivel, B., Aronow, B., Campbell, K., and Nakafuku, M. (2013). Environmental impact on direct neuronal reprogramming in vivo in the adult brain. Nat. Commun. *4*, 1–12.

Grealish, S., Drouin-Ouellet, J., and Parmar, M. (2016). Brain repair and reprogramming: the route to clinical translation. J. Intern. Med. *280*, 265–275.

Greig, L.C., Woodworth, M.B., Galazo, M.J., Padmanabhan, H., and Macklis, J.D. (2013). Molecular logic of neocortical projection neuron specification, development and diversity.

Guazzi, S., Strangio, A., Franzi, A.T., and Bianchi, M.E. (2003). HMGB1, an architectural chromatin protein and extracellular signalling factor, has a spatially and

temporally restricted expression pattern in mouse brain. Gene Expr. Patterns.

Guillemot, F. (2007). Cell fate specification in the mammalian telencephalon. Prog. Neurobiol. *83*, 37–52.

Guo, Z., Zhang, L., Wu, Z., Chen, Y., Wang, F., and Chen, G. (2014). In vivo direct reprogramming of reactive glial cells into functional neurons after brain injury and in an Alzheimer's disease model. Cell Stem Cell *14*, 188–202.

Hébert, J.M., and Fishell, G. (2008). The genetics of early telencephalon patterning: some assembly required. Nat. Rev. Neurosci. *9*, pages 678–685.

Heinrich, C., Blum, R., Gascón, S., Masserdotti, G., Tripathi, P., Sánchez, R., Tiedt, S., Schroeder, T., Götz, M., and Berninger, B. (2010). Directing astroglia from the cerebral cortex into subtype specific functional neurons. PLoS Biol.

Heinrich, C., Gasc, S., Masserdotti, G., Lepier, A., Sanchez, R., Simon-Ebert, T., Schroeder, T., and Berninger, B. (2011). Generation of subtype-specific neurons from postnatal astroglia of the mouse cerebral cortex. Nat. Protoc. *6*.

Heinrich, C., Bergami, M., Gascón, S., Lepier, A., Viganò, F., Dimou, L., Sutor, B., Berninger, B., and Götz, M. (2014). Sox2-Mediated Conversion of NG2 Glia into Induced Neurons in the Injured Adult Cerebral Cortex. Stem Cell Reports.

Heinrich, C., Spagnoli, F.M., and Berninger, B. (2015). In vivo reprogramming for tissue repair. Nat. Publ. Gr. *17*.

Heins, N., Malatesta, P., Cecconi, F., Nakafuku, M., Tucker, K.L., Hack, M.A., Chapouton, P., Barde, Y.A., and Goötz, M. (2002). Glial cells generate neurons: The role of the transcription factor Pax6. Nat. Neurosci. *5*, 308–315.

Henke, R.M., Savage, T.K., Meredith, D.M., Glasgow, S.M., Hori, K., Dumas, J., MacDonald, R.J., and Johnson, J.E. (2009). Neurog2 is a direct downstream target of the Ptf1a-Rbpj transcription complex in dorsal spinal cord. Development *136*, 2945–2954.

Henson, E.S., and Gibson, S.B. (2006). Surviving cell death through epidermal growth factor (EGF) signal transduction pathways: Implications for cancer therapy. Cell. Signal. *18*, 2089–2097.

Hock, R., Furusawa, T., Ueda, T., and Bustin, M. (2007). HMG chromosomal proteins in development and disease.

Holth, L.T., Thorlacius, E.A., and Reeves, R. (1997). Effects of Epidermal Growth Factor and Estrogen on the Regulation of the HMG-I/Y Gene in Human Mammary Epithelial Cell Lines. DNA Cell Biol. *16*, 1299–1309.

Hsieh, J. (2012). Orchestrating transcriptional control of adult neurogenesis. Genes Dev. *26*, 1010–1021.

Huang, D.W., Sherman, B.T., and Lempicki, R.A. (2009a). Bioinformatics enrichment tools: paths toward the comprehensive functional analysis of large gene lists. Nucleic Acids Res. *37*, 1–13.

Huang, D.W., Sherman, B.T., and Lempicki, R.A. (2009b). Systematic and integrative analysis of large gene lists using DAVID bioinformatics resources. Nat. Protoc. *4*, 44–57.

Huh, C.J., Zhang, B., Victor, M.B., Dahiya, S., Batista, L.F., Horvath, S., and Yoo, A.S. (2016). Maintenance of age in human neurons generated by microRNA-based neuronal conversion of fibroblasts. Elife *5*, e18648.

Hulsen, T., de Vlieg, J., and Alkema, W. (2008). BioVenn – a web application for the comparison and visualization of biological lists using area-proportional Venn diagrams. BMC Genomics *9*, 488.

Ito, K., and Suda, T. (2014). Metabolic requirements for the maintenance of self-renewing stem cells. Nat. Rev. Mol. Cell Biol. *15*, 243–256.

Ito, Y., and Bustin, M. (2002). Immunohistochemical Localization of the Nucleosome-Binding Protein HMGN3 in Mouse Brain. J. Histochem. Cytochem. Histochem Cytochem *50*.

Iwafuchi-Doi, M., and Zaret, K.S. (2014). Pioneer transcription factors in cell reprogramming. Genes Dev. *28*, 2679–2692.

Izzo, A., Kamieniarz, K., and Schneider, R. (2008). The histone H1 family: specific members, specific functions? Biol. Chem. *389*, 333–343.

Jørgensen, H.F., Terry, A., Beretta, C., Pereira, C.F., Leleu, M., Chen, Z.-F., Kelly, C., Merkenschlager, M., and Fisher, A.G. (2009). REST selectively represses a subset of RE1-containing neuronal genes in mouse embryonic stem cells. Development *136*, 715–721.

Kalinowska-Herok, M., and Widłak, P. (2008). High mobility group proteins stimulate DNA cleavage by apoptotic endonuclease DFF40/CAD due to HMG-box interactions with DNA. Acta Biochim. Pol.

Karow, M., Sá Nchez, R., Schichor, C., Masserdotti, G., Ortega, F., Heinrich, C., Gascó, S., Khan, M.A., Lie, D.C., Dellavalle, A., et al. (2012). Reprogramming of Pericyte-Derived Cells of the Adult Human Brain into Induced Neuronal Cells. Cell Stem Cell *11*, 471–476.

Kim, J.H., Lee, S.-R., Li, L.-H., Park, H.-J., Park, J.-H., Lee, K.Y., Kim, M.-K., Shin, B.A., and Choi, S.-Y. (2011). High Cleavage Efficiency of a 2A Peptide Derived from Porcine Teschovirus-1 in Human Cell Lines, Zebrafish and Mice. PLoS One *6*, e18556.

Kimura, A., Matsuda, T., Sakai, A., Murao, N., and Nakashima, K. (2018). HMGB2 expression is associated with transition from a quiescent to an activated state of adult neural stem cells. Dev. Dyn. *247*, 229–238.

Kishi, Y., Fujii, Y., Hirabayashi, Y., and Gotoh, Y. (2012). HMGA regulates the global chromatin state and neurogenic potential in neocortical precursor cells. Nat. Neurosci.

Kisseleva, T., Bhattacharya, S., Braunstein, J., and Schindler, C.. (2002). Signaling through the JAK/STAT pathway, recent advances and future challenges. Gene *285*, 1–24.

Klempin, F., Gertz, K., and Kronenberg, G. (2017). Redox homeostasis: unlocking the bottleneck in glia-to-neuron conversion. Stem Cell Investig. *4*, 7.

Knoth, R., Singec, I., Ditter, M., Pantazis, G., Capetian, P., Meyer, R.P., Horvat, V., Volk, B., and Kempermann, G. (2010). Murine Features of Neurogenesis in the Human Hippocampus across the Lifespan from 0 to 100 Years. PLoS One *5*, e8809.

Kokoeva, M. V., Yin, H., and Flier, J.S. (2005). Neurogenesis in the hypothalamus of adult mice: Potential role in energy balance. Science (80-.).

Kriegstein, A., and Alvarez-Buylla, A. (2009). The Glial Nature of Embryonic and Adult Neural Stem Cells. Annu. Rev. Neurosci.

Kronenberg, G., Gertz, K., Cheung, G., Buffo, A., Kettenmann, H., Götz, M., and Endres, M. (2010). Modulation of fate determinants Olig2 and Pax6 in resident glia evokes spiking neuroblasts in a model of mild brain ischemia. Stroke *41*, 2944–2949.

Langmead, B., Trapnell, C., Pop, M., and Salzberg, S.L. (2009). Ultrafast and memory-efficient alignment of short DNA sequences to the human genome. Genome Biol. *10*, R25.

Lazarini, F., and Lledo, P.-M. (2011). Is adult neurogenesis essential for olfaction? Trends Neurosci. *34*, 20–30.

Lepko, T. (2012). The role of the HMG proteins in adult neurogenesis.

Li, H. (2011). A statistical framework for SNP calling, mutation discovery, association mapping and population genetical parameter estimation from sequencing data. Bioinformatics *27*, 2987–2993.

Li, H., Handsaker, B., Wysoker, A., Fennell, T., Ruan, J., Homer, N., Marth, G., Abecasis, G., and Durbin, R. (2009). The Sequence Alignment/Map format and SAMtools. Bioinformatics *25*, 2078–2079.

Li, M., Sun, L., Luo, Y., Xie, C., Pang, Y., and Li, Y. (2014). High-mobility group box 1 released from astrocytes promotes the proliferation of cultured neural stem/progenitor cells. Int. J. Mol. Med.

Lim, D.A., Suárez-Fariñas, M., Naef, F., Hacker, C.R., Menn, B., Takebayashi, H., Magnasco, M., Patil, N., and Alvarez-Buylla, A. (2006). In vivo transcriptional profile analysis reveals RNA splicing and chromatin remodeling as prominent processes for adult neurogenesis. Mol. Cell. Neurosci.

Liu, M.L., Zang, T., Zou, Y., Chang, J.C., Gibson, J.R., Huber, K.M., and Zhang, C.L. (2013). Small molecules enable neurogenin 2 to efficiently convert human fibroblasts into cholinergic neurons. Nat. Commun. *4*, 2183.

Liu, M.L., Zang, T., and Zhang, C.L. (2016). Direct Lineage Reprogramming Reveals Disease-Specific Phenotypes of Motor Neurons from Human ALS Patients. Cell Rep. *14*, 115–128.

Liu, Y., Miao, Q., Yuan, J., Zhang, P., Li, S., Rao, Z., Zhao, W., Ye, Q., Geng, J., Zhang, X., et al. (2015). Ascl1 Converts Dorsal Midbrain Astrocytes into Functional Neurons In Vivo.

Lodato, S., and Arlotta, P. (2015). Generating Neuronal Diversity in the Mammalian Cerebral Cortex. Annu. Rev. Cell Dev. Biol. *31*, 699–720.

Lunt, S.Y., and Vander Heiden, M.G. (2011). Aerobic Glycolysis: Meeting the Metabolic Requirements of Cell Proliferation. Annu. Rev. Cell Dev. Biol. *27*, 441–464.

Magistretti, P.J., and Allaman, I. (2015). A cellular perspective on brain energy metabolism and functional imaging. Neuron *86*, 883–901.

Malarkey, C.S., and Churchill, M.E.A. (2012). The high mobility group box: The ultimate utility player of a cell. Trends Biochem. Sci.

Mall, M., Kareta, M.S., Chanda, S., Ahlenius, H., Perotti, N., Zhou, B., Grieder, S.D., Ge, X., Drake, S., Ang, C.E., et al. (2017). Myt1l safeguards neuronal identity by actively repressing many non-neuronal fates Normal differentiation and induced reprogramming require the activation of target cell programs and silencing of donor cell programs.

Marro, S., Pang, Z.P., Yang, N., Tsai, M.-C., Qu, K., Chang, H.Y., Südhof, T.C., and Wernig, M. (2011). Direct Lineage Conversion of Terminally Differentiated

Hepatocytes to Functional Neurons. Cell Stem Cell *9*, 374–382.

Marshall, C.A.G., Novitch, B.G., and Goldman, J.E. (2005). Olig2 directs astrocyte and oligodendrocyte formation in postnatal subventricular zone cells. J. Neurosci. *25*, 7289–7298.

Masserdotti, G., Gillotin, S., Sutor, B., Drechsel, D., Irmler, M., Jørgensen, H.F., Sass, S., Theis, F.J., Beckers, J., Berninger, B., et al. (2015). Transcriptional Mechanisms of Proneural Factors and REST in Regulating Neuronal Reprogramming of Astrocytes. Cell Stem Cell *17*, 74–88.

Masserdotti, G., Gascón, S., and Götz, M. (2016). Direct neuronal reprogramming: learning from and for development. Development *143*, 2494–2510.

Mattar, P., Britz, O., Johannes, C., Nieto, M., Ma, L., Rebeyka, A., Klenin, N., Polleux, F., Guillemot, F., and Schuurmans, C. (2004). A screen for downstream effectors of Neurogenin2 in the embryonic neocortex. Dev. Biol. *273*, 373–389.

Mattugini, N., Merl-Pham, J., Petrozziello, E., Schindler, L., Bernhagen, J., Hauck, S.M., and Götz, M. (2018). Influence of white matter injury on gray matter reactive gliosis upon stab wound in the adult murine cerebral cortex. Glia 1–19.

Meneghini, V., Bortolotto, V., Francese, M.T., Dellarole, A., Carraro, L., Terzieva, S., and Grilli, M. (2013). High-Mobility Group Box-1 Protein and $_{NL}$-Amyloid Oligomers Promote Neuronal Differentiation of Adult Hippocampal Neural Progenitors via Receptor for Advanced Glycation End Products/Nuclear Factor-□B Axis: Relevance for Alzheimer's Disease. J. Neurosci. *33*, 6047–6059.

Merkle, F.T., Tramontin, A.D., García-Verdugo, J.M., and Alvarez-Buylla, A. (2004). Radial glia give rise to adult neural stem cells in the subventricular zone. Proc. Natl. Acad. Sci. *101*, 17528–17532.

Mertens, J., Paquola, A.C.M., Ku, M., Hatch, E., Böhnke, L., Ladjevardi, S., McGrath, S., Campbell, B., Lee, H., Herdy, J.R., et al. (2015). Directly Reprogrammed Human Neurons Retain Aging-Associated Transcriptomic Signatures and Reveal Age-Related Nucleocytoplasmic Defects. Cell Stem Cell *17*, 705–718.

Ming, G. li, and Song, H. (2011). Adult Neurogenesis in the Mammalian Brain: Significant Answers and Significant Questions. Neuron.

Mirzadeh, Z., Merkle, F.T., Soriano-Navarro, M., Garcia-Verdugo, J.M., and Alvarez-Buylla, A. (2008). Neural Stem Cells Confer Unique Pinwheel Architecture to the Ventricular Surface in Neurogenic Regions of the Adult Brain. Cell Stem Cell *3*, 265–

278.

Moleri, S., Cappellano, G., Gaudenzi, G., Cermenati, S., Cotelli, F., Horner, D.S., and Beltrame, M. (2011). The HMGB protein gene family in zebrafish: Evolution and embryonic expression patterns. Gene Expr. Patterns.

Molyneaux, B.J., Arlotta, P., Menezes, J.R.L., and Macklis, J.D. (2007). Neuronal subtype specification in the cerebral cortex. Nat. Rev. Neurosci. *8*.

Müller, S., Ronfani, L., and Bianchi, M.E. (2004). Regulated expression and subcellular localization of HMGB1, a chromatin protein with a cytokine function. In Journal of Internal Medicine, p.

Nagao, M., Lanjakornsiripan, D., Itoh, Y., Kishi, Y., Ogata, T., and Gotoh, Y. (2014). High Mobility Group Nucleosome-Binding Family Proteins Promote Astrocyte Differentiation of Neural Precursor Cells. Stem Cells *32*, 2983–2997.

Nat, R., Apostolova, G., and Dechant, G. (2013). Telencephalic Neurogenesis Versus Telencephalic Differentiation of Pluripotent Stem Cells. In Trends in Cell Signaling Pathways in Neuronal Fate Decision, (InTech), p.

Ninkovic, J., and Götz, M. (2013). Fate specification in the adult brain - lessons for eliciting neurogenesis from glial cells. BioEssays.

Ninkovic, J., Steiner-Mezzadri, A., Jawerka, M., Akinci, U., Masserdotti, G., Petricca, S., Fischer, J., Von Holst, A., Beckers, J., Lie, C.D., et al. (2013). The BAF Complex Interacts with Pax6 in Adult Neural Progenitors to Establish a Neurogenic Cross-Regulatory Transcriptional Network. Cell Stem Cell *13*, 403–418.

Nishino, J., Kim, I., Chada, K., and Morrison, S.J. (2008). Hmga2 promotes neural stem cell self-renewal in young, but not old, mice by reducing p16Ink4a and p19Arf expression. Cell *135*, 227–239.

Niu, W., Zang, T., Zou, Y., Fang, S., Smith, D.K., Bachoo, R., and Zhang, C.-L. (2013). In vivo reprogramming of astrocytes to neuroblasts in the adult brain. Nat. Cell Biol. *15*.

Niu, W., Zang, T., Smith, D.K., Vue, T.Y., Zou, Y., Bachoo, R., Johnson, J.E., and Zhang, C.-L. (2015). SOX2 reprograms resident astrocytes into neural progenitors in the adult brain. Stem Cell Reports *4*, 780–794.

Noctor, S.C., Martínez-Cerdeño, V., and Kriegstein, A.R. (2007). Contribution of Intermediate Progenitor Cells to Cortical Histogenesis. Arch. Neurol. *64*, 639.

Ochiai, W., Nakatani, S., Takahara, T., Kainuma, M., Masaoka, M., Minobe, S., Namihira, M., Nakashima, K., Sakakibara, A., Ogawa, M., et al. (2009).

Periventricular notch activation and asymmetric Ngn2 and Tbr2 expression in pair-generated neocortical daughter cells. Mol. Cell. Neurosci. *40*, 225–233.

Ohtaka-Maruyama, C., and Okado, H. (2015). Molecular Pathways Underlying Projection Neuron Production and Migration during Cerebral Cortical Development. Front. Neurosci. *9*, 447.

Ory, D.S., Neugeborent, B.A., and Mulligantt, R.C. (1996). A stable human-derived packaging cell line for production of high titer retrovirus/vesicular stomatitis virus G pseudotypes. Proc. Natl. Acad. Sci. *93*, 11400–11406.

Ozturk, N., Singh, I., Mehta, A., Braun, T., and Barreto, G. (2014). HMGA proteins as modulators of chromatin structure during transcriptional activation. Front. Cell Dev. Biol. *2*, 5.

Pang, Z.P., Yang, N., Vierbuchen, T., Ostermeier, A., Fuentes, D.R., Yang, T.Q., Citri, A., Sebastiano, V., Marro, S., Südhof, T.C., et al. (2011). Induction of human neuronal cells by defined transcription factors. Nature *476*, 220–223.

Paridaen, J.T., and Huttner, W.B. (2014). Neurogenesis during development of the vertebrate central nervous system. EMBO Rep. *15*, 351–364.

Parker, T.M., Nguyen, A.H., Rabang, J.R., Patil, A.-A., and Agrawal, D.K. (2017). The danger zone: Systematic review of the role of HMGB1 danger signalling in traumatic brain injury. Brain Inj. *31*, 2–8.

Pataskar, A., Jung, J., Smialowski, P., Noack, F., Calegari, F., Straub, T., and Tiwari, V.K. (2016). NeuroD1 reprograms chromatin and transcription factor landscapes to induce the neuronal program. EMBO J. *35*, 24–45.

Patel, T., Tursun, B., Rahe, D.P., and Hobert, O. (2012). Removal of Polycomb Repressive Complex 2 Makes C. elegans Germ Cells Susceptible to Direct Conversion into Specific Somatic Cell Types. Cell Rep. *2*, 1178–1186.

Petryniak, M.A., Potter, G.B., Rowitch, D.H., and Rubenstein, J.L.R. (2007). Dlx1 and Dlx2 control neuronal versus oligodendroglial cell fate acquisition in the developing forebrain. Neuron *55*, 417–433.

Pfisterer, U., Kirkeby, A., Torper, O., Wood, J., Nelander, J., Dufour, A., Björklund, A., Lindvall, O., Jakobsson, J., Parmar, M., et al. (2011). Direct conversion of human fibroblasts to dopaminergic neurons. Proc. Natl. Acad. Sci. *108*, 10343–10348.

Pilz, G.-A., Shitamukai, A., Reillo, I., Pacary, E., Schwausch, J., Stahl, R., Ninkovic, J., Snippert, H.J., Clevers, H., Godinho, L., et al. (2013). Amplification of progenitors in the mammalian telencephalon includes a new radial glial cell type. Nat. Commun.

4, 2125.

Pimentel, H., Bray, N.L., Puente, S., Melsted, P., and Pachter, L. (2017). Differential analysis of RNA-seq incorporating quantification uncertainty. Nat. Methods *14*, 687–690.

Postnikov, Y. V., and Bustin, M. (2016). Functional interplay between histone H1 and HMG proteins in chromatin. Biochim. Biophys. Acta - Gene Regul. Mech.

Pusterla, T., De Marchis, F., Palumbo, R., and Bianchi, M.E. (2009). High mobility group B2 is secreted by myeloid cells and has mitogenic and chemoattractant activities similar to high mobility group B1. Autoimmunity.

Quadrato, G., Zhang, A.C., and Arlotta, P. (2016). Stressed out? Healing Tips for Newly Reprogrammed Neurons. Cell Stem Cell *18*, 297–299.

Reeves, R. (2001). Molecular biology of HMGA proteins: hubs of nuclear function. Gene *277*, 63–81.

Reeves, R. (2015). High mobility group (HMG) proteins: Modulators of chromatin structure and DNA repair in mammalian cells. DNA Repair (Amst).

Rivetti di Val Cervo, P., Romanov, R.A., Spigolon, G., Masini, D., Martín-Montañez, E., Toledo, E.M., La Manno, G., Feyder, M., Pifl, C., Ng, Y.-H., et al. (2017). Induction of functional dopamine neurons from human astrocytes in vitro and mouse astrocytes in a Parkinson's disease model. Nat. Publ. Gr. *35*.

Robel, S., Berninger, B., and Götz, M. (2011). The stem cell potential of glia: Lessons from reactive gliosis. Nat. Rev. Neurosci. *12*, 88–104.

Robins, S.C., Stewart, I., McNay, D.E., Taylor, V., Giachino, C., Goetz, M., Ninkovic, J., Briancon, N., Maratos-Flier, E., Flier, J.S., et al. (2013). α-Tanycytes of the adult hypothalamic third ventricle include distinct populations of FGF-responsive neural progenitors. Nat. Commun. *4*, 2049.

Rojczyk-Gołębiewska, E., Pałasz, A., and Wiaderkiewicz, R. (2014). Hypothalamic subependymal niche: A novel site of the adult neurogenesis. Cell. Mol. Neurobiol.

Ronfani, L., Ferraguti, M., Croci, L., Ovitt, C.E., Schöler, H.R., Consalez, G.G., and Bianchi, M.E. (2001). Reduced fertility and spermatogenesis defects in mice lacking chromosomal protein Hmgb2. Development *128*, 1265–1273.

Rouaux, C., and Arlotta, P. (2013). Direct lineage reprogramming of post-mitotic callosal neurons into corticofugal neurons in vivo. Nat. Cell Biol. *15*.

Rowitch, D.Hd. genetics of vertebrate glial-cell specification, and Kriegstein, A.R. (2010). Developmental genetics of vertebrate glial-cell specification. Nat. Rev. *468*,

214–222.

RStudio (2015). RStudio: Integrated Development for R. RStudio, Inc.

Sanes, D.H., Reh, T.A., Harris, W.A., Sanes, D.H., Reh, T.A., and Harris, W.A. (2012). Polarity and segmentation. In Development of the Nervous System, (Elsevier), pp. 23–48.

Schieber, M., and Chandel, N.S. (2014). ROS function in redox signaling and oxidative stress. Curr. Biol. *24*, R453-62.

Schindelin, J., Arganda-Carreras, I., Frise, E., Kaynig, V., Longair, M., Pietzsch, T., Preibisch, S., Rueden, C., Saalfeld, S., Schmid, B., et al. (2012). Fiji: an open-source platform for biological-image analysis. Nat. Methods *9*, 676–682.

Schuurmans, C., and Guillemot, F. (2002). Molecular mechanisms underlying cell fate specification in the developing telencephalon. Curr. Opin. Neurobiol. *12*, 26–34.

Seo, S., Lim, J.-W., Yellajoshyula, D., Chang, L.-W., and Kroll, K.L. (2007). Neurogenin and NeuroD direct transcriptional targets and their regulatory enhancers. EMBO J. *26*, 5093–5108.

Shin, J., Berg, D.A., Zhu, Y., Shin, J.Y., Song, J., Bonaguidi, M.A., Enikolopov, G., Nauen, D.W., Christian, K.M., Ming, G.L., et al. (2015). Single-Cell RNA-Seq with Waterfall Reveals Molecular Cascades underlying Adult Neurogenesis. Cell Stem Cell.

Silver, J., Schwab, M.E., and Popovich, P.G. (2014). Central nervous system regenerative failure: role of oligodendrocytes, astrocytes, and microglia. Cold Spring Harb. Perspect. Biol. *7*, a020602.

Sirko, S., Behrendt, G., Johansson, P.A., Tripathi, P., Costa, M., Bek, S., Heinrich, C., Tiedt, S., Colak, D., Dichgans, M., et al. (2013). Reactive glia in the injured brain acquire stem cell properties in response to sonic hedgehog glia. Cell Stem Cell.

Sirko, S., Irmler, M., Gascón, S., Bek, S., Schneider, S., Dimou, L., Obermann, J., De Souza Paiva, D., Poirier, F., Beckers, J., et al. (2015). Astrocyte reactivity after brain injury-: The role of galectins 1 and 3. Glia *63*, 2340–2361.

Smith, D.K., and Zhang, C.-L. (2015). Regeneration through reprogramming adult cell identity in vivo. Am. J. Pathol. *185*, 2619–2628.

Smith, D.K., Yang, J., Liu, M.-L., and Zhang, C.-L. (2016). Small molecules modulate chromatin accessibility to promote NEUROG2- mediated fibroblast-to-neuron reprogramming. Stem Cell Reports *7*, 955–969.

Sofroniew, M. V (2009). Molecular dissection of reactive astrogliosis and glial scar

formation. Trends Neurosci. *32*, 638–647.

Sofroniew, M. V, and Vinters, H. V (2010). Astrocytes: biology and pathology. Acta Neuropathol. *119*, 7–35.

Son, E.Y., Ichida, J.K., Wainger, B.J., Toma, J.S., Rafuse, V.F., Woolf, C.J., and Eggan, K. (2011). Conversion of Mouse and Human Fibroblasts into Functional Spinal Motor Neurons. Cell Stem Cell *9*, 205–218.

Sorrells, S.F., Paredes, M.F., Cebrian-Silla, A., Sandoval, K., Qi, D., Kelley, K.W., James, D., Mayer, S., Chang, J., Auguste, K.I., et al. (2018). Human hippocampal neurogenesis drops sharply in children to undetectable levels in adults. Nat. Publ. Gr.

Spalding, K.L., Bergmann, O., Alkass, K., Bernard, S., Salehpour, M., Huttner, H.B., Boström, E., Westerlund, I., Vial, C., Buchholz, B.A., et al. (2013). Dynamics of Hippocampal Neurogenesis in Adult Humans. Cell *153*, 1219–1227.

Štros, M. (2010). HMGB proteins: Interactions with DNA and chromatin. Biochim. Biophys. Acta - Gene Regul. Mech. *1799*, 101–113.

Štros, M., Launholt, D., and Grasser, K.D. (2007). The HMG-box: A versatile protein domain occurring in a wide variety of DNA-binding proteins. Cell. Mol. Life Sci.

Su, Z., Niu, W., Liu, M.-L., Zou, Y., and Zhang, C.-L. (2014). In vivo conversion of astrocytes to neurons in the injured adult spinal cord. Nat. Commun. *5*, 3338.

Taudt, A., Nguyen, M.A., Heinig, M., Johannes, F., and Colome-Tatche, M. (2016). chromstaR: Tracking combinatorial chromatin state dynamics in space and time. BioRxiv 038612.

Taupin, P., and Gage, F.H. (2002). Adult neurogenesis and neural stem cells of the central nervous system in mammals. J. Neurosci. Res.

Taverna, E., Götz, M., and Huttner, W.B. (2014). The Cell Biology of Neurogenesis: Toward an Understanding of the Development and Evolution of the Neocortex. Annu. Rev. Cell Dev. Biol.

Tole, S., and Hébert, J.M. (2013). Telencephalon Patterning. In Comprehensive Developmental Neuroscience: Patterning and Cell Type Specification in the Developing CNS and PNS, J.L. (John L. Rubenstein, and P. Rakic, eds. (Academic Press), pp. 3–24.

Tong, C.K., Han, Y.-G., Shah, J.K., Obernier, K., Guinto, C.D., and Alvarez-Buylla, A. (2014). Primary cilia are required in a unique subpopulation of neural progenitors. Proc. Natl. Acad. Sci. U. S. A. *111*, 12438–12443.

Torper, O., Pfisterer, U., Wolf, D.A., Pereira, M., Lau, S., Jakobsson, J., Bjorklund,

A., Grealish, S., and Parmar, M. (2013). Generation of induced neurons via direct conversion in vivo. Proc. Natl. Acad. Sci. *110*, 7038–7043.

Torper, O., Ottosson, D.R., Pereira, M., Lau, S., Cardoso, T., Grealish, S., and Parmar, M. (2015). In Vivo Reprogramming of Striatal NG2 Glia into Functional Neurons that Integrate into Local Host Circuitry. Cell Rep. *12*, 474–481.

Treutlein, B., Lee, Q.Y., Camp, J.G., Mall, M., Koh, W., Ali, S., Shariati, M., Sim, S., Neff, N.F., Skotheim, J.M., et al. (2016). Dissecting direct reprogramming from fibroblast to neuron using single-cell RNA-seq. Nature *534*, 391–395.

Tsacopoulos, M., and Magistretti, P.J. (1996). Metabolic coupling between glia and neurons. J. Neurosci. *16*, 877–885.

Tsunemoto, R.K., Eade, K.T., Blanchard, J.W., and Baldwin, K.K. (2015). Forward engineering neuronal diversity using direct reprogramming. EMBO J. *34*, 1445–1455.

Ueda, T., and Yoshida, M. (2010). HMGB proteins and transcriptional regulation. Biochim. Biophys. Acta - Gene Regul. Mech.

Vierbuchen, T., Ostermeier, A., Pang, Z.P., Kokubu, Y., Südhof, T.C., and Wernig, M. (2010). Direct conversion of fibroblasts to functional neurons by defined factors. Nature *463*, 1035–1041.

Wang, L.-L., and Zhang, C.-L. (2018). Engineering new neurons: in vivo reprogramming in mammalian brain and spinal cord. Cell Tissue Res. *371*, 201–212.

Wapinski, O.L., Vierbuchen, T., Qu, K., Lee, Q.Y., Chanda, S., Fuentes, D.R., Giresi, P.G., Ng, Y.H., Marro, S., Neff, N.F., et al. (2013). Hierarchical mechanisms for direct reprogramming of fibroblasts to neurons. Cell *155*, 621–635.

Wapinski, O.L., Lee, Q.Y., Chen, A.C., Li, R., Corces, M.R., Ang, C.E., Treutlein, B., Xiang, C., Baubet, V., Suchy, F.P., et al. (2017). Rapid Chromatin Switch in the Direct Reprogramming of Fibroblasts to Neurons. Cell Rep. *20*, 3236–3247.

Xue, Y., Ouyang, K., Huang, J., Zhou, Y., Ouyang, H., Li, H., Wang, G., Wu, Q., Wei, C., Bi, Y., et al. (2013). Direct conversion of fibroblasts to neurons by reprogramming PTB-regulated microRNA circuits. Cell *152*, 82–96.

Xue, Y., Qian, H., Hu, J., Zhou, B., Zhou, Y., Hu, X., Karakhanyan, A., Pang, Z., and Fu, X.-D. (2016). Sequential regulatory loops as key gatekeepers for neuronal reprogramming in human cells. Nat. Neurosci. *19*, 807–815.

Yang, X., Liaw, L., Prudovsky, I., Brooks, P.C., Vary, C., Oxburgh, L., and Friesel, R. (2015). Fibroblast growth factor signaling in the vasculature. Curr. Atheroscler. Rep. *17*, 509.

Yu, G., Wang, L.-G., and He, Q.-Y. (2015a). ChIPseeker: an R/Bioconductor package for ChIP peak annotation, comparison and visualization. Bioinformatics *31*, 2382–2383.

Yu, K.-R., Shin, J.-H., Kim, J.-J., Koog, M.G., Lee, J.Y., Choi, S.W., Kim, H.-S., Seo, Y., Lee, S., Shin, T., et al. (2015b). Rapid and Efficient Direct Conversion of Human Adult Somatic Cells into Neural Stem Cells by HMGA2/let-7b. CellReports *10*, 441–452.

8 List of publications

Heimann, G., Canhos, L.L., Frik, J., Jäger, G., **Lepko, T.**, Ninkovic, J., Götz, M., and Sirko, S. (2017). Changes in the Proliferative Program Limit Astrocyte Homeostasis in the Aged Post-Traumatic Murine Cerebral Cortex. Cereb. Cortex 27, 4213–4228.

Di Giaimo, R.*, Durovic, T.*, Kociaj, A., **Lepko, T.**, Irmler, M., Cernilogar, F.M., Schotta, G., Barbosa, J., Trümbach, D., Baumgart, E.V., Beckers, J., Wurst, W., and Ninkovic, J. (2018). Aryl hydrocarbon receptor pathway defines time frame for restorative neurogenesis. Cell Reports, in revision.

Lepko, T.*, Pusch, M.*, Müller, T., Schulte, D., Hasler, J., Huttner, H.B., Vandenbroucke R., Vandendriessche C., Martin-Villalba, A., Zhao, S., LLorens-Bobadilla, E., Schneider, A., Fischer, A., Götz, M.*, and Ninkovic, J.* (2018). Choroid Plexus Releases miR-204 Regulating the Number of Neural Stem Cells in the Adult Brain. EMBO J., in revision.

Sanchez-Gonzalez, R., Koupourtidou, C., Breunig, C.T., **Lepko, T.**, Zambusi, A., Novoselc, K.T., Charlène, G., Durovic, T., Aschenbroich, S., Fischer, J., Schwarz, V., Sirko, S., Straka, H., Merl-Pham, J., Huttner, H.B., Irmler, M., Unger, N., Dimou, L., Beckers, J., Wurst, W., Trümbach, D., Götz, M., Hauck, S., Stricker, S.H., Bareyre, F., and Ninkovic, J. (2018). Key role of innate immune pathways in regulating glial scar formation and recovery after central nervous system injury. In submission to Nature.

* Equal contribution

9 Affidavit

Eidesstattliche Versicherung/Affidavit

Hiermit versichere ich an Eides statt, dass ich die vorliegende Dissertation “The Role of Chromatin Associated Protein HMGB2 in Setting up Permissive Chromatin States for Direct Glia to Neuron Conversion” selbstständig angefertigt habe, mich außer der angegebenen keiner weiteren Hilfsmittel bedient und alle Erkenntnisse, die aus dem Schrifttum ganz oder annähernd übernommen sind, als solche kenntlich gemacht und nach ihrer Herkunft unter Bezeichnung der Fundstelle einzeln nachgewiesen habe.

I hereby confirm that the dissertation “The Role of Chromatin Associated Protein HMGB2 in Setting up Permissive Chromatin States for Direct Glia to Neuron Conversion” is the result of my own work and that I have only used sources or materials listed and specified in the dissertation.

München, den 18.04.2018 Tjaša Lepko

10 List of contributions

The following people listed below contributed materials provided help with experiments or helped with the analysis of data.

Prof. Dr. Jovica Ninkovic (LMU, Munich) performed initial experiments of EGF+FGF and FGF cultures reprogramming (Fig. 15d), analysed their differences based on the cellular marker expression (Fig. 16a-f) and performed the RNA-seq analysis.

The mass spectrometry analysis was performed by Dr. Stefanie Hauck and Dr. Juliane Merl-Pham at the Research Unit Protein Science at the Helmholtz Zentrum München.

Maren Büttner and Aaron Taudt, both from Institute of Computational Biology (ICB) at the Helmholtz Zentrum München performed ATAC-seq analysis.

Dr. Alexandra Lepier (LMU, Munich) kindly prepared the Hmgb2 overexpression construct.

Dr. Lorenza Ronfani (Core Facility for Conditional Mutagenesis, San Raffaele Scientific Institute, Milan, Italy) kindly provided us with the Hmgb2-/- mouse line.

Jesica Frik (LMU, Munich) shared some sections used for the analysis in Fig. 26.

Tjaša Lepko Prof. Dr. Jovica Ninkovic

11 Acknowledgements

My first gratitude belongs to my supervisors Prof. Dr. Jovica Ninkovic and Prof. Dr. Magdalena Götz, for the great opportunity to carry out my PhD study in this lab.

I would like to thank Jovica for a continuous support and guidance during these early steps of my research career, for his patience, kindness, motivation, and enthusiasm. I really enjoyed our meetings and I hold in high regard that he always found the time for the supervision. Thanks for sharing his expertise and brilliant ideas. It was really a joy to work with and learn from such a great scientist.

I would like to express my sincere gratitude to Magdalena, for her wonderful support over these years of my PhD. Her knowledge, ideas, and suggestions gave an extremely valuable input to the project. Her enthusiasm and motivation for science have been after all these years still a great inspiration for me. It was the privilege to work in her lab and I am truly thankful for everything that I've learned from her.

To the Graduate School of Systemic Neurosciences, I would like to thank for the excellent organisation, offering many courses of the highest quality and the financial support enabling me to attend the outstanding conferences. It was a pleasure being part of it. Special thanks to the GSN coordinators for always being so kind and helpful. I would also like to thank to HELENA Helmholtz Graduate School for the financial support and organizing excellent workshops. Many thanks also to the members of my Thesis Advisory Committee, Prof. Dr. Sandra Hake and Dr. Raymond Poot, for taking their time and giving valuable advice and suggestions to the project.

Further I owe the warmest thanks to Andrea Steiner-Mezzadri for her never-ending help, giving all the possible support and making sure that everything in the lab runs smoothly. I would like to thank for her patience, encouragement and being available all the time for me. This thesis would not have been possible without her support. I would also like to thank Emily Violette Baumgart, Angelika Waiser, Sarah Hubinger, and Sabine Ulbricht for their great technical support, kindness and always being prepared to help.

At this point, I would also like to thank my “old office” members, Filippo Calzolari, Judith Fischer-Sternjak and Rossella Di Giaimo for the great atmosphere, valuable advice, and discussions. I really enjoyed all the time we spent together and it has been a pleasure to know you all.

Next, I warmly want to thank our “Fish group” - Christina, Anita, Alessandro, Klara, Tamara, Sven, Rosario, Veronika, for the entertaining atmosphere and fantastic company in the lab. You are great colleagues, making my time being a graduate student really enjoyable. Thank you for all your support and sharing all good and less good days with me.

My appreciation also goes to previous graduate students and friends, Stefania Petricca, Vidya Ramesh, and Elisa Murenu, for helping me with my experiments and answering thousands of my questions. Thank you for taking your time, for your kind help and chilling atmosphere, I had a great time to work with you. Big thanks also to Miriam Esgleas for her kindness and for her unlimited help. I am grateful fur everything what I’ve learned from you. To Sonia Najas Sales big thanks for nice discussions and her positive energy and always offering her help. I would also like to thank Anna Köferle for her great support in the lab and outside of it especially during this last stage of my PhD. My special thank goes also to Melanie Pusch for the opportunity to continue work on her project and all her help anytime I need.

I would also like to express my gratitude to Dr. Sergio Gascon, Dr. Giacomo Masserdotti and Carmen Mayer for their kind collaboration and performing some of the reprogramming experiments.

A very special thank goes to our secretaries Elsa Melo and Lana Polero for their great help taking over all of the non-scientific work.

During my six years of the PhD the every single person lab member contributed to a great working environment and a really nice atmosphere. Many thanks for all the help and support, this PhD would not have been possible without you.

Most importantly, I would like to thank my mother for her never ending encouragement, confidence, patience, and understanding. Thanks for supporting me and helping me any time I needed.

In the end, I would like to especially thank to my boyfriend Miha Modic for standing all this time beside me, for his patience and unlimited support. Words cannot express how grateful I am to have him in my life for the past 10 years. Thank you for giving me the trust, encouragement and unlimited love. I would never achieve this point without you. Thank you for always, always being there for me.